

Diffusion in zeolites : towards a microscopic understanding

Citation for published version (APA):

Schuring, D. (2002). *Diffusion in zeolites : towards a microscopic understanding*. [Phd Thesis 1 (Research TU/e / Graduation TU/e), Chemical Engineering and Chemistry]. Technische Universiteit Eindhoven.
<https://doi.org/10.6100/IR558779>

DOI:

[10.6100/IR558779](https://doi.org/10.6100/IR558779)

Document status and date:

Published: 01/01/2002

Document Version:

Publisher's PDF, also known as Version of Record (includes final page, issue and volume numbers)

Please check the document version of this publication:

- A submitted manuscript is the version of the article upon submission and before peer-review. There can be important differences between the submitted version and the official published version of record. People interested in the research are advised to contact the author for the final version of the publication, or visit the DOI to the publisher's website.
- The final author version and the galley proof are versions of the publication after peer review.
- The final published version features the final layout of the paper including the volume, issue and page numbers.

[Link to publication](#)

General rights

Copyright and moral rights for the publications made accessible in the public portal are retained by the authors and/or other copyright owners and it is a condition of accessing publications that users recognise and abide by the legal requirements associated with these rights.

- Users may download and print one copy of any publication from the public portal for the purpose of private study or research.
- You may not further distribute the material or use it for any profit-making activity or commercial gain
- You may freely distribute the URL identifying the publication in the public portal.

If the publication is distributed under the terms of Article 25fa of the Dutch Copyright Act, indicated by the "Taverne" license above, please follow below link for the End User Agreement:

www.tue.nl/taverne

Take down policy

If you believe that this document breaches copyright please contact us at:

openaccess@tue.nl

providing details and we will investigate your claim.

Diffusion in Zeolites:

Towards a Microscopic Understanding

PROEFSCHRIFT

ter verkrijging van de graad van doctor
aan de Technische Universiteit Eindhoven,
op gezag van de Rector Magnificus,
prof.dr. R.A. van Santen,
voor een commissie aangewezen
door het College voor Promoties
in het openbaar te verdedigen
op dinsdag 5 november 2002 om 16.00 uur

door

Danny Schuring

geboren te Amersfoort

Dit proefschrift is goedgekeurd door de promotoren:

prof.dr. R.A. van Santen

en

prof.dr. P.A.J. Hilbers

CIP-DATA LIBRARY TECHNISCHE UNIVERSITEIT EINDHOVEN

Schuring, Danny.

Diffusion in zeolites : towards a microscopic understanding / by Danny Schuring. - Eindhoven: Technische Universiteit Eindhoven, 2002.

Proefschrift. - ISBN 90-386-2624-X

NUR 913

Trefwoorden: heterogene katalyse ; zeolieten / poreuze materialen ;
diffusie / adsorptie / fysisch-chemische simulatie en modellering /
moleculaire dynamica / alkanen / radiochemie ; positron-emissie

Subject headings: heterogeneous catalysis ; zeolites / porous materials ;
diffusion / adsorption / physiochemical simulation and modeling /
molecular dynamics / alkanes / radiochemistry ; positron emission

Printed at *Universiteitsdrukkerij*, Eindhoven University of Technology.

The work described in this thesis has been carried out at the Schuit Institute of Catalysis (part of NIOK, the Netherlands School for Catalysis Research), Eindhoven University of Technology, The Netherlands.

Contents

1	Introduction	1
1.1	Catalysis	1
1.1.1	The principles of catalysis	2
1.1.2	Zeolites	3
1.1.3	Zeolites and the catalytic cycle	5
1.2	Diffusion	6
1.2.1	Diffusion in gases and liquids	6
1.2.2	Diffusion in microporous materials	7
1.3	The study of diffusion in zeolites	8
1.4	Computational techniques	8
1.5	Questions to be answered	9
1.6	Overview of this thesis	10
1.7	References	11
2	Diffusion in Zeolites: Concepts and Techniques	13
2.1	Intracrystalline diffusion	13
2.1.1	From gas-phase to micropore diffusion	13
2.1.2	Diffusion in zeolites	14
2.2	Self-diffusion versus transport diffusion	15
2.2.1	Fickian diffusion	15
2.2.2	Self-diffusion	16
2.2.3	The Darken relation	17
2.3	Factors influencing the diffusivity	18
2.3.1	Adsorbate concentration	18
2.3.2	Temperature	19
2.4	Anomalous diffusion in zeolites	20
2.5	Experimental techniques: an overview	21
2.5.1	Macroscopic techniques	22
2.5.2	Microscopic techniques	23
2.5.3	Comparing the results of different techniques	24
2.6	Positron Emission Profiling	25

iv CONTENTS

2.6.1	Detection principles	26
2.6.2	Production of radioactively labelled molecules	27
2.6.3	Diffusion experiments	28
2.7	Simulating diffusion in zeolites	28
2.7.1	Classical diffusion theory	29
2.7.2	Molecular dynamics simulations	30
2.7.3	Dynamic Monte Carlo methods	31
2.7.4	Other techniques	32
2.8	Final remarks	33
2.9	References	34
3	Molecular Dynamics of Alkanes in Zeolites	37
3.1	Introduction	37
3.2	Model and calculations	39
3.2.1	The zeolite model	39
3.2.2	The alkane model	41
3.2.3	Calculations	41
3.3	Comparison with other studies	43
3.4	Diffusion in single-file pore systems	44
3.5	Concentration dependence of the diffusivity	46
3.6	Chainlength dependence	51
3.7	Diffusion of branched alkanes	53
3.8	Conclusions	54
3.9	References	55
4	Diffusion in Single-File Systems	57
4.1	Introduction	57
4.2	Methodology	59
4.2.1	Hard-sphere dynamics	59
4.2.2	Molecular dynamics with Lennard-Jones type interactions	61
4.2.3	Computational procedure	63
4.3	Diffusion inside an unstructured tube	64
4.3.1	The mean-square displacement	64
4.3.2	Concentration dependence	66
4.3.3	Influence of boundary conditions	66
4.4	Diffusion in a structured tube	68
4.4.1	The mean-square displacement in a structured tube	69
4.4.2	Dependence on outer pore diameter	72
4.4.3	Changing the pore geometry and interactions	75
4.4.4	Finite size effects in a structured tube	76

4.5	Implications and conclusions	78
4.6	References	81
5	Measurement and Simulation of Binary Diffusion in Zeolites	83
5.1	Introduction	83
5.2	Experimental setup	85
5.3	Modeling the tracer exchange process	86
5.3.1	The model equations	87
5.3.2	Solving the model	89
5.3.3	Adsorption/desorption at the crystal boundary	89
5.3.4	Influence of the diffusion and adsorption constants	92
5.4	Results and discussion	92
5.4.1	Adsorption of single components: comparison with literature	94
5.4.2	Binary adsorption: Results and comparison with CBMC . .	96
5.4.3	Multicomponent diffusion	98
5.5	Conclusions	101
5.6	References	102
6	The Influence of Siting on Adsorption and Diffusion	105
6.1	Introduction	105
6.2	Modeling the diffusion in a 2-D pore network	107
6.2.1	Dynamic Monte Carlo simulations	107
6.2.2	The lattice-gas model	108
6.2.3	Computational details	111
6.3	Adsorption of Single-component systems	112
6.3.1	Influence of preferential siting	112
6.3.2	Influence of lateral interactions	115
6.4	Single-component diffusion	117
6.4.1	Influence of the lattice topology	117
6.4.2	Influence of preferential siting	118
6.5	Influence of site blocking	120
6.5.1	Diffusivity at varying coverages	120
6.5.2	Blocking at constant coverage	122
6.6	Binary diffusion	122
6.6.1	Diffusivity versus coverage	122
6.6.2	Influence of the mixture composition	124
6.7	Conclusions	126
6.8	References	129

vi CONTENTS

7 Concluding Remarks	133
7.1 Diffusion in zeolites: where do we stand now?	133
7.2 The results: an overview	134
7.2.1 Molecular dynamics: modeling on microscopic scale	134
7.2.2 Single-file diffusion: simple systems with complex behaviour	135
7.2.3 Diffusion in mixtures	135
7.2.4 DMC: a coarse-grained model of diffusion	136
7.3 The big picture	136
7.3.1 The importance of intermolecular interactions	136
7.3.2 The limitations of DMC	137
7.3.3 Macroscopic versus microscopic viewpoints	137
7.3.4 Theory versus experiment	138
Summary	141
Samenvatting	143
Dankwoord	145
Publications	147
Curriculum Vitae	149

1

Introduction

In this chapter some background information, necessary for understanding the relevance of the study conducted in this thesis, will be given. A short introduction is given on catalysis, zeolites, and their use. The importance of diffusion and adsorption for the catalytic performance of these materials is discussed, as well as the diffusive process itself, both in the gas phase, as well as in microporous materials. Finally, a short overview is given of the contents of this thesis.

Although the research presented in this thesis is performed in the inorganic chemistry and catalysis group at the Eindhoven University of Technology, this thesis does not contain any chemical (catalytic) reactions. Instead, it deals with a subject of physical chemistry, the diffusion of molecules in zeolites. At first sight, these two subjects do not seem to be too closely related. Diffusion can however be a very important parameter when understanding the catalytic performance of chemical reactors, something which will hopefully become clear in the next few sections. This chapter is aimed at only giving a general overview of the field, a more detailed description of the diffusion can be found in the next chapter.

1.1 Catalysis

Nowadays, catalysis plays a very important role in the chemical industries. Although most people only know of the existence of catalysts because they have one underneath their car, nearly all products originating from the chemical industries (more than 90%!)¹ in one way or the other are produced utilizing these materials. Some of the most important processes are the production of high-quality fuels from crude oil, the production of ammonia, of all kinds of plastics, and increasingly also in

2 Introduction

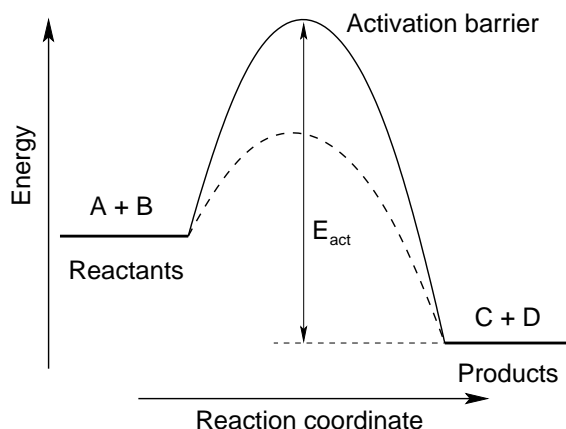


Figure 1.1: *The principle of catalysis: a catalyst reduces the height of the activation barrier between reactant and product.*

the production of pharmaceuticals. Basically, the motivation of applying catalysts is twofold: because of economical interest, and because of environmental issues. From an economical point of view, the use of a catalyst in the production process can reduce costs because it enables the use of milder conditions under which the reaction takes place, thus reducing the amount of energy that has to be put into the production process, and possibly also the demands for the equipment used in the production (e.g. due to pressure or temperature reductions). From an environmental point of view, catalysts can be used to remove or convert toxic species into harmless ones (like e.g. in the automotive catalyst) and reduce the amount of waste products in certain processes. It is obvious that often the two reasons for using a catalyst go hand-in-hand, as the removal of waste products from a production process is often quite expensive, and a reduction of energy demands is also attractive from an environmental point of view.

1.1.1 The principles of catalysis

Catalysts are thus extremely useful, but how do they work? The word “catalysis” was first defined by Berzelius in his annual review of chemistry in 1836² as a *chemical event that changes the composition of a mixture, but not the catalyst*. At that time, a number of catalytic processes were already known, but the explanation of catalysis was far from clear and of a quite metaphysical nature.³ It was Friedrich Ostwald who first forwarded the explanation of catalysis, which is still believed to be the correct one. As is shown schematically in figure 1.1, when a reactant is converted to its products it has to overcome a certain energy barrier. This is due to the fact that certain changes have to take place inside the molecules, like breaking bonds between the



(a)

(b)

Figure 1.2: Scanning electron micrographs of a sample of silicalite-1 crystals showing the regular, coffin-like shape of this zeolites. Pictures were taken from Zhu et al.⁴

atoms, or bending certain parts of the molecule. A catalyst can provide an alternative pathway from reactant to product, which has a lower activation barrier and thus requires a lower amount of energy. It however does not change the equilibrium between reactant and product, as the energy levels at which these reside are not altered.

A lot of different materials are capable of catalyzing reactions, and a huge number of different catalysts are nowadays available for all kinds of processes. These can be divided in *homogeneous* and *heterogeneous* catalysts, depending on whether the catalyst particles are in the same phase as the reactants or not. A lot of different processes in the human body are catalyzed by these homogeneous catalysts (but, in this case, they are called enzymes). Metal surfaces form a large class of heterogeneous catalysts, of which platinum is of course one of the more well-known examples. Another interesting group of materials which are now extensively used are the so-called *zeolites*.

1.1.2 Zeolites

Since the 1960's, zeolites (the name zeolite is derived from the greek words for *to boil* and *stone*) have been applied in an increasing number of catalytic processes. Zeolites are crystalline microporous materials (see figure 1.2) whose composition is very similar to sand, as it is mainly composed of silicon and oxygen atoms. The silicons are tetrahedrally surrounded by oxygens, and using these basic building blocks, all kinds of structures can be created with pores and cavities of varying dimensions. Up to now, 136 different structures have been reported,⁵ of which about 40 are naturally occurring, and the rest has been synthesized in a laboratory. Basically, these materials

4 Introduction

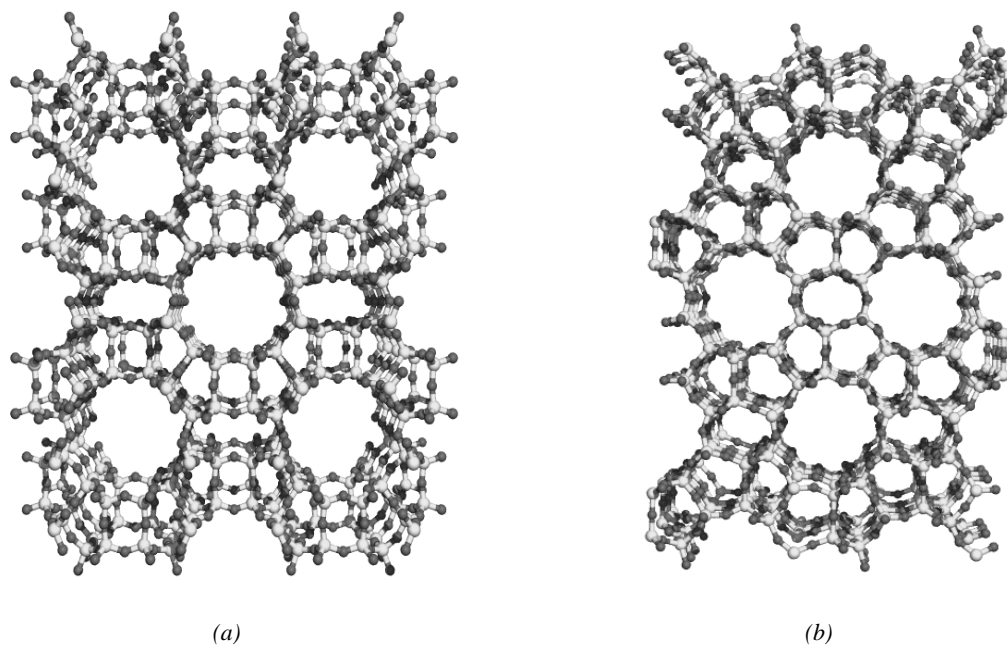


Figure 1.3: The structures of zeolites mordenite (a) and silicalite (b). The pores in the zeolite structure are clearly visible.

look like sponges, but with a very regular structure and pore sizes which are typically of molecular dimensions. Two of the more important zeolites are depicted in figure 1.3, namely *mordenite* and *silicalite-1*. The regularly shaped channels in these zeolites can be clearly seen. The different zeolites differ in pore diameter, pore shape and the way these pores are interconnected. Zeolite mordenite has a one-dimensional pore system consisting of channels with a diameter of about 7 Å, while the pores of silicalite-1 form a three-dimensional network of straight and zig-zag channels (shown schematically in figure 1.4) with a diameter of around 5.5 Å.

What makes these materials suited as a catalyst is the fact that part of the silicon atoms in the framework can be substituted by other cations like aluminum, sodium or potassium. As a result of the different valency of these cations, charges are created in the framework which have to be compensated by the addition of protons. These protons form acidic (Brønsted) sites, which behave basically in the same way as the protons in an acidic solution. A great advantage of using zeolites however is that these catalysts, because of the specific structure of the pores and cages, not all products can be easily formed, and as a result can dramatically enhance the *selectivity* (i.e. the fraction of desired products of all products that are formed) of the reaction.

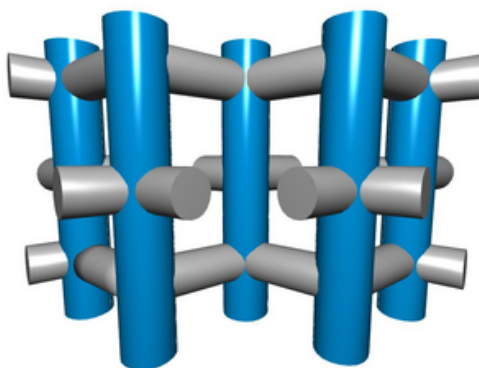


Figure 1.4: A schematic representation of the pore network of silicalite containing straight and zigzag channels.

Furthermore, these materials can also act as a support for other catalytic materials (like e.g. platinum or palladium), and in this way catalysts can be produced with a very high surface area and different catalytic functions can be united into one particle.

Among the most important applications of zeolites is the use of these materials to catalyze the conversion of crude oil to more useful products like gasoline, kerosine and other smaller hydrocarbons. A number of different reactions are involved in this conversion, like hydrocracking, hydro-isomerization, aromatization, and the dehydrogenation of cyclohexanes. The catalytic cracking alone is one of the largest applications of catalysts, with a worldwide production of more than 500 million tons per year.⁶ One example of the processes nowadays performed in oil refineries is the so-called Hysomer process, developed by Shell for the hydro-isomerization of linear alkanes to branched ones. This process makes use of platinum-loaded H-Mordenite, and is a typical example in which the zeolite acts as a bifunctional catalyst.⁷ The platinum is responsible for the dehydrogenation and hydrogenation of the alkanes, while the acid sites of the zeolites catalyze the conversion of linear alkenes to branched ones. This process is especially useful as it can increase the octane number of the products.

1.1.3 Zeolites and the catalytic cycle

As is clear from the previous section, in these materials the catalytically active sites are not directly accessible to the reacting molecules. As is usually the case for heterogeneous catalysts, a number of different steps are needed in order to convert the reactants into the desired products. These steps are schematically depicted in figure 1.5. As the feed stream is usually in the gas or liquid phase, *adsorption* on the zeolite surface and into the zeolite pores first has to take place. In order to react, the

6 Introduction

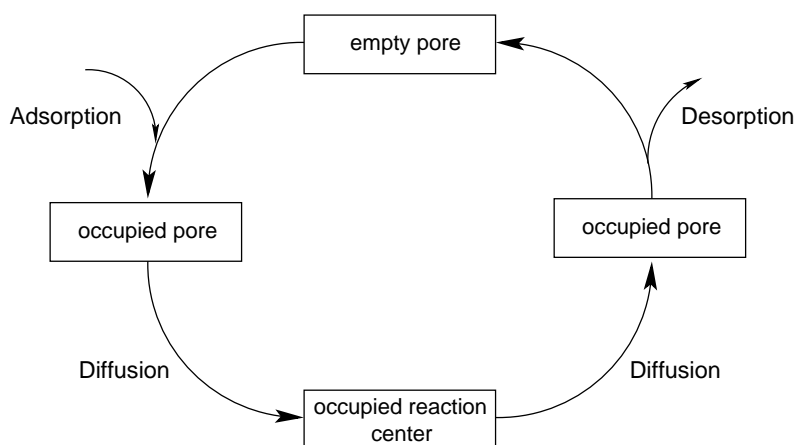


Figure 1.5: The catalytic cycle in zeolite catalysis: The zeolite pores are occupied by adsorption from the gas phase, after which the adsorbed species diffuse to the reactive centers.

molecules then have to be transported to the reactive sites inside these pores. This transport process is called *diffusion*. Once the reactants have reached the catalytically active sites, the necessary chemical reactions can finally take place, and the conversion into products takes place. As these products have to be extracted from the reactor in one way or the other and the catalytic sites have to be freed again in order to facilitate the next reaction, they now have to be transported away from these sites and out of the zeolite pore again. Again, diffusion, and the subsequent desorption of products takes care of that again. As the conversion of reactants can only occur when a significant amount of them are able to reach the active sites, and the resulting products are removed sufficiently fast from these sites, one can imagine that both adsorption and diffusion can significantly determine the catalytic behaviour of a system.

1.2 Diffusion

1.2.1 Diffusion in gases and liquids

Diffusion in liquids, gases and solids has been studied for more than a century now.⁸ The discovery of Brownian motion, which is closely related to diffusion, and the subsequent search for explaining this behaviour significantly contributed to the acceptance of the atomic view of matter and kinetic theory of gases and liquids. Diffusion is caused by the thermal motion and subsequent collisions of the molecules. Two types of diffusion can be distinguished: *transport* diffusion resulting from a concentration gradient, and *self*-diffusion which takes place in a system which is at

equilibrium. The flux due to transport diffusion can be described using Fick's First Law of Diffusion:

$$\vec{J} = -D \cdot \nabla c \quad (1.1)$$

in which D is the diffusion constant and c the concentration. Self-diffusion is usually expressed in terms of a self-diffusion constant D_c . In the case of tracer diffusion, where the labelled molecules mix with unlabelled molecules with the same properties, the transport and self-diffusivity are identical. But, although transport and self-diffusion generally occur by essentially the same microscopic principle, usually these coefficients for transport and self-diffusion are not the same.

1.2.2 Diffusion in microporous materials

Diffusion in zeolites differs from ordinary diffusion in the sense that the molecules have to move through channels of molecular dimensions. As a result, there is a constant interaction between the diffusing molecules and the zeolite framework, and the molecular motion is thus also strongly influenced by the exact size and shape of these channels instead of the temperature and concentration only. While in the case of gases and liquids the behaviour and exact value of the diffusivity can be calculated with relative ease, the exact values of these are much harder to predict for zeolites. The interactions between molecules and the pore wall for example lead to large differences in the diffusivities of different alkane isomers, as the more bulky branched isomers have a much larger interaction with the zeolite framework. A special type of diffusion can be observed in one-dimensional zeolites, called *single-file* diffusion. This type of diffusion results from the fact that some types of molecules are unable to pass each other in the narrow pores of the zeolites, and leads to a significant reduction of the mobility in these systems. Clearly, these effects are not present in pure liquids and gases.

From an industrial point of view, it is important to be able to predict and describe the mass transfer through the packed-bed reactors used in the chemical industries. A better understanding of this phenomenon will aid in the optimization and development of industrial applications of these materials in separation and catalytic processes. For this purpose, the transport diffusivities are needed. A number of different experimental techniques are nowadays available for determining these values.⁹ There is however no reliable theory that can easily predict the diffusivity for different components in different zeolites, as it is often hard to relate these values to the underlying microscopic mechanisms.^{10, 11} Furthermore, large discrepancies often exist between values obtained from different techniques, and performing these experiments is often not straightforward. It would thus be advantageous to have a good understanding of what can happen inside these zeolites, and what kind of influence this will have on a reactor scale.

8 Introduction

From a fundamental point of view, the study of diffusion is also interesting as the interactions between molecules and the zeolite can lead to all kinds of unexpected behaviour. The dependencies on for example the concentration of the diffusing molecules is expected to be completely different, as also the topology of the zeolite pore network plays an important role in this behaviour. The diffusion of mixtures of different molecules is also less straightforward. These kind of effects can be readily studied using zeolites, as in a sense, due to their regular structure, they can act as models for more complicated systems like for example amorphous materials. Furthermore, a thorough understanding of the underlying microscopic mechanisms involved will aid in understanding the interaction between transport properties and the reactivity in these materials.

1.3 The study of diffusion in zeolites

As was already mentioned in the previous section a number of different techniques are available for studying the diffusion in zeolites. The most common technique is to follow the time response of an adsorbate-adsorbent system after changing the pressure or composition of the surrounding atmosphere. By analyzing the response curves the contributing diffusion coefficients can then be calculated.¹² A number of different sorption techniques are nowadays available, which all have their advantages and disadvantages. A special class of techniques form the ones in which labelled molecules are used, as these techniques are capable of measuring the diffusion under equilibrium conditions and can thus probe the *tracer*- or self-diffusivity. More recently, two new techniques have been introduced to directly probe the self-diffusivity in these materials called pulse-field gradient NMR (PFG-NMR)¹³ and Quasi-Elastic Neutron Scattering (QENS).¹⁴ Both techniques are capable of measuring the mean-square displacement of the molecules inside the zeolite pores.

1.4 Computational techniques

Since the beginning of the 1980's, an increasing number of theoretical studies have been conducted.¹⁵ Due to the increase in computational power, different methods originating from the field of statistical mechanics could now be applied to the study of diffusion and adsorption in these microporous materials. Monte Carlo techniques could now be applied to investigate the adsorptive behaviour of molecules. Lattice dynamics studies served to study the influence of the lattice topology on reactions and transport phenomena. Molecular dynamics simulations gave a more detailed description of the diffusive and adsorptive processes, and have proven to be successful

in studying the diffusive behaviour. Nowadays, even quantum chemical calculations can be applied.¹⁶

One of the main reasons why theoretical methods have received an increasing amount of attention is that they potentially provide an inexpensive and time-effective way to determine the diffusive and adsorptive behaviour of adsorbents in zeolites. As experimental techniques are often very expensive and time-consuming, and the interpretation of the results is not always unambiguous, the development of reliable theoretical methods can significantly contribute to the prediction of transport phenomena. Using theoretical methods, the different parameters of interest (pore structure, concentration, temperature) can furthermore easily be varied, and their influence on the parameters of interest readily be calculated. Furthermore, the microscopic understanding resulting from these model studies often help in understanding the experimental results. In this respect, a close synergy between experiment and theory is of fundamental importance to both fields.

1.5 Questions to be answered

Although an extensive amount of research is nowadays available in literature on the subject of diffusion in zeolites, a number of questions still remain in this field. One of the most important problems is the apparent discrepancy between the results obtained from different techniques, especially when comparing macroscopic and microscopic methods. As the interactions between adsorbates and the zeolite taking place on a molecular scale are the main cause for the completely different behaviour compared to the gas phase, a better insight into the effect of these interactions might help in clarifying this problem. This will therefore be one of the main focusses of the research presented in this thesis.

As was already discussed in the previous section, theoretical methods are, although they only provide an approximative description of reality, excellently suited for investigating the diffusive process on a microscopic scale. These will therefore be the primary tools used in this thesis. Using these, the influence of different experimental parameters (zeolite structure, type of adsorbate, concentration, temperature) on the diffusivity are determined. The controversy in literature regarding the occurrence of single-file diffusion in zeolites with one-dimensional pore structures seems to indicate that a study of the fundamentals of this process might also help in understanding the problems encountered in zeolite science. The diffusion of binary mixtures provides an excellent test-case in which the interrelation between adsorbate-adsorbate and adsorbate-zeolite interactions can be investigated. The same holds for systems in which molecules have a preference of residing in certain regions of the pore structure. All these problems will hopefully provide us with some idea of what

10 Introduction

microscopic phenomena influence the mobility of the adsorbates in the zeolite, and what the consequences will be on a macroscopic scale.

1.6 Overview of this thesis

Now that it is clear why the study of diffusion in zeolites is of interest, it is time to have a more in-depth look at this field of research. In the upcoming chapters, a short overview will be given of the current insights in the diffusion of molecules in microporous materials, and different techniques will be applied to study some of the phenomena present in these systems. The different chapters are written in such a way, that they can in principle be read separately.

Chapter 2 starts with a short overview of the basic concepts of diffusion in zeolites. After that, a short overview is given of both the experimental and theoretical techniques that are available to study the subject. As the details of the methods used in this thesis are described in the respective chapters in which they are applied, only the basic principles will be discussed. The aim is to provide an overview of the most important available techniques, together with some of their advantages and disadvantages.

In chapter 3, molecular dynamics simulations have been applied to study the influence of the zeolite structure, size of the diffusing molecules, and pore loading on the diffusivity. As this technique is capable of quite accurately describing the process on a microscopic level, it is particularly suited to study this phenomenon on a microscopic scale. Although the simulations themselves are computationally demanding, different parameters like the ones mentioned before can be easily varied and their influences studied without having to worry about influencing other factors.

Chapter 4 focusses on the more fundamental subject of single-file diffusion. This type of diffusion can be observed in zeolites with one-dimensional pore structures, and results in anomalous diffusive behaviour which significantly alters the behaviour on a microscopic scale, but also has a great impact on the behaviour on a macroscopic scale. Using very simple model systems, some of the basic factors leading to this behaviour are studied, and, although these results are generally applicable to all single-file systems, the consequences for the diffusive behaviour in zeolites are discussed.

In Chapter 5, the more practical subject of diffusion in binary mixtures is considered. In this case, a mixture of *n*-hexane and 2-methylpentane in silicalite was used, as this is a system which is also quite interesting from an industrial point of view. For this study, an experimental technique called Positron Emission Profiling (PEP) was used. In order to be able to interpret the results, a mathematical model describing the flow in zeolite packed-bed reactors was developed, and this model will be discussed

in detail here. The obtained results raise some questions regarding the influence of the siting of different components inside the zeolite pore network on the diffusive behaviour.

One of the questions raised in chapter 5 is investigated further in chapter 6. Using dynamic Monte Carlo simulations, the diffusive behaviour of particles on a 2-dimensional pore network is studied. As these simulations make use of a coarse-grained model of the zeolite pore network, these simulations can be performed at much larger time- and length scales than for example molecular dynamics simulations. Although these simulations do not give a detailed description of the interactions on a microscopic scale, some of the essential features can be easily included and their influences can be readily investigated. In this case, the effects of the preferential siting of particles for a certain type of adsorption site in the lattice on the single- and binary-component diffusion and adsorption will be studied.

This thesis will finish with chapter 7, which will give a general overview of the results obtained in the previous chapters, and summarizes the conclusions that can be drawn from this research. Some general insights will be considered which have been obtained from the research in this thesis.

1.7 References

- ¹ J. M. Thomas and W. J. Thomas, *Principles and practice of heterogeneous catalysis*, VCH, Weinheim, Germany (1996).
- ² J. J. Berzelius, *Jahresber. Chem.* **15**, 242–244 (1836).
- ³ R. A. van Santen and J. W. Niemantsverdriet, *Chemical kinetics and catalysis*, Plenum Press, New York, New York (1995).
- ⁴ W. Zhu, F. Kapteijn, and J. A. Moulijn, *Microporous Mesoporous Mater.* **47**, 157–171 (2001).
- ⁵ C. Baerlocher, W. M. Meier, and D. H. Olson, *Atlas of zeolite framework types*, Elsevier, Amsterdam, The Netherlands, 5th ed. (2001).
- ⁶ R. A. van Santen, P. W. N. M. van Leeuwen, J. A. Moulijn, and B. A. Averill (Eds.), *Catalysis: An integrated approach, second, revised and enlarged edition*, Elsevier, Amsterdam, The Netherlands, 2nd ed. (1999).
- ⁷ P. B. Weisz, *Polyfunctional heterogeneous catalysis*, in: *Advances in catalysis and related subjects*, D. D. Eley, P. W. Selwood, and P. B. Weisz, eds., vol. 13, pp. 137–190, Academic Press, New York (1962).
- ⁸ W. Jost, *Diffusion in solids, liquids and gases*, Academic Press, New York (1960).
- ⁹ J. Kärger and D. M. Ruthven, *Diffusion in zeolites and other microporous solids*, John Wiley & Sons, Inc., New York (1992).
- ¹⁰ N. Y. Chen, T. F. Degnan Jr., and C. M. Smith, *Molecular transport and reaction in zeolites - design and application of shape selective catalysis*, VCH Publishers, New York (1994).
- ¹¹ N. Benes and H. Verweij, *Langmuir* **15**(23), 8292–8299 (1999).

12 Introduction

- ¹² D. M. Ruthven, *Principles of adsorption and adsorption processes*, John Wiley & Sons, New York (1984).
- ¹³ J. Kärgler and H. Pfeifer, *Zeolites* **7**, 90–107 (1987).
- ¹⁴ H. Jobic, M. Beé, and G. J. Kearley, *J. Phys. Chem.* **98**, 4660–4665 (1994).
- ¹⁵ F. J. Keil, R. Krishna, and M.-O. Coppens, *Rev. Chem. Eng.* **16**(2), 71–197 (2000).
- ¹⁶ L. Benco, T. Demuth, J. Hafner, F. Hutschka, and H. Toulhoat, *J. Chem. Phys.* **114**(14), 6327–6334 (2001).

2

Diffusion in Zeolites: Concepts and Techniques

Nowadays a number of different techniques, both experimental and theoretical, are available to study the diffusion in zeolites. Roughly, these methods can be divided in macroscopic and microscopic methods, depending on the time- or lengthscale at which they probe the diffusive process. In this chapter, a short overview is given of the different techniques available. The emphasis will be more on the theoretical methods, as these were used for the largest part of the research in this thesis. Some extra attention will furthermore be paid on the methods applied in this thesis.

2.1 Intracrystalline diffusion

2.1.1 From gas-phase to micropore diffusion

As was already discussed in the introduction, the diffusion of molecules through the pores of a zeolite crystal differs greatly from gaseous diffusion. In gases the diffusion is controlled by the interactions (or collisions) between the different molecules due to their thermal motion. As gases and liquids form an isotropic medium, different properties like the average collision rate, collision rate and mean free path can be calculated relatively easy using kinetic theory, based on the laws of classical mechanics.¹ More sophisticated theories, which also account for intermolecular interactions, vibration and rotation of the molecules, and quantum effects are nowadays available and are quite capable of describing the behaviour of a variety of systems.

The diffusion of molecules in pores can be classified in a number of different

14 Diffusion in Zeolites: Concepts and Techniques

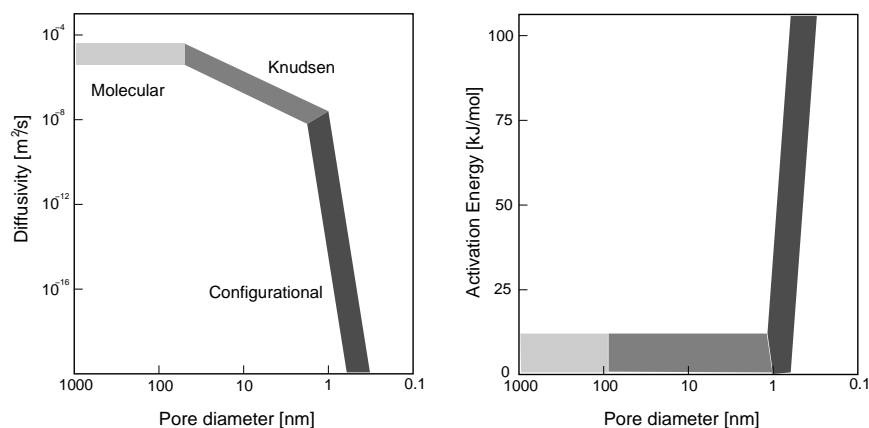


Figure 2.1: Effect of pore size on the diffusivity and activation energy of diffusion (taken from Post²).

regimes depending on the pore diameter (see figure 2.1). For large pore diameters, of the order of $1 \mu\text{m}$ or larger, usually called *macropores*, collisions between the molecules occurs much more frequently than collisions with the wall, and molecular diffusion is the dominant mechanism. Typically, the diffusion constants of gases are around $10^{-5} \text{m}^2 \cdot \text{s}^{-1}$. As the size of the pores decreases, the number of collisions with the wall increases until it finally becomes smaller than the mean free path (the average distance travelled by a molecule between two collisions) of the gas molecules. At this point, Knudsen diffusion takes over and the mobility starts to depend on the dimensions of the pore.³ At even smaller pore sizes, in the range of 20\AA and smaller when the pore diameter become comparable to the size of the molecules, these will continuously feel the interaction with the walls. Diffusion in the micropores of a zeolite usually takes place in this regime, and is called *configurational* diffusion.⁴

2.1.2 Diffusion in zeolites

The mechanism by which the molecules move through the pores in the configurational regime is comparable to that of surface diffusion of adsorbed molecules on a surface. Due to the small distance between the molecules and the pore wall, the molecules are more or less physically bonded to it, and the mechanism is comparable to surface diffusion. The diffusivity in this regime will depend strongly on the pore diameter, the structure of the pore wall, the interactions between the surface atoms and the diffusing molecules, the shape of the diffusing molecules and the way the channels are connected. As a result, it is very difficult to derive generalized equations relating the forementioned properties to the diffusion coefficient one finds for these systems. The values of these coefficients furthermore span an enormous range

from 10^{-8} to as low as $10^{-20} \text{ m}^2 \cdot \text{s}^{-1}$.⁵ Compared to the gas phase, the diffusivity of the molecules inside the zeolite channels is thus greatly reduced, and a much stronger temperature dependence is often observed. The fact that the particles have to move through the pore network also introduces correlation effects, which can also greatly enhance the concentration dependence.

2.2 Self-diffusion versus transport diffusion

2.2.1 Fickian diffusion

The foundations of the theory of diffusion were laid by Fick in the 19th century. In one dimension, the flow of a certain species can be related to the gradient of the concentration according to Fick's first law⁶

$$J = -D_t \left(\frac{\partial C}{\partial x} \right) \quad (2.1)$$

in which C is the concentration, x is the spatial coordinate, and D_t is the (transport) diffusion coefficient. The diffusion coefficient is thus defined as a proportionality constant between the rate of flow and the concentration gradient. Although the above equation is a convenient starting point, it does not reflect the true driving force of diffusion. As diffusion is nothing more than the macroscopic manifestation of the tendency of a system to approach equilibrium, the driving force should be the gradient of the chemical potential μ . Using irreversible thermodynamics, the Onsager relation can be derived:

$$J = -L \frac{\partial \mu}{\partial x} \quad (2.2)$$

in which L is the phenomenological Onsager coefficient. This equation indeed explicitly identifies the cause for diffusive flow, and will prove to be useful when trying to relate the transport diffusion to self-diffusion.

The pioneering work on zeolitic diffusion, performed by Barrer and Jost,⁷ was based on the application of Fick's equation. Assuming a concentration-independent diffusion constant, eq. 2.1 can be transformed into a diffusion equation known as Fick's second law:

$$\frac{\partial C}{\partial t} = -D_t \left(\frac{\partial^2 C}{\partial x^2} \right) \quad (2.3)$$

This equation gives the change of concentration in a finite volume element with time. In the approach of Barrer and Jost, the diffusivity is assumed to be isotropic throughout the crystal, as D_t is independent of the direction in which the particles diffuse.

16 Diffusion in Zeolites: Concepts and Techniques

Assuming spherical particles, Fick's second law can be readily solved in radial coordinates. As a result, all information about the exact shape and connectivity of the pore structure is lost, and only reflected by the value of the diffusion constant.

2.2.2 Self-diffusion

While for the transport diffusion a gradient in the chemical potential is necessary, self-diffusion is an equilibrium process. This type of diffusion can be monitored by labeling some of the molecules inside the zeolite pores and following how the labeled and unlabeled molecules are mixed. Eq. 2.1 can again be used to describe the flow of the labelled components:

$$J_i^* = -D_s \left. \frac{\partial C^*}{\partial x_i} \right|_{C=\text{constant}} \quad (2.4)$$

in which the asterix refers to the labelled component, and D_s in this case is the self-diffusion constant. Alternatively, the self-diffusion constant can be related to a microscopic quantity called the mean-square displacement, as was shown by Einstein in his study on Brownian motion.⁸ The mean-square displacement is defined as:

$$\langle r^2(t) \rangle = \langle |\vec{r}(t) - \vec{r}(0)|^2 \rangle = \frac{1}{N} \sum_{i=1}^N (\vec{r}^i(t) - \vec{r}^i(0))^2 \quad (2.5)$$

in which N is the number of particles in the system and $\vec{r}^i(t)$ is the position of particle i at time t , which is nothing more than the average of the squared distance a particle has travelled at time t . By assuming that the particles move according to a random walk, it can be shown that for sufficiently long times this mean-square displacement will be linearly dependent on time:⁹

$$\langle |\vec{r}^2(t)| \rangle = 6D_s t \quad (2.6)$$

for diffusion in the z direction only. This equation is known as the Einstein relation. It can be shown that the diffusion constant in this equation and equation 2.4 are equivalent.¹⁰

An alternative way to define the self-diffusivity based on the microscopic properties of the diffusing molecules is by making use of the Green-Kubo relations.¹¹ Using this relation, the self-diffusivity can be calculated from the velocity auto-correlation function, a quantity that expresses correlations between velocities at different times:

$$D_s = \frac{1}{3} \int_0^{\infty} \langle \vec{v}(0) \cdot \vec{v}(t) \rangle dt \quad (2.7)$$

Although it is difficult to measure the velocity auto-correlation function experimentally, this equation can be conveniently used in theoretical methods.

2.2.3 The Darken relation

As was already noted in section 2.2.1 the driving force of diffusion is the gradient of the chemical potential. The chemical potential can be related to the concentration by considering the equilibrium vapor phase:

$$\mu = \mu^0 + R_g T \ln p \quad (2.8)$$

in which p is the partial pressure of the component. Using this equation yields the so-called *Darken equation* (although Darken was not the first to derive this particular equation),¹² which relates the two constants D_t and L to each other:

$$D_t = R_g T L \left(\frac{\partial \ln p}{\partial \ln C} \right) = D_0 \left(\frac{\partial \ln p}{\partial \ln C} \right) = D_0 \cdot \Gamma \quad (2.9)$$

D_0 is generally referred to as the *corrected* or *Maxwell-Stefan* diffusivity, and Γ is called the thermodynamic correction factor, which corrects for the non-linearity between the pressure and the concentration of the adsorbent. Often, the corrected diffusivity is used in experimental studies where the transport diffusion is measured. Although D_0 can still depend on the concentration, in systems near the saturation limit, or in the low concentration (Henry's Law) regime this dependence has been experimentally shown to be quite small, and the use of the corrected diffusivity helps in directly comparing experimental results under different conditions.⁹

A similar expression as eq. 2.9 is also used to relate the transport and self-diffusion to each other:

$$D_t(q) = D_s(0) \left(\frac{d \ln p}{d \ln q} \right) \quad (2.10)$$

in which q is the concentration of the species adsorbed in the pores. This equation implies that the self- and transport-diffusivity coincide at low concentrations. Although the derivation of this relation is rather straightforward,⁹ the assumption is made that the diffusive process in both completely different experimental situations can be described in a similar fashion. In general this does not have to be the case and deviations from the above expression can be expected.¹³ Recently, Paschek and Krishna¹⁴ have suggested that eq. 2.9 can indeed be used to relate the transport diffusivity to the Maxwell-Stefan or corrected diffusivity, but that an extra relation is needed to link the corrected and self-diffusivity:

$$D_s = \frac{D_0}{1 + \theta} \quad (2.11)$$

in which θ is the coverage inside the pores of the zeolite.

18 Diffusion in Zeolites: Concepts and Techniques

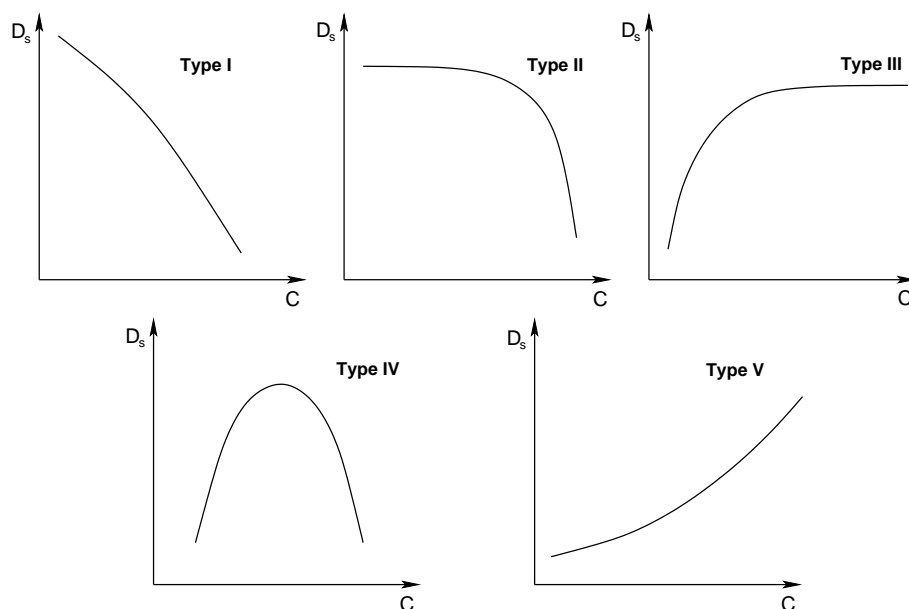


Figure 2.2: Types of concentration dependence of the intracrystalline self-diffusion.

2.3 Factors influencing the diffusivity

2.3.1 Adsorbate concentration

In zeolites, the diffusivity of the adsorbates can be strongly dependent on the concentration. As the diffusion of molecules in zeolites takes place in channels where it is difficult or impossible to pass each other, encounters between different molecules will have a much more pronounced influence on the mobility. Barrer¹⁵ explained the concentration dependence of the diffusivity in zeolites using a simple jump model. Assuming that the particle has an elementary diffusion rate D_s^0 at infinite dilution to move from one site to another, the diffusivity will be proportional to the chance that a neighbouring site is empty:

$$D_s(\theta) = D_s^0 \cdot (1 - \theta) \quad (2.12)$$

This equation makes use of the fact that, in the mean-field approximation, the average coverage of a site will be equal to θ . That the actual situation can be rather more complicated has been demonstrated by a number of authors,^{16–18} who have shown that correlation effects can have a strong impact on the dependence of the diffusivity.

According to Kärger and Pfeifer,¹⁹ five different types of concentration dependence of the self-diffusivity (observed with NMR measurements) can be observed, as shown in figure 2.2. These different dependencies can be attributed to differences in

the interactions between the framework atoms and the diffusing molecules, like for example interactions with different cations in the zeolite, or the presence of strong and weak adsorption sites. In addition the pore topology can also have a significant influence on the diffusivity, as was shown by Coppens *et al.*¹⁸ This is mainly due to the stronger correlations present in systems with lower connectivity. As a result, there is an increased chance that a molecule will move back into its previous location as the chance of finding an empty space there is larger, and a larger decrease in mobility with increasing pore loading is observed.⁹ The prediction of the concentration dependence for different systems however remains difficult, and further investigations on this dependence remain of interest.

2.3.2 Temperature

As the molecules are continuously moving in the forcefield of the zeolite channels, the diffusion process can be described as an activated process, and the temperature dependence can accordingly be described by an Arrhenius-type equation:²⁰

$$D(T) = D_0 \cdot \exp \left[-\frac{E_{act}}{R_g T} \right] \quad (2.13)$$

with D_0 the diffusivity at infinite temperature, and E_{act} the activation energy of diffusion. This dependency is usually explained by assuming that diffusion takes place via a sequence of activated hops.²¹ The pre-exponential term D_0 is related to the elementary rate at which particles attempt to hop to a neighbouring adsorption site, while the exponential expresses the chance that the particles are able to overcome the free energy barrier E_{act} between these sites. Although this will certainly be an oversimplified picture of the true diffusion process, many experimental and theoretical studies have shown that it is capable of accurately describing the temperature dependence in these systems.

Experimentally, the activation energy can thus be determined by measuring the diffusivity at different temperatures. Some care should however be taken when interpreting these results. As the concentration of molecules inside the zeolite also depends on the temperature and measurements are often performed at finite loadings, the combined effect of temperature and loading dependence is measured. With increasing temperature, the loading of the zeolite crystals usually decreases. Assuming a type I concentration dependence, in addition to the increased mobility of the molecules due to the higher temperatures, this can also lead to an increase of the diffusion rate. As a result, the measured activation energy can in this case be much higher than the real activation energy, and this value will also depend on the gas-phase pressure at which the measurements are performed. This effect has recently been demonstrated for 3-methylpentane in silicalite,²² but the exact influence of the

20 Diffusion in Zeolites: Concepts and Techniques

concentration dependence of course depends on the concentration dependence of the system. Ways to circumvent this problem is by measuring at very low coverages, or choosing experimental conditions in such a way that the concentration inside the zeolite remains constant. For systems with a moderate dependence of the diffusivity on the concentration the effect might be small, but this dependence can possibly complicate the comparison of activation energies of diffusion for different experimental conditions, especially when considering that the activation energy itself might also depend on the temperature (see chapter 3 of this thesis).

An additional point complicating the comparison of the measured temperature dependence is the different definitions used for the diffusion constant. The above equation is used for both transport as well as self-diffusion, but the temperature dependence of these two quantities does not necessarily has to be the same. In addition, two different definitions are commonly used in literature for the transport diffusivity. The diffusion constant D_c , as encountered before, is defined directly by Fick's First law by considering the gradient of the total adsorbed phase in the crystals. Alternatively, Haynes²³ proposed the use of a micropore diffusion constant D_x , assuming that most of the molecules are adsorbed on the pore wall and immobile, and only a small fraction is able to move with a diffusivity equal to this constant. These two diffusion constants can be related to each other via²⁴

$$D_x = \varepsilon_x(1 + K_a)D_c \quad (2.14)$$

in which ε_x is the porosity of the zeolite crystals, and K_a is the equilibrium adsorption constant. In most cases $K_a \gg 1$, and D_x thus has an activation energy equal to the sum of the heat of adsorption and the activation energy for diffusion. Some questions however remain regarding the use of this diffusion constant, as in the narrow pores of the zeolite there is always a strong interaction between adsorbate and adsorbant and a gas-phase cannot really exist in this environment. Resultingly, the distinction between a gas and adsorbed phase seems rather arbitrary, and the use of D_c as diffusivity of the molecules is more appropriate.

2.4 Anomalous diffusion in zeolites

Another fascinating example of the completely different behaviour of diffusing molecules in zeolites compared to the gas phase is the occurrence of anomalous diffusion in some zeolites. Anomalous diffusion can occur for example when molecules diffuse through a zeolite with a one-dimensional channel network (i.e. the pores are not interconnected with each other). This type of diffusion is known as *single-file* diffusion,²⁵ and is characterized by a dramatic decrease in mobility of the molecules.

As a result, this type of diffusion is expected to have a large impact on the catalytic behaviour of these zeolites.^{26–28}

In single-file systems, the Einstein relation (eq. 2.6) does no longer hold, and in the long-time limit, the mean-square displacement obeys the following equation:²⁹

$$\langle r^2(t) \rangle = 2 \cdot F \cdot \sqrt{t} \quad (2.15)$$

in which F is the single-file mobility factor. Due to the large correlation effects present in this system, this mobility factor strongly depends on the pore loading θ .³⁰

$$F = l^2 \frac{1 - \theta}{\theta} \frac{1}{\sqrt{2\pi\tau}} \quad (2.16)$$

In this equation, l is the (average) hopping length, and τ the average time between two attempted hops. A lot of questions however remain regarding this subject, and recent studies have for example shown that, on large timescales, the Einstein relation can again be valid for these systems.³¹ As a result, a lot of discrepancies still exist between different experimental studies on this field.

2.5 Experimental techniques: an overview

As is clear from the previous sections, the prediction of diffusion rates inside zeolites is difficult, but of great practical importance. Therefore, there has always been a lot of interest in experimental techniques capable of measuring the molecular migration in these systems. Nowadays, a number of different techniques are available, which all have their advantages and disadvantages. These methods can roughly be divided in two different categories (although other classifications are possible): macroscopic and microscopic methods. Macroscopic techniques typically use a bed of zeolite crystals or a zeolite membrane, and measure the response to a change of the adsorbate concentration in the surrounding gas phase. The interpretation of the response is mostly based on a description of the diffusion via Fick's law (eq. 2.2.1). As these experiments measure the response to a concentration change, these methods usually measure the transport diffusivity, although some techniques are also capable of measuring self-diffusion by making use of labelled molecules. The microscopic techniques are capable of measuring the mobility of adsorbates on a much shorter time- and lengthscale than the previous techniques. These techniques can in principle measure the propagation of molecules through a single zeolite crystal, and can directly probe the underlying microscopic mechanisms of diffusion.

In the next few paragraphs, a short overview will be given of different experimental techniques. This overview will in no way be complete, but rather give a general idea of the techniques and their basic principles which are available nowadays. A

22 Diffusion in Zeolites: Concepts and Techniques

distinction is being made between macroscopic and microscopic methods. A number of excellent, and more exhaustive reviews regarding the different experimental techniques can be found in literature.^{2, 9, 32–34}

2.5.1 Macroscopic techniques

Membrane permeation: Permeation measurements are one of the earliest ways to determine the diffusivity through porous solids.⁹ With this technique, the flux of the adsorbate through a parallel sides slab or membrane is measured under conditions in which the concentrations at both faces are known. As the flux is related to the diffusivity of the adsorbate via Fick's law, this quantity can thus be directly calculated. The pressure can either be kept constant (like e.g. in the Wicke-Kallenbach method), or a constant pressure gradient is applied. Although the technique is rather straightforward, its application to zeolites depends on the availability of zeolite membranes, which have only recently become available.³⁵

Uptake methods: Uptake methods are based on the measurement of the response of the zeolitic host-guest system to a change in the pressure or concentration of the surrounding gas phase. If the influence of non-diffusive processes can be eliminated, either experimentally or through suitable data analysis, the contributing diffusion coefficients may be calculated from the observed response curves.^{9, 36, 37} Usually, this analysis relies on analytical solutions of the diffusion equations that describe the mass transfer inside the zeolite crystals. For the measurement of the response of the system, different techniques can be used. Examples are the gravimetric method, which uses a vacuum microbalance to measure the change in weight of the zeolite sample after exposure to a change in the gas phase, and volumetric methods which measure the change in the amount of gas phase molecules in the sorption vessel. More recently, the tapered element oscillating microbalance (TEOM) technique has been introduced, which measures the uptake in a zeolite sample via a change in eigenfrequency of the oscillating tube holding the sample.³⁸

Chromatographic methods: The chromatographic technique has been introduced as an alternative to the uptake methods, as the use of a steady-state flow can significantly reduce the influence of heat and external mass transfer resistance of the system. The technique is based on the measurement of the response of a chromatographic column filled with pellets composed of zeolite crystals to a perturbation in the sorbate concentration at the inlet. The conventional methods use either a pulse or step injection of the sorbate, after which the desired diffusion constants can be extracted by using moments analysis, which relates the time lag and broadening of the response curve to the diffusive and adsorptive properties, or by fitting an approximate analytical solution to the measured response of the column.^{23, 39} More recently, with the advent of fast computers, more accurate numerical models can also be used to

analyze the results.^{24, 40}

A number of variations on the traditional chromatographic techniques have been introduced in the passed decades. By injecting radiochemically labelled molecules, this method can for example be used to study tracer diffusion, provided that the injected pulse is sufficiently small (see e.g. Hyun and Dannyer⁴¹). The frequency response method⁴² uses a sinusoidally varying perturbation of the inlet concentration, and obtains information from the phase shift and amplitude of the response of the chromatographic column. The zero-length column (ZLC) method⁴³ uses a very small gas volume which is equilibrated with the sorbate of interest and subsequently purged with an inert gas at a high flowrate in order to further decrease external mass transfer resistances. More recently, TAP experiments^{44, 45} have been introduced that measure the pulse response of a bed under ultra-high vacuum conditions using a mass spectrometer.

2.5.2 Microscopic techniques

Pulsed Field Gradient NMR: The Pulsed Field Gradient (PFG) NMR^{10, 19} technique makes use of the spatial dependence of the nuclear magnetic resonance frequency in an inhomogeneous magnetic field. This inhomogeneous magnetic field increases linearly with the spatial coordinate z , and is superimposed over the constant magnetic field. In the PFG-NMR technique, this field is only applied during two equal, short time intervals, separated by time t . The resulting NMR signal, generated by an appropriate sequence of radiofrequent pulses, will be proportional to the propagator of the diffusing molecules. This propagator denotes the probability density that during a time interval t a molecule is shifted over a certain distance, which is determined by the field gradient that is applied during the experiments. As a result, from these experiments the self-diffusion constant and mean-square displacement can be calculated inside the zeolite crystals. Typically, the displacements measured using this technique are in the order of micrometers, much smaller than the typical lengthscales encountered in the macroscopic methods.

Other NMR techniques: Apart from PFG-NMR, other techniques based on NMR spectroscopy have been introduced. Nuclear spin interactions probed by solid-state NMR are generally anisotropic, and as a result encode for the molecular orientation with respect to the external magnetic field. By studying the motional averaging or time-correlation functions of these interactions, information can be obtained about the rotational motion of the molecules.⁴⁶⁻⁴⁸ By assuming a certain relation between rotational and translational mobility (i.e. molecules have to reorient in a certain way to move from one site to another⁴⁹) the elementary diffusion rates can be extracted. More recently, Magusin *et al.*⁵⁰ have introduced a technique which makes use of the different chemical environments of molecules in the different cages of zeolite ZK-

24 Diffusion in Zeolites: Concepts and Techniques

5. This difference is used to selectively label the molecules in one of the cages and measure the elementary exchange rate. Although the above-mentioned techniques can only be applied to a small number of zeolite-sorbate systems, their main advantage is that they are capable of measuring systems with extremely low mobility (D_s in the order of $10^{-20} \text{ m}^2 \cdot \text{s}^{-1}$).

Quasi-Elastic Neutron Scattering: Quasi-elastic neutron scattering (QENS) has been introduced in the early 90's as an alternative to PFG-NMR measurements to measure the intracrystalline diffusion in zeolites.⁵¹ This technique is based on the analysis of the quasi-elastic broadening in the energy of the scattered neutron beam. The broadening is caused by an energy transfer between the incident wave and the diffusing molecules, which in its turn depends on the elementary diffusion process of the particles. From these experiments, the self-diffusivity can be determined, and the mean jump length may be estimated. The application of this technique is limited to species with higher mobilities, and the diffusion paths covered during a measurement are typically of the order of a few nanometers.

Interference microscopy: A technique that has recently been introduced in the study of diffusion in zeolite crystals is interference microscopy.⁵² It is based on the measurement of the change in optical density of the zeolite crystallites during transient adsorption or desorption. The optical density in the zeolite is determined by the integral of the sorbate concentration in the observation direction. By using a microscope, pixel sizes of $1 \times 1 \mu\text{m}$ can be achieved, and localized concentration measurements on zeolite crystals can be performed. As the method measures concentration changes, this technique is capable of measuring the transport-diffusion on a microscopic scale. Alternatively, infrared absorbance can be used instead of the optical density for measuring the concentration.⁵³

2.5.3 Comparing the results of different techniques

As will have become clear from the previous section, there is a vast amount of techniques available for studying the diffusion in zeolites. These techniques all vary in their basic principles, the time- and length scales at which the diffusion process is measured, and the underlying assumptions made to analyze the experiments. As a result, the range of diffusivities accessible to the different methods will be different. This is illustrated in figure 2.3, in which the range of diffusivities that can typically be measured by different techniques is plotted. This makes a direct comparison between different techniques harder to accomplish. All techniques furthermore rely on certain assumptions, and for the macroscopic techniques complex, but approximative models are used for determining the diffusivity, which should be treated with some caution.⁵⁴ The fact that some methods determine the transport diffusivities, while others probe the self-diffusion in these systems, further complicates the situation. These equilib-

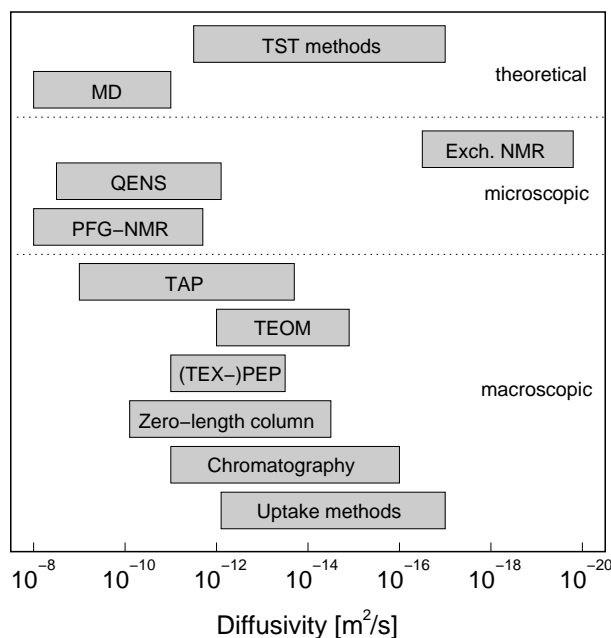


Figure 2.3: Range of diffusivities that can be determined with different methods. As some of the ranges depend on the size of the zeolite crystals, for all techniques a size of $10 \mu\text{m}$ was assumed.

rium and non-equilibrium results can in principle be related to each other using the equations discussed in section 2.2.3, but the application of these equations might not be unambiguous. It will therefore not come as a big surprise that often large discrepancies exist between different experimental studies.^{2, 9, 55} Although a number of different explanations for these discrepancies have been forwarded, a definitive answer to this problem has not been obtained. Continuous efforts are being put in the experimental verifications of different explanations, and this subject will remain an important challenge for future zeolite research.

2.6 Positron Emission Profiling

Now that a short review has been given on the different experimental techniques available, some extra attention will be given to the technique that is used in this thesis: Positron Emission Profiling (PEP). In principle, PEP is a chromatographic technique using labelled molecules, but instead of measuring the response at the exit of the reactor, this technique is capable of measuring the concentration at different positions inside the reactor. As the technique furthermore uses a standard laboratory-scale

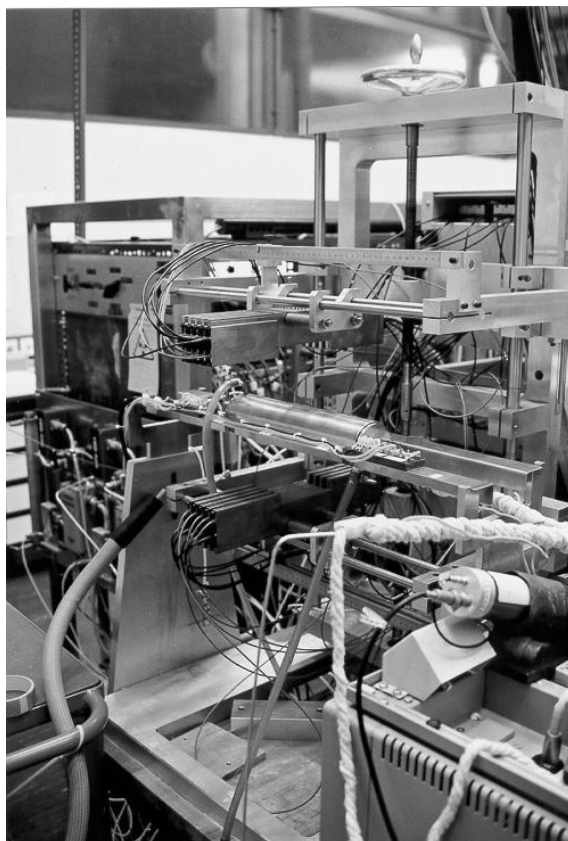


Figure 2.4: *Picture of the PEP detector showing the two rows of detectors, with the furnace containing the packed-bed reactor in between them.*

packed-bed reactor, experiments can be performed under typical reaction conditions.

2.6.1 Detection principles

The detection principle of PEP is identical to that of its 3-dimensional analogue in nuclear medicine, called Positron Emission Tomography, from which it has been derived.⁵⁶ Due to the increased time and position resolution, this detector is optimized for the measurement of the concentration along the axial direction of cylindrical flow reactors. As the radiochemical label of the injected molecules, positron (β^+) emitting isotopes have to be used. Once a positron has been emitted, it will almost immediately annihilate with an electron from the surrounding medium, producing a pair of γ photons travelling in opposite directions. From the coincident detection of these γ photons, information can be obtained on the position at which the β^+ decay took

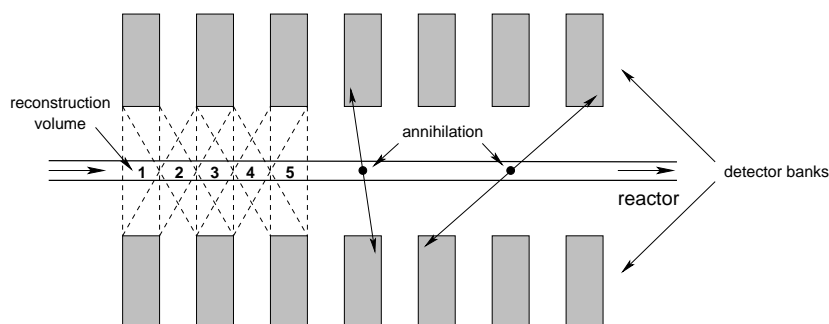


Figure 2.5: Schematic picture of the PEP detector setup with the two detector banks (not all detector elements are displayed). The first five reconstruction positions are displayed.

place.

The PEP detector consists of two arrays of nine independent detection elements each and is mounted horizontally, with the reactor and furnace placed between the upper and lower detection banks (see figure 2.4). Each detection element consists of a bismuth germanium oxide (BGO) scintillation crystal coupled to a photomultiplier. Each of these detectors in a bank can form a detection pair with each of the elements in the opposite bank, creating a total of 81 detection pairs. By coincident detection of the two γ photons produced during the positron-electron annihilation by one of these detection pairs, the position along the cylindrical axis of the bed at which this event took place can be reconstructed as the intersection of a line drawn between the two detectors and this axis (see figure 2.5).⁵⁷ As some detection pairs measure at the same intersection point with the reactor axis, a total of 17 unique, equidistant detection points are formed at which the number of annihilations can be measured as a function of time. The maximum obtainable spatial resolution is about 3 mm, while the temporal resolution is equal to 0.5 seconds.⁵⁸ As the number of annihilations is proportional to the number of decays of the positron-emitting isotopes, information can be obtained about the concentration of labelled molecules inside the reactor as a function of time and position.

2.6.2 Production of radioactively labelled molecules

As the PEP technique relies on the coincident detection of γ photons produced by the decay of positron-emitting isotopes and the subsequent annihilation of these particles, the adsorbates under study have to be labelled with these isotopes. For the experiments presented in this thesis, carbon-11 (^{11}C) was used. As the half-life of these isotopes is only 20.4 minutes, the radio-labelled molecules have to be produced on-site. First, ^{11}C is produced by irradiating a nitrogen target with highly energetic (12 MeV) protons produced by a cyclotron. Subsequently, a homologation process is

28 Diffusion in Zeolites: Concepts and Techniques

used to produce labelled hydrocarbons ranging from propane to hexane,⁵⁹ which can be trapped and injected into the reactor.

2.6.3 Diffusion experiments

With the PEP setup, two different types of experiments can be conducted. In the first type of experiments, the labelled molecules are injected as a small pulse in a steady-state feed stream of either an inert carrier gas, or of unlabelled molecules of the same kind. The propagation of the pulse through the reactor can then be followed using the PEP detector. Information about the diffusive processes can be obtained from the delay and broadening of the pulse, and quantitative information can be obtained by analysis of the measurements using an appropriate model, as will be discussed in more detail in the next section. In the second type of experiment, which is called tracer exchange-PEP (TEX-PEP),⁶⁰ the labelled molecules are constantly “leaked” into the feed stream, instead of injected as a single pulse. The PEP detector can again be used to measure the tracer exchange once the injection has started. By switching off the injection of labelled molecules after equilibrium is reached, the subsequent re-exchange can be followed as well. Again, information can be obtained by fitting appropriate models to the time evolution of the tracer exchange at the various positions along the reactor bed. This technique will be applied to the study of binary mixtures, and described in more detail in chapter 5.

The PEP technique has a number of different advantages over more conventional techniques. First of all, it is capable of measuring the in-situ concentration inside a packed bed reactor, which enables it to study phenomena which would otherwise remain invisible.⁶¹ Furthermore, this enables one to observe the evolution of a pulse or step change inside the reactor itself, therefore excluding the influence of reactor exit effects and minimizing the influence of entrance effects. Due to the penetrating power of the γ photons used in the detection, no special requirements are being put on the experimental system holding the zeolite sample, and standard plug-flow reactors can be used under typical conditions also found in the laboratory. Finally, the use of radiochemically labelled molecules makes this method particularly suited to study the diffusion of mixtures, as one of the components can be selectively labelled.

2.7 Simulating diffusion in zeolites

Theoretical methods nowadays form a valuable addition to the available experimental methods. The first theoretical foundations of zeolitic diffusion were based on classical diffusion theory, based on Fick’s second law of diffusion (see section 2.2.1). These studies focussed on the description of the diffusive behaviour of systems used

in experiments to determine the diffusivity. With the advent of faster computers, more complex calculations could be conducted. Using microscopic simulation methods like molecular dynamics and transition-state theory, predictions could now be made regarding the elementary rate of diffusion based on an atomistic model of the zeolite-adsorbate system. In this thesis, a number of different techniques will be used to simulate the diffusion in zeolites. A short overview will be given of the available techniques.

2.7.1 Classical diffusion theory

Theoretical methods based on classical diffusion theory have been used to describe the mass transfer in zeolitic systems since the start of this research field. The basis of this method is formed by Fick's second law of diffusion (eq. 2.3). Assuming that mass transfer occurs via diffusion, and that the zeolite crystals are spherically shaped, a mass balance over the zeolite particle gives

$$\frac{\partial q}{\partial t} = D_c \left(\frac{\partial^2 q}{\partial r^2} + \frac{2}{r} \frac{\partial q}{\partial r} \right) \quad (2.17)$$

in which q is the adsorbed phase concentration, D_c the diffusion constant, and r is the radial coordinate. This expression can be used to describe the uptake of a zeolite sample, assuming that micropore diffusion is the rate-controlling step. The effect of micropore diffusion is contained in the constant D_c , and as a result, this method itself is not capable of predicting the value of this constant, but merely describes what happens to the zeolitic system on a macroscopic scale. Assuming a step change in the concentration, this equation can be solved analytically:⁹

$$\frac{q(t) - q_0}{q_\infty - q_0} = 1 - \frac{6}{\pi^2} \sum_{n=1}^{\infty} \frac{1}{n^2} \exp\left(-\frac{n^2 \pi^2 D_c t}{r_c^2}\right) \quad (2.18)$$

in which $q(t)$, q_0 and q_∞ are the adsorbed phase concentrations at time t , at time 0, and the equilibrium value at infinite time, respectively. r_c is the radius of the catalyst particle. The situation becomes more complex when more than one type of resistance significantly contribute to the mass transfer in the zeolite sample. As the zeolite crystals are often pressed in pellets, when the diffusion in the micropores is relatively fast, the uptake can also be influenced by macropore diffusion and external film resistances, and more complex equations are needed to describe the uptake.

In case of a chromatographic experiment, mass transfer also occurs via the constant flow through the reactor bed. In this case, a mass balance is also needed that describes the flow in the bed:⁹

$$\frac{\partial c}{\partial t} = D_L \frac{\partial^2 c}{\partial z^2} - v \frac{\partial c}{\partial z} - \left(\frac{1 - \varepsilon}{\varepsilon} \right) \frac{\partial q}{\partial t} \quad (2.19)$$

30 Diffusion in Zeolites: Concepts and Techniques

In this equation, c is the gas-phase concentration in the bed, D_L is the axial diffusion coefficient, z the coordinate along the reactor axis, v the velocity of the flowing gas, and ε the porosity of the bed. Additionally, when using a biporous bed, an equation is needed that describes the mass transfer in the macroparticles, resulting from macropore diffusion.^{23, 62} This leads to a set of three coupled differential equations, which are difficult to solve analytically. Originally, approximative models were therefore used, like the linear driving force model,⁴⁰ or by assuming that certain contributions to the mass transfer could be neglected. Nowadays, numerical methods can be used to solve this set of differential equations, and the contribution of the different processes to the overall behaviour of the zeolite bed can be analyzed. A more detailed description of this method will be given in chapter 5.

2.7.2 Molecular dynamics simulations

A completely different type of simulations is formed by molecular dynamics. While the previous method is based on a phenomenological description of the behaviour of a zeolite system, in these type of simulations a detailed, atomistic model is built of the zeolite-sorbate system. At the start of the calculations, a small slab of the zeolite crystal (with typical dimensions in the order of 50 to 100 Å) is reproduced by defining the positions of the framework atoms. Often, all-silica structures are used, as the presence of cations and their resulting long-range electrostatic interactions seriously complicate the simulations.³⁴ Interactions between the atoms are usually modelled by using two-body potentials. For the adsorption and diffusion of alkanes, dispersive forces are the dominating interactions, and usually, Lennard-Jones potentials are used:

$$V(r_{ij}) = 4\varepsilon_{ij} \left[\left(\frac{\sigma_{ij}}{r_{ij}} \right)^{12} - \left(\frac{\sigma_{ij}}{r_{ij}} \right)^6 \right] \quad (2.20)$$

in which r_{ij} is the distance between the two interacting atoms, ε_{ij} is the energy parameter, and σ_{ij} the size parameter of the potential for the interaction between atoms i and j . The interaction parameters can in principle be calculated by some type of combination rule from the properties of the individual atoms.⁶³ However, as the above equation is only an approximation of the real interactions between sorbate and zeolite, these values are usually chosen so that the model is capable of reproducing some reference experimental data for the system under study.⁶⁴ Although there are some general forcefields available, calculations with these often do not lead to adequate results.⁶⁵

In addition to these interatomic potentials, potentials have to be defined that describe the behaviour of the adsorbates, like bond bending, torsion, and bond vibrations which give a total contribution V_{internal} . A more detailed description of these

interactions can be found in chapter 3. Once all interactions are defined, the total potential energy felt by a single atom can be calculated by summing all individual two-body interaction energies:

$$V_{\text{tot}}^i = V_{\text{zeo}}^i + V_{\text{inter}}^i + V_{\text{internal}}^i = \sum_{j=1}^N V(r_{ij}) + \sum_{k=1}^M V(r_{ik}) + V_{\text{internal}}^i \quad (2.21)$$

in which N is the number of framework atoms, and M is the total number of atoms from other sorbates. The forces acting on the atom can be calculated from the gradient of the total potential energy of this particle:

$$\vec{F}^i = -\nabla V_{\text{tot}}^i \quad (2.22)$$

The molecular dynamics simulation now proceeds by calculating the time evolution of the system by using Newton's equations of motion:

$$m^i \ddot{\vec{r}}^i = \vec{F}^i \quad (2.23)$$

with m^i the mass of atom i . Given the initial positions and velocities of the atoms, Newton's equation can be integrated, and the positions of the adsorbates can be calculated as a function of time. For this integration, different techniques are available,⁶⁶ but all these methods are based on taking sufficiently small timesteps, modifying the positions of the atoms, after which the interactions are recalculated. This process is repeated until the desired timespan has been covered. During the simulation, the various parameters of interest, like the mean-square displacement or the velocity auto-correlation function, can be calculated and stored. From these parameters, the diffusivity can be calculated.

Although this technique has proven to be very useful and is capable of providing reasonable values for the diffusivities,^{67, 68} it also has some disadvantages. As the interactions between all atoms in the system have to be calculated after each timestep, these methods are computationally demanding. Therefore, only rather small systems with a limited amount sorbate molecules can be simulated, and the timescale is limited to the order of nanoseconds. Furthermore, approximations often have to be made to reduce computer time, like assuming a rigid zeolite structure, using united-atom models, and assuming an all-silica structure, which makes these simulations less realistic. Nevertheless, these simulations are capable of probing the elementary mechanisms of diffusion on a microscopic scale, and can help in gaining more insight in its fundamentals.

2.7.3 Dynamic Monte Carlo methods

The Dynamic (or Kinetic) Monte Carlo (DMC) technique is based on a stochastic description of the diffusion in zeolites, as was already forwarded by Barrer in 1941.¹⁵

32 Diffusion in Zeolites: Concepts and Techniques

In this technique, the zeolite crystal is modeled as a network of interconnected pores. Transport of molecules proceeds via a sequence of jumps from one adsorption site to another. For adsorbates with high activation energies, this seems a reasonable assumption, as the residence time of these molecules in the low-energy regions of the zeolite is large compared to the time it spends travelling from one site to another. In principle, the dynamic Monte Carlo technique provides a numerical solution to a stochastic description based on a Markovian master equation, which describes the evolution over time of the system through jumps between configurations in phase space.⁶⁸ These stochastic descriptions have been applied by a number of authors to address the problem of diffusion in high-occupancy and blocked zeolites,^{17, 69} but have proven to be difficult to solve for these complex systems.

A first step for performing DMC simulations is the definition of the zeolite pore network. Often, simple square or cubic lattices are used, but sometimes more detailed models are developed that try to accurately mimic the adsorption sites and connectivity of the real system under study. The next step is to assign appropriate hopping rates to the different possible jumps which describe the elementary diffusion process. Given an initial configuration, the time evolution of the system is then calculated by creating a list of all possible events, assigning a tentative time for each of these events according to a Poisson-distribution, and executing the first possible event. The system time is then updated to the time of this event, and the event list is updated, after which the next event is executed, and so on. A number of different algorithms are available for advancing the time, which differ in implementation, but are conceptually identical.⁷⁰

As the DMC simulations use a coarse-grained model of the zeolite-adsorbate system, this method is computationally much less demanding than molecular dynamics simulations. This method can therefore be used to simulate on much larger time- and lengthscales than this method, and can be used to study the influence of the microscopic hopping mechanism on a mesoscopic scale. This coarse-graining is however also the greatest disadvantage of the method: in order to achieve the timescale of these simulations, a lot of details regarding the zeolite-adsorbate and adsorbate-adsorbate interactions are lost. Furthermore, not all systems might be suitably represented by a hopping mechanism.

2.7.4 Other techniques

In addition to the methods described above, which have been applied in this thesis, a number of other techniques are available. As an alternative to MD simulations, transition state methods can be used to calculate the diffusion constants from atomistic models of the zeolite-sorbate system. This method is especially suitable for the more bulky molecules inside small-pore zeolites, as these molecules typically have

low diffusion rates. The basic principle behind this type of calculations is the rate at which a molecule moves over an activation barrier is determined by the product of the probability of finding the molecule at the top of this barrier, and a dynamic term describing the rate at which the barrier is crossed.⁷¹ One of the main tasks of these methods is thus to calculate the free energy profile in the zeolite, often by using umbrella-sampling or similar techniques.^{72–74}

A technique that has recently received an increasing amount of attention is the Maxwell-Stefan theory of diffusion. This macroscopic approach is based on the Maxwell-Stefan formulation of diffusion, which relates the flux due to the diffusive motion to the gradient of the chemical potential in the system. The interaction with the zeolite is modelled as if the adsorbate diffuses in a mixture with giant dust molecules, which are essentially motionless.⁷⁵ This method has proven to be especially useful in describing the behaviour of mixtures.^{35, 76, 77}

2.8 Final remarks

As is evident from the previous section, the number of techniques available for studying the diffusion in zeolites is numerous. Historically, experimental techniques that measure the diffusivity on a macroscopic scale have always played an important role in this field of research. With the introduction of new techniques capable of measuring the diffusion processes on a microscopic scale, it has become clear that the macroscopic techniques don't always reveal the underlying processes, and are often difficult to interpret. Not in the least place, this is due to the simultaneous occurrence of a number of different processes during these experiments, which are hard to separate from each other. The interpretation of these methods often have to rely on models in which the zeolite crystals are assumed to be isotropic, while in reality a strong diffusion anisotropy can exist. Furthermore, the completely different time- and lengthscales of the different techniques might be another cause, as on a large timescale different mechanisms can manifest themselves than on short timescales.

Theoretical methods are a valuable addition to the available experimental techniques. Although these methods can only provide an approximate description of the real system, different characteristics of the system can be easily varied, and their influences systematically studied. In this respect, they can provide valuable answers to the questions that have been raised from the different experiments. Furthermore, a lot of experimental methods rely on an accurate description of the flow inside the zeolite bed. In the coming chapters, different theoretical techniques will be used to further clarify some of the open questions still present in zeolite research.

2.9 References

- ¹ W. Kauzmann, *Kinetic theory of gases*, Addison-Wesley, Reading (1966).
- ² M. F. M. Post, *Diffusion in zeolite molecular sieves*, in: *Introduction to zeolite science and practice*, H. van Bekkum, E. M. Flanigen, and J. C. Jansen, eds., vol. 58 of *Studies in surface science and catalysis*, pp. 391–443, Elsevier, Amsterdam (1991).
- ³ N. Wakao and S. Kagueli, *Heat and mass transfer in packed beds*, Gordon and Breach Science, London (1982).
- ⁴ P. B. Weisz, *Chem. Tech.* **3**, 498–505 (1973).
- ⁵ N. Y. Chen, T. F. Degnan Jr., and C. M. Smith, *Molecular transport and reaction in zeolites - design and application of shape selective catalysis*, VCH Publishers, New York (1994).
- ⁶ A. Fick, *Ann. Phys.* **94**, 59–86 (1855).
- ⁷ R. M. Barrer and W. Jost, *Trans. Faraday Soc.* **45**, 928–930 (1949).
- ⁸ A. Einstein, *Ann. Phys.* **17**, 549–560 (1905).
- ⁹ J. Kärger and D. M. Ruthven, *Diffusion in zeolites and other microporous solids*, John Wiley & Sons, Inc., New York (1992).
- ¹⁰ J. Kärger, H. Pfeifer, and W. Heink, *Adv. Magn. Res.* **12**, 1 (1988).
- ¹¹ D. N. Theodorou, R. Q. Snurr, and A. T. Bell, *Molecular dynamics and diffusion in microporous materials*, in: *Comprehensive Supramolecular Chemistry: Solid-state supramolecular chemistry - Two- and three-dimensional inorganic networks*, vol. 7, G. Alberti and T. Bein, eds., pp. 507–548, Pergamon, Oxford (1996).
- ¹² L. S. Darken, *Trans. AIME* **175**, 184–192 (1948).
- ¹³ A. I. Skoulidas and D. S. Sholl, *J. Phys. Chem. B* **105**(16), 3151–3154 (2001).
- ¹⁴ D. Paschek and R. Krishna, *Chem. Phys. Lett.* **333**, 278–284 (2001).
- ¹⁵ R. M. Barrer, *Trans. Faraday Soc.* **37**, 590–594 (1941).
- ¹⁶ D. N. Theodorou and J. Wei, *J. Catal.* **83**, 205–224 (1983).
- ¹⁷ J. Tsikoyiannis and J. Wei, *Chem. Engng Sci.* **46**(1), 233–253 (1991).
- ¹⁸ M.-O. Coppens, A. T. Bell, and A. K. Chakraborty, *Chem. Engng. Sci.* **53**(11), 2053–2061 (1998).
- ¹⁹ J. Kärger and H. Pfeifer, *Zeolites* **7**, 90–107 (1987).
- ²⁰ J. Xiao and J. Wei, *Chem. Engng Sci.* **47**(5), 1123–1141 (1992).
- ²¹ L. Riekert, *Adv. Catal.* **21**, 281 (1970).
- ²² A. O. Koriabkina, D. Schuring, A. M. de Jong, and R. A. van Santen, *J. Phys. Chem. B* (2002), submitted for publication.
- ²³ H. W. Haynes and P. N. Sarma, *AIChE J.* **19**(5), 1043–1046 (1973).
- ²⁴ N. J. Noordhoek, L. J. van IJzendoorn, B. G. Anderson, F. J. de Gauw, R. A. van Santen, and M. J. A. de Voigt, *Ind. Eng. Chem. Res.* **37**(3), 825–833 (1998).
- ²⁵ J. Kärger, M. Petzold, H. Pfeifer, S. Ernst, and J. Weitkamp, *J. Catal.* **136**, 283–299 (1992).
- ²⁶ C. Rödenbeck, J. Kärger, and K. Hahn, *J. Catal.* **157**, 656–664 (1995).
- ²⁷ C. Rödenbeck, J. Kärger, and K. Hahn, *J. Catal.* **176**, 513–526 (1998).
- ²⁸ F. J. M. M. de Gauw, J. van Grondelle, and R. A. van Santen, *J. Catal.* **204**, 53–63 (2001).
- ²⁹ D. G. Levitt, *Phys. Rev. A* **8**(6), 3050–3054 (1973).
- ³⁰ K. Hahn and J. Kärger, *J. Phys. Chem.* **100**(1), 316–326 (1996).

- ³¹ P. H. Nelson and S. M. Auerbach, *J. Chem. Phys.* **110**(18), 9235–9243 (1999).
- ³² R. M. Barrer, *Zeolites and clay minerals as sorbents and molecular sieves*, Academic Press, London (1978).
- ³³ J. Kärger, *Determination of diffusion coefficients in porous media*, in: *Handbook of heterogeneous catalysis*, G. Ertl, H. Knözinger, and J. Weitkamp, eds., pp. 1253–1261, VCH, Weinheim (1997).
- ³⁴ J. Kärger, S. Vasenkov, and S. M. Auerbach, *Diffusion in zeolites*, in: *Handbook of zeolite catalysts and microporous materials*, S. M. Auerbach, K. A. Carrado, and P. K. Dutta, eds., Marcel Dekker, New York (2002).
- ³⁵ J. M. van de Graaf, *Permeation and separation properties of supported silicalite-1 membranes - A modeling approach*, Ph.D. thesis, Delft University of Technology, Delft, The Netherlands (1999).
- ³⁶ W. Boersma-Klein and J. A. Moulijn, *Chem. Eng. Sci.* **34**(7), 959–969 (1979).
- ³⁷ D. M. Ruthven, *Principles of adsorption and adsorption processes*, John Wiley & Sons, New York (1984).
- ³⁸ W. Zhu, J. M. van de Graaf, L. J. P. van den Broeke, F. Kapteijn, and J. A. Moulijn, *Ind. Eng. Chem. Res.* **37**(5), 1934–1942 (1998).
- ³⁹ B. G. Anderson, N. J. Noordhoek, F. J. M. M. de Gauw, L. J. van IJzendoorn, M. J. A. de Voigt, and R. A. van Santen, *Ind. Eng. Chem. Res.* **37**(3), 815–824 (1998).
- ⁴⁰ N. S. Raghavan and D. M. Ruthven, *Chem. Eng. Sci.* **40**, 699–706 (1985).
- ⁴¹ S. H. Hyun and R. P. Danner, *AIChE J.* **31**(7), 1077–1085 (1985).
- ⁴² D. Shen and L. V. C. Rees, *Zeolites* **11**, 666–671 (1991).
- ⁴³ M. Eic and D. Ruthven, *Zeolites* **8**, 40–45 (1988).
- ⁴⁴ O. P. Keipert and M. Baerns, *Chem. Eng. Sci.* **53**(20), 3623–3634 (1998).
- ⁴⁵ T. A. Nijhuis, L. J. P. van den Broeke, M. J. G. Linders, J. M. van de Graaf, F. Kapteijn, M. Makkee, and J. A. Moulijn, *Chem. Eng. Sci.* **54**(4423–4436) (1999).
- ⁴⁶ L. F. Gladden, J. A. Sousa-Gonçalves, and P. Alexander, *J. Phys. Chem. B* **101**(48), 10121–10127 (1997).
- ⁴⁷ D. J. Schaefer, D. E. Favre, M. Wilhelm, S. J. Weigel, and B. F. Chmelka, *J. Am. Chem. Soc.* **119**(39), 9252–9267 (1997).
- ⁴⁸ D. E. Favre, D. J. Schaefer, S. M. Auerbach, and B. F. Chmelka, *Phys. Rev. Lett.* **81**(26), 5852–5855 (1998).
- ⁴⁹ S. M. Auerbach and H. I. Metiu, *J. Chem. Phys.* **106**(7), 2893–2905 (2000).
- ⁵⁰ P. C. M. M. Magusin, D. Schuring, E. M. van Oers, J. W. de Haan, and R. A. van Santen, *Magn. Reson. Chem.* **37**, S108–S117 (1999).
- ⁵¹ H. Jovic, M. Beé, and G. J. Kearley, *J. Phys. Chem.* **98**, 4660–4665 (1994).
- ⁵² U. Schemmert, J. Kärger, and J. Weitkamp, *Microporous Mesoporous Mater.* **32**, 101–110 (1999).
- ⁵³ Y. S. Lin, N. Yamamoto, Y. Choi, T. Yamaguchi, T. Okubo, and S.-I. Nakao, *Microporous Mesoporous Mater.* **38**, 207–220 (2000).
- ⁵⁴ N. Benes and H. Verweij, *Langmuir* **15**(23), 8292–8299 (1999).
- ⁵⁵ J. Kärger and D. M. Ruthven, *Zeolites* **9**, 267–281 (1989).
- ⁵⁶ B. G. Anderson, A. M. de Jong, and R. A. van Santen, *In situ measurement of heterogeneous catalytic reactor phenomena using positron emission*, in: *In-situ spectroscopy in heterogeneous catalysis*, J. A. Haw, ed., pp. 195–237, Wiley-VCH, Weinheim (2002).

36 Diffusion in Zeolites: Concepts and Techniques

- ⁵⁷ A. V. G. Mangnus, *A detection system for positron emission profiling*, Ph.D. thesis, Eindhoven University of Technology, Eindhoven, The Netherlands (2000).
- ⁵⁸ A. V. G. Mangnus, L. J. van IJzendoorn, J. J. M. de Goeij, R. H. Cunningham, R. A. van Santen, and M. J. A. de Voigt, *Nucl. Instr. and Meth. in Phys. Res. B* **99**, 649–652 (1995).
- ⁵⁹ R. H. Cunningham, A. V. G. Mangnus, J. van Grondelle, and R. A. van Santen, *J. Molec. Catal. A: Chem.* **107**, 153–158 (1996).
- ⁶⁰ R. R. Schumacher, B. G. Anderson, N. J. Noordhoek, F. J. M. M. de Gauw, A. M. de Jong, M. J. A. de Voigt, and R. A. van Santen, *Microporous Mesoporous Mater.* **35–36**, 315–326 (2000).
- ⁶¹ N. J. Noordhoek, D. Schuring, F. J. M. M. de Gauw, B. G. Anderson, A. M. de Jong, M. J. A. de Voigt, and R. A. van Santen, *Ind. Eng. Chem. Res.* **41**(8), 1973–1985 (2002).
- ⁶² N. J. Noordhoek, *Positron emission profiling study of hydrocarbon conversion on zeolites*, Ph.D. thesis, Eindhoven University of Technology, Eindhoven, The Netherlands (2000).
- ⁶³ I. M. Torrens, *Interatomic potentials*, Academic Press, New York (1972).
- ⁶⁴ S. M. Auerbach, F. Jousse, and D. P. Vercauteren, *Dynamics of sorbed molecules in zeolites*, in: *Computer modelling of microporous and mesoporous materials*, C. R. A. Catlow, R. A. van Santen, and B. Smit, eds., Academic Press, London (2002), in press.
- ⁶⁵ M. D. Macedonia and E. J. Maginn, *Mol. Phys.* **96**(9), 1375–1390 (1999).
- ⁶⁶ M. P. Allen and D. J. Tildesley, *Computer simulation of liquids*, Clarendon, Oxford (1987).
- ⁶⁷ P. Demontis and G. B. Suffritti, *Chem. Rev.* **97**(8), 2845–2878 (1997).
- ⁶⁸ F. J. Keil, R. Krishna, and M.-O. Coppens, *Rev. Chem. Eng.* **16**(2), 71–197 (2000).
- ⁶⁹ S. Sundaresan and C. K. Hall, *Chem. Eng. Sci.* **41**(6), 1631–1645 (1986).
- ⁷⁰ J. Segers, *Algorithms for the simulation of surface processes*, Ph.D. thesis, Eindhoven University of Technology, Eindhoven (1999).
- ⁷¹ B. Smit, L. D. J. C. Loyens, and G. L. M. M. Verbist, *Faraday Discuss.* **106**, 93–104 (1997).
- ⁷² R. L. June, A. T. Bell, and D. N. Theodorou, *J. Phys. Chem.* **95**(22), 8866–8878 (1991).
- ⁷³ T. Mosell, G. Schrimpf, and J. Brickmann, *J. Phys. Chem.* **100**(11), 4582–4590 (1996).
- ⁷⁴ T. J. H. Vlugt, C. Dellago, and B. Smit, *J. Chem. Phys.* **113**(19), 8791–8799 (2000).
- ⁷⁵ R. Krishna and J. A. Wesselingh, *Chem. Eng. Sci.* **52**(6), 861–911 (1997).
- ⁷⁶ R. Krishna, *Chem. Phys. Lett.* **355**, 483–489 (2002).
- ⁷⁷ R. Krishna and D. Paschek, *Phys. Chem. Chem. Phys.* **4**, 1891–1898 (2002).

3

Molecular Dynamics of Alkanes in Zeolites

Molecular dynamics simulations are a powerful tool to investigate the diffusion of alkanes in zeolites on a microscopic scale. With this type of simulations, alkane-zeolite interactions are described using forcefields and atomistic models of the zeolite and adsorbents. This technique was used to study the diffusion of linear and branched alkanes in different zeolites. The concentration dependence was investigated, as well as chain-length and temperature dependency.

3.1 Introduction

The diffusive and adsorptive properties of alkanes in zeolite molecular sieves have been the focus of numerous experimental and theoretical studies. Not only are these properties important from a fundamental point of view, but also because zeolites are used in a number of important petroleum refining processes such as hydro-isomerization and catalytic cracking.¹ Furthermore zeolites are increasingly used for separation processes. For all these applications the dynamic behaviour of the molecules inside the zeolite micropores play an essential role in determining its catalytic and separating properties. A thorough understanding of this behaviour will thus aid in the design and efficient operation of catalysts.

Experimentally, a number of different techniques are available for measuring the

[†]Reproduced in part from D. Schuring, A.P.J. Jansen, and R.A. van Santen, "Concentration and Chainlength Dependence of the Diffusivity of Alkanes in Zeolites Studied with MD Simulations", *J. Phys. Chem. B* **104**(5), 941–948 (2000). © 2000 American Chemical Society.

38 Molecular Dynamics of Alkanes in Zeolites

diffusivity in zeolites which can roughly be divided in macroscopic and microscopic methods. Macroscopic methods typically relate the dynamic response of a zeolite sample to small perturbations in the concentration of the sorbate, and measure the Fickian or transport diffusivity. Examples include the zero-length column technique (ZLC),² the frequency response method,³ and, recently, Positron Emission Profiling (PEP).⁴ With microscopic techniques such as pulsed-field gradient NMR (PFG-NMR),⁵ 1D-exchange ¹³C NMR⁶ and quasi-elastic neutron scattering (QENS),⁷ one can directly measure the self-diffusion of the molecules under equilibrium conditions. The results obtained with these microscopic methods (the self-diffusivity) can be directly compared with the Fickian diffusivity obtained from macroscopic techniques by using the “Darken equation”.⁸ Although in some cases results from both these techniques agree reasonably well, often one can find large discrepancies between the results of these different methods. The source of these discrepancies still remains the subject of much debate.

In recent years, molecular simulations have become an increasingly important tool for studying sorbates in zeolites. A number of different methods are available.⁹ Configurational-bias Monte Carlo (CBMC) can be used to effectively compute equilibrium properties and adsorption isotherms for even large alkanes.¹⁰ With molecular dynamics simulations (MD) both equilibrium as well as the dynamical behaviour of a system can be studied. These simulations allow the user to follow the time evolution of a model system over a given length of time, which make them ideally suited to get insight into the microscopic mechanism of the process involved. Drawback of this method however is that they are relatively time-consuming, limiting its applicability to small systems and timescales and thus to systems with relatively small activation energies. In order to overcome these problems and be able to study reaction kinetics as well, Kinetic Monte-Carlo simulations can be used in which diffusion is modelled as a jump from one adsorption site to another.^{11–13}

Most of the molecular dynamics studies up to now have focussed on the simulation of small linear alkanes such as *n*-butane and *n*-hexane in MFI-type zeolites.¹⁴ Runnebaum and Maginn have performed a similar study for alkanes up to *n*-C₂₀.¹⁵ Interestingly, they found that the self-diffusivity along the [010] axis of MFI is a periodic function of chain length, which they ascribed to a resonant diffusion mechanism. Furthermore it is noteworthy that only small variations of the self-diffusion coefficient with chainlength were observed, which seems in contrast with the results found in macroscopic experiments. Studies in other (all-silica) zeolite structures have mostly been limited to methane.

In this chapter molecular dynamics simulations have been used to investigate the diffusion of alkanes ranging from methane to *n*-dodecane in four different zeolites: Silicalite (MFI), Mordenite (MOR), Ferrierite (FER) and ZSM-22 (TON). The choice

of these zeolites make it possible to compare the effects of pore size and topology on the self-diffusion of these sorbates. For *n*-butane, the concentration dependence of the diffusivity and activation energy was studied. Furthermore the chainlength dependency of the diffusion constant was investigated. By performing simulations at higher temperatures, the motion of branched alkanes could be studied as well. In the next sections, the models and simulation methodology will be given, followed by a presentation and discussion of the results obtained in this study. First, a comparison will be made between results obtained in this study and previous experimental and theoretical work. next, the concentration dependence of the diffusivity of *n*-butane in the different systems is discussed. The next section discusses the chainlength dependence of the diffusion constant in zeolites MOR, FER and TON. Finally, the diffusion of branched alkanes is discussed.

3.2 Model and calculations

3.2.1 The zeolite model

In the simulations described in this study four different zeolite structures were used. Zeolite Silicalite is the silicious form of ZSM-5 and has a channel system of two sets of interconnected 10-ring pores (diameter approx. 5.5 Å), forming “zigzag” channels in the [100] direction and “straight” channels in the [010] direction. Silicalite thus exhibits a 3-dimensional pore structure, in which the two channels meet in a relatively open “intersection” region. Zeolite Ferrierite (FER) also has a 3-dimensional pore structure with straight 10-ring channels in the [001] direction, interconnected via cages with 8-ring windows. Mordenite (MOR) has 12-ring channels along the [001] direction which are connected by 8-ring pores in the [010] direction. Previous studies however showed that these 8-ring channels are inaccessible to most alkanes, making it essentially a zeolite with a 1-dimensional pore system. ZSM-22 (TON) also is 1-dimensional with 10-ring pores in the [001] direction. The sizes of the simulation boxes used are shown in table 3.I.

In our work the zeolites are assumed to be purely silicious. Previous studies have shown that even with this assumption a fairly good agreement with experiment (in which acidic zeolites are indeed used) can be achieved¹⁶ and that the silicon-aluminium ratio hardly influences the observed self-diffusion coefficient.¹⁷ The zeolite structures were extracted from the zeolite database available in the MSI Cerius² software package.¹⁸ The zeolite structure was furthermore assumed to be rigid to reduce computational requirements. For small alkanes this assumption has been shown not to have a great influence on the calculated diffusivity,¹⁹ but for bulkier alkanes some effects might occur.

40 Molecular Dynamics of Alkanes in Zeolites

Table 3.I: Simulation box dimensions as used in the simulations. The largest simulation box of Mordenite was used for simulations at low loadings.

Zeolite	Size (no. of unit cells)	Size (Å)
Mordenite	$2 \times 2 \times 4$	$36.2 \times 41.0 \times 30.1$
Mordenite	$2 \times 2 \times 12$	$36.2 \times 41.0 \times 90.3$
ZSM-5	$2 \times 2 \times 4$	$40.1 \times 39.8 \times 53.7$
ZSM-22	$4 \times 3 \times 8$	$55.4 \times 52.3 \times 40.3$
Ferrierite	$2 \times 3 \times 6$	$38.3 \times 42.4 \times 44.9$

Table 3.II: Parameters for the torsion potentials of linear and branched alkanes. A CH_3 group connected to a CH group is denoted by CHb_3 , the letter i is used to indicate either a CH_2 or CH_3 group.

Beads	C_0/k_B [K]	C_1/k_B [K]	C_2/k_B [K]	C_3/k_B [K]
$CH_i-CH_2-CH_2-CH_i$	1009.728	2018.446	136.341	-3164.52
$CH_i-CH_2-CH_2-CH$	1009.728	2018.446	136.341	-3164.52
$CH_i-CH_2-CH-CHb_3$	373.0512	919.0441	268.1541	-1737.216

Table 3.III: Lennard-Jones potential parameters for the interactions between pseudo atoms of alkanes. Parameters for interactions between different types of beads were calculated using the Lorentz-Berthelot rules: $\epsilon_{ij} = \sqrt{\epsilon_i \epsilon_j}$ and $\sigma_{ij} = \frac{1}{2}(\sigma_i + \sigma_j)$.

Beads	ϵ/k_B [K]	σ [Å]
CH_4-CH_4	148	3.73
CH_3-CH_3	98.1	3.77
CH_2-CH_2	47.0	3.93
$CH-CH$	12.0	4.1

Table 3.IV: Lennard-Jones Parameters for the zeolite-alkane interactions.

(Pseudo)atoms	ϵ/k_B [K]	σ [Å]
$O-CH_4$	96.5	3.64
$O-CH_3$	87.5	3.64
$O-CH_2$	54.4	3.64
$O-CH$	58.0	3.64
$O-CHb_3$	80.0	3.64

3.2.2 The alkane model

Following the work of Reykaert and Bellemans²⁰ the alkane molecules are modelled using united atom models, whereby the methyl and methylene groups are treated as single interaction centres. The bond length is kept fixed at 1.54 Å and bond angles between three adjacent atoms were allowed to fluctuate under the influence of a harmonic potential:²¹

$$u_{bb}(\theta_i) = \frac{1}{2} \cdot k_\theta \cdot (\theta_i - \theta_0)^2 \quad (3.1)$$

in which θ_0 is the equilibrium bond angle of 114° and k_θ the force constant, taken equal to 62500 K·rad⁻².²² Torsion is modelled using a four-term cosine expansion in the dihedral angle:²³

$$u_{torsion}(\phi_i) = \sum_{n=0}^3 C_n \cos^n(\phi_i) \quad (3.2)$$

with the parameters C_n given in table 3.II. Note that a different torsion potential is needed when describing branched alkanes. The alkane beads can interact with each other via a Lennard-Jones potential:

$$u_{ij}^{lj} = 4\epsilon_{ij} \left[\left(\frac{\sigma_{ij}}{r_{ij}} \right)^{12} - \left(\frac{\sigma_{ij}}{r_{ij}} \right)^6 \right] \quad (3.3)$$

Intramolecular interactions between beads of the same molecule are only included when they are separated by more than three bonds. These interactions prevent the backbone of the alkane from crossing over itself. The interaction parameters are shown in table 3.III and were taken from Vlucht et al.²⁴ For the intermolecular potentials a cut-off radius of 13 Å was used and the usual tail corrections were applied.²⁵

Zeolite-alkane intermolecular interactions are also modelled using a Lennard-Jones interaction. As is common in these kind of simulations the interactions between the alkane beads and the zeolite silicon atoms are neglected.²⁶ To account for the absence of the silicon atoms, modified oxygen interaction parameters were used. These parameters were obtained from fitting Configurational-Bias Monte Carlo simulations to adsorption data.¹⁰ The parameters used are summarized in table 3.IV. The interactions were truncated at 13.8 Å.

3.2.3 Calculations

The models described above were used in a canonical (NVT) MD simulation. In these simulations a Verlet algorithm²⁵ was used for the integration of the equations of motion, using a timestep of 0.5 fs. The bond lengths were kept fixed using a Shake algorithm.⁹ To maintain a constant temperature, a Nosé-Hoover thermostat²⁷ was

42 Molecular Dynamics of Alkanes in Zeolites

applied with a time constant of 2 ps. Furthermore, periodic boundary conditions were applied. During the simulation, the different contributions to the potential energy and the total energy can be monitored in order to check if the system is equilibrated. From the entire run the average potential energy contributions are calculated.

The self-diffusion coefficient can be calculated using the Einstein relation:

$$D_s = \frac{1}{6} \lim_{t \rightarrow \infty} \frac{d}{dt} \langle |\vec{r}(t) - \vec{r}(0)|^2 \rangle \quad (3.4)$$

in which the term between brackets is the ensemble average of the mean-square displacement (MSD) of the molecules. This mean-square displacement is monitored during the simulation using an order- n algorithm.⁹ According to the previous equation the diffusion coefficient can then be calculated by a linear fit of the MSD versus time. The temperature dependency of the self-diffusion constant is governed by the Arrhenius equation:

$$D_s = D_0 \exp \left[-\frac{E_{act}}{RT} \right] \quad (3.5)$$

in which D_0 is the diffusion constant at infinite temperature, E_{act} the activation energy for diffusion, R the gas constant and T the temperature.

Prior to a simulation run, a predetermined number of molecules were placed inside the zeolite simulation box. In zeolites having one-dimensional pore structures, no exchange of the molecules between different pores takes place. Experimental determination of the diffusivity typically involves the averaging of the movements over a large number of pores, so that fluctuations of the number of molecules inside the channels are averaged out. In the simulations performed in this study however only a fairly limited number (≈ 20) of pores are monitored. In order to still be able to extract reliable information regarding the concentration dependence of the self-diffusion coefficient, care has to be taken that every pore contains an equal amount of molecules.

To ascertain a quick equilibration of the molecules, low-energy starting configurations were generated by using a Monte Carlo simulation previous to the simulation run. After the generation of these low-energy configurations, an MD run of 125 ps was sufficient to equilibrate the system. An additional run of 1 to 5 ns was then conducted in which the mean-square displacement and the equilibrium properties were calculated. The number of molecules inside the simulation boxes varied from 8 to 144 molecules, depending on the concentration which was modelled. In order to get good statistics for the measured diffusivity at low concentration, several simulations at equal loading were performed using different starting configurations and the average results of all simulations were used. In this way it was ensured that an ensemble average of at least 100 molecules was taken, which provided sufficient accuracy.

Table 3.V: Comparison of simulation results in Silicalite with literature values from MD simulations and PFG-NMR measurements.

Molecule	Temp. [K]	MD (lit) [m ² /s]	PFG-NMR [m ² /s]	this work [m ² /s]
methane (2 mol./U.C.)	298	1.26×10^{-8} ²⁸	1.05×10^{-8} ²⁹	1.07×10^{-8}
ethane (4 mol./U.C.)	298	5.9×10^{-9} ³⁰	3.8×10^{-9} ²⁹	2.85×10^{-9}
propane (4 mol./U.C.)	298	1.9×10^{-9} ³⁰	2.8×10^{-9} ²⁹	2.49×10^{-9}
<i>n</i> -butane (4 mol./U.C.)	333	2.93×10^{-9} ³¹	7.0×10^{-10} ¹⁷	1.88×10^{-9}
<i>n</i> -pentane (4 mol./U.C.)	333	–	3.9×10^{-10} ¹⁷	9.85×10^{-10}
<i>n</i> -hexane (4 mol./U.C.)	333	1.42×10^{-9} ³¹	1.2×10^{-10} ¹⁷	1.78×10^{-10}

3.3 Comparison with other studies

In order to check the model used in this study, a number of simulations were conducted using methane, butane, pentane and hexane in all-silica ZSM-5. As there is a fair amount of data on these systems available in literature, a comparison can be made with previous investigations. The results are shown in table 3.V. In this table, both previous theoretical work (MD simulations) and experimental data are shown. For the experimental values only PFG-NMR results were included, as these measurements are supposed to measure the true microscopic diffusion rate. Values from macroscopic techniques are often many orders of magnitude smaller,⁸ but even in the PFG-NMR data differences as big as one order of magnitude can be found.

The diffusion constant for methane, ethane and propane are in excellent agreement with both other simulations^{28, 30, 32} and PFG-NMR measurements.²⁹ The calculated diffusivities of butane and hexane in this study are lower than in previous studies,^{14, 31} due to small differences in the adsorbate-zeolite interaction parameters which results in a somewhat stronger interaction. A comparison with experimental data^{17, 33} shows that the simulations overestimate the diffusivity of butane and pentane. For these two molecules the calculated diffusivity is a factor of two larger than from PFG-NMR measurements, which does not seem significant if one considers the large variations in the experimental data available. For hexane, an excellent agreement is again obtained, in contrast with earlier studies. Clearly, Molecular Dynamics simulations provide a good order-of-magnitude estimate of the diffusivity, even for longer alkanes.

For *n*-butane, the diffusivity was calculated at a number of different temperatures ranging from 298 to 523 K. Using eq. 5, the activation energy was calculated to be 4.2 kJ/mol. This result is in good agreement with the 4.40 kJ/mol obtained from MD simulations of Hernández and Catlow,³¹ but somewhat lower than the value of 6.69

44 Molecular Dynamics of Alkanes in Zeolites

kJ/mol found by Runnebaum and Maginn.¹⁵ The calculated activation energy is also in good agreement with the value of about 5 kJ/mol obtained from QENS by Jobic et al.³⁴ The value found by Datema et al.³³ (8.1 kJ/mol) is significantly higher, but as we will see later this might be due to the high loading of 7 molecules per unit cell at which the activation energy was determined.

Unfortunately, as far as the authors know no PFG-NMR or QENS data exist for alkanes in zeolites Mordenite, Ferrierite, and ZSM-22, so no comparison could be made with experimental results in these systems. No theoretically calculated data was available for comparison as well.

3.4 Diffusion in single-file pore systems

As was already discussed in a previous section, diffusion in a number of different zeolites was studied. Two of the zeolite structures, Mordenite and ZSM-22, contain single-file pores. In these systems, deviations from normal diffusion behaviour, in which the MSD is proportional to time, might be expected.⁸ For a single file of infinite length and for large t the MSD is proportional to the square root of time:³⁵

$$\langle |\vec{r}(t) - \vec{r}(0)|^2 \rangle = 2 \cdot F \cdot \sqrt{t} \quad (3.6)$$

in which F is the single-file mobility. This behaviour is a result of the fact that the molecules cannot pass each other inside the pores. Although the occurrence of this kind of behaviour can be predicted from first principles, the experimental evidence of single-file diffusion is still contradictory and a continuing subject of discussion.³⁵ Molecular dynamics studies of these systems have, as far as the authors know, been rather limited and mostly confined to simple systems.³⁵⁻³⁸

Figure 3.1 shows the mean-square displacement of *n*-butane in zeolite Mordenite at a loading of 1 and 1.5 molecules per unit cell (corresponding to 28.6 and 42.9% of the maximum loading, respectively). Clearly, no single-file diffusion behaviour is observed. Even at maximum pore filling (3.5 molecules/U.C., not shown in fig. 3.1, the MSD is still proportional to t , indicating normal diffusion behaviour. The same observation holds for zeolite ZSM-22. One possible explanation for the absence of single-file diffusion behaviour could be that the model does not accurately represent the physical properties of the system. One of the possibilities could be the assumption of periodic boundary conditions, as the boundaries seem to strongly influence the behaviour of the system.³⁵ However, increasing the simulation box size by a factor of five (and accordingly the number of molecules) did not result in deviations from the results found with the standard simulation box size. Furthermore boundary effects should not be significant if the box size is significantly larger than the average distance travelled by the molecules during the simulations.

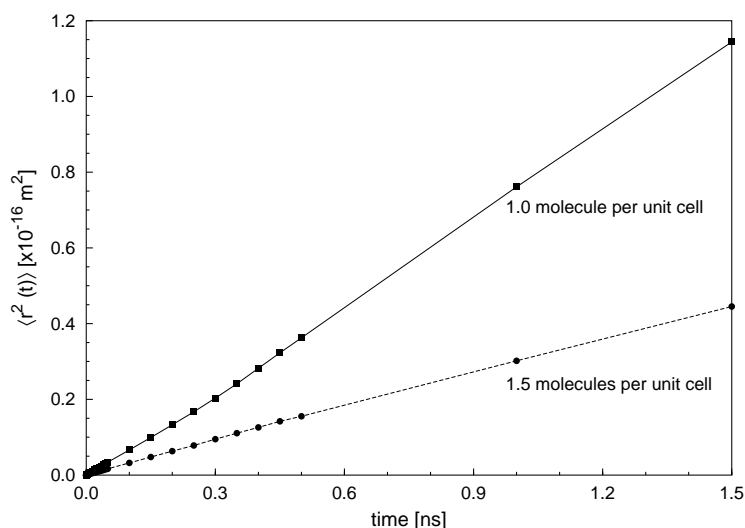


Figure 3.1: Mean-square displacement of *n*-butane in Mordenite at 333 K at a loading of 1.0 and 1.5 molecules per unit cell. The markers indicate the actual time at which the mean-square displacement is evaluated in the simulation, the lines merely serve as a “guide to the eye”. Clearly, no single-file diffusion behaviour is observed.

Another possible explanation for deviations from single-file behaviour might be the possibility that particles can pass each other in the pores.³⁵ This could be checked by monitoring the particle passages during the simulation run. On the timescale of the simulation, no particle passages were detected for *n*-butane, ruling out this possible explanation. Particle passages were indeed observed for methane and ethane in zeolite Mordenite.

As was already stated the \sqrt{t} dependence of the MSD is only valid for the long-time limit. On a short timescale, the molecules essentially behave as isolated particles and the normal diffusion behaviour will be observed. The timescale of the simulations might thus be another explanation for the absence of single-file diffusion. This anomalous diffusion however should play a role when the distance travelled by the molecules exceeds the average distance between the adsorbates. For a loading of 1.5 molecules per unit cell the average distance is approximately 10 Å, while during a simulation run of 1.5 ns they travel approximately 65 Å. For all other simulations, the average distance travelled by the molecules was indeed larger than the average intermolecular distance, showing that the timescale of the simulations should be sufficient to allow for the observation of single-file diffusion.

The normal diffusion behaviour observed during the simulations could thus be caused by the real physical nature of the molecular motion inside the pores. In the types of zeolites studied, diffusion barriers for linear alkanes are rather low. Jousse

et al.³⁹ already pointed out that for these low barriers, the diffusive motion can no longer be modelled as a series of uncorrelated jumps because the transition-state approximation no longer holds. Kramers showed that transition state theory is only valid if $E_b > 5kT$.⁴⁰ This condition ensures that the time the molecules spend on the adsorption sites is much larger than the time to jump from one site to the other, thus allowing for sufficient thermalization. In our case, this condition is clearly not met, as the required activation barrier (at 333 K) equals 13.8 kJ/mol, much higher than the typical barriers of ± 5 kJ/mol in these zeolites. A “hopping-like” diffusion mechanism, in which the particles move as random walkers, therefore might not give an accurate description of this motion. Instead the particles “memorize” their direction of motion when moving from one minimum-energy site to another so that the motion is no longer uncorrelated and close to ballistic. Furthermore the intermolecular interactions are not of a hard-sphere type, and effects such as cluster formation can influence the diffusive behaviour.^{41, 42} A more thorough treatment of the fundamentals of single-file diffusion will be given in chapter 4.

3.5 Concentration dependence of the diffusivity

As is already evident from figure 3.1, the diffusivity strongly depends on the zeolite loading. To study this concentration dependence the diffusion of *n*-butane was simulated in zeolites Mordenite, Silicalite, Ferrierite and ZSM-22 at different loadings. Figure 3.2 shows the calculated self-diffusion coefficients as a function of loading. The concentration is normalized on the maximum pore loading of the different zeolites. The maximum pore loading was determined from experimental data⁴³ (when possible) or grand-canonical CBMC simulations. These values were determined to be 3.5, 9, 3.5 and 1.5 molecules per unit cell for Mordenite, Silicalite, Ferrierite, and ZSM-22, respectively.

At low loadings, the molecules have the highest mobility in zeolite Mordenite, due to the fact that it has large 12-ring pores instead of the smaller 10-ring pores of the other zeolites. Diffusion in silicalite is faster than in Ferrierite and ZSM-22 because of its slightly larger pore diameter and its 3-dimensional pore structure. More remarkable is the differences in mobility in zeolites Ferrierite and ZSM-22. Both zeolites have pores of comparable dimensions, and although FER has a 3-dimensional pore structure, on the timescale of the simulations only 1-dimensional diffusion was observed, as is the case in ZSM-22. However, the presence of the 8-ring windows and cages in FER significantly increases the freedom of movement of the molecules.

For all zeolites, the diffusivity decreases as a function of the loading. This is a result of the more frequent occurrence of molecular collisions between the different molecules at higher concentrations. At sufficiently low loadings, the molecules no

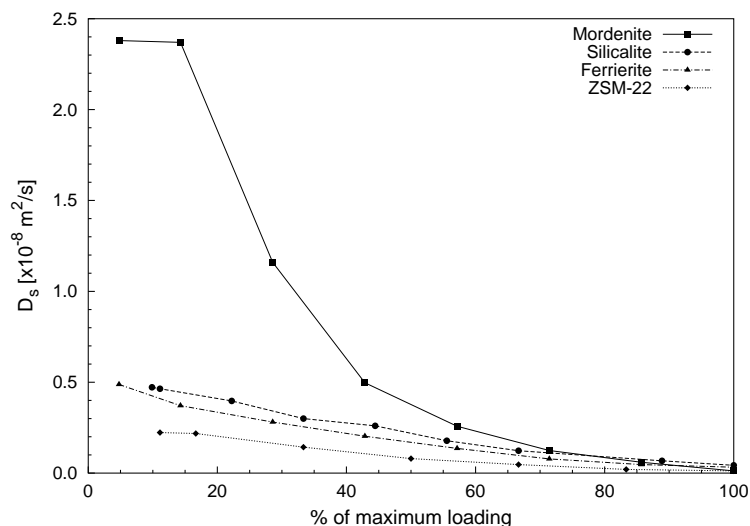


Figure 3.2: Self-diffusion coefficient of *n*-butane as a function of zeolite loading for zeolites Mordenite, Silicalite, Ferrierite and ZSM-22 at 333 K.

longer “feel” each others presence and D_s tends to the limiting value at infinite dilution, as can be clearly seen at loadings below 20 % for zeolites MOR and TON. Diffusion in the large-pore zeolite MOR depends more strongly on the concentration than in other zeolites. Because of these large pores the molecular motions are less restricted by the zeolite structure, making the effect of alkane-alkane interaction more dramatic. Near the maximum loading of the zeolites, the self-diffusion coefficient has the same order of magnitude in all zeolites ($\approx 4 \times 10^{-10} \text{ m}^2\text{s}^{-1}$). This indicates that in this regime the diffusional motion is dominated by the alkane-alkane interaction rather than the zeolite framework. This is further supported by figure 3.3, which shows a comparison of the *n*- and *i*-butane diffusivity as a function of loading. The branched alkane has more interaction with the zeolite structure, resulting in a lower mobility at low loadings. However, at high loadings the diffusivity of *n*- and *i*-butane is again comparable and the structural differences between the molecules do not seem to have a large influence any more.

Figures 3.4, 3.5 and 3.6 show the ensemble averages of the alkane-zeolite, alkane-alkane and torsion potential energy as a function of loading in all four zeolites. The alkane-zeolite interaction is roughly a factor of 10 larger than all other energy contributions. For zeolites Silicalite and ZSM-22 the interaction between the alkanes and the framework does not depend on the loading. The interaction energy in Mordenite and Ferrierite decreases slightly with higher loadings, indicating that the molecules are forced into energetically less favorable conformations. This can also be con-

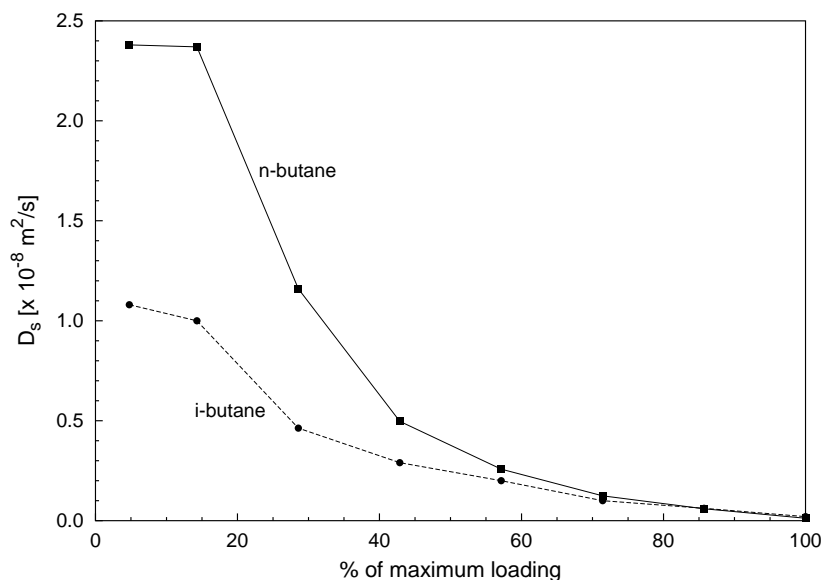


Figure 3.3: Self-diffusion coefficient as a function of zeolite loading for n- and i-butane in Mordenite at 333 K. At high loadings, the mobility of the linear and branched alkane are almost equal.

cluded from the torsional potential energy which also increases with loading in these systems. A strong increase of the alkane-alkane interactions is seen for all zeolites, as can be expected because the molecules are more likely to encounter each other at higher loadings. In the large-pore zeolite MOR, these interactions are the strongest because the molecules can partly reside next to each other in the pore cross-section. In FER and MFI (both 3-dimensional), these interactions are strikingly similar, and seem to linearly depend on the concentration. The bond-bending energy did not show any dependence on the concentrations, and is therefore not shown.

For zeolite Mordenite, the concentration dependence of the activation energy for diffusion was investigated as well. The results are shown in figure 3.7. Diffusion of *n*-butane in Mordenite at low loadings has a rather low activation energy of 4.4 kJ/mol. At higher loadings the activation energy however increases and at 3 molecules per unit cell a value of 9.1 kJ/mol is found, more than twice the value at infinite dilution. This clearly shows that another type of interaction is taking over the molecular motion at higher concentrations than zeolite-alkane interactions. The dominance of alkane-alkane collisions at high loadings cause an enhanced temperature dependency, as the mobility increases at higher temperature and therefore the molecules are less hindered by each others presence.

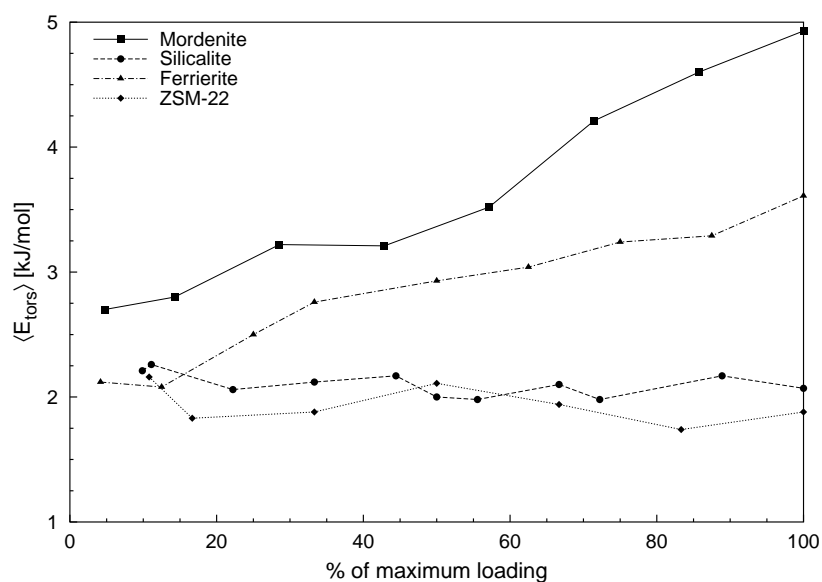


Figure 3.4: Ensemble-averaged torsional potential energy as a function of loading for n-butane in zeolites Mordenite, Silicalite, Ferrierite and ZSM-22 at 333 K.

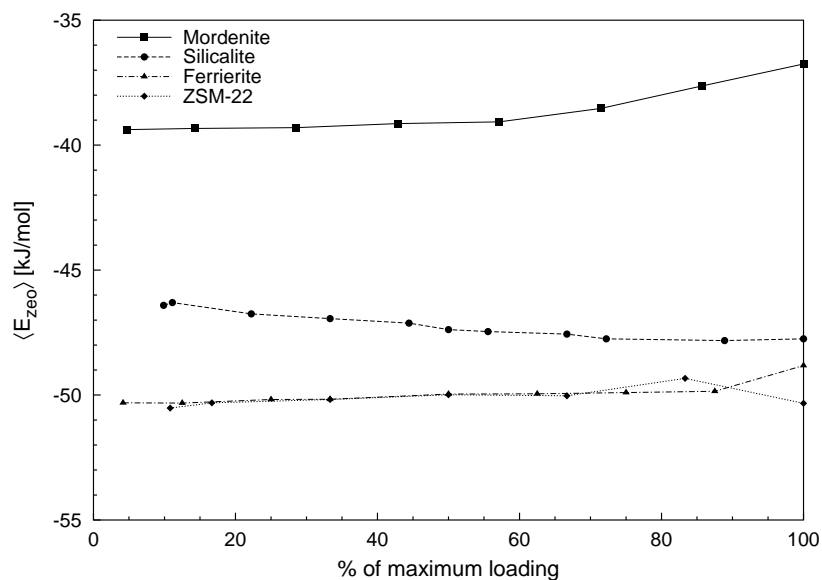


Figure 3.5: Ensemble-averaged alkane-zeolite potential energy of n-butane as a function of loading in different zeolites.

50 Molecular Dynamics of Alkanes in Zeolites

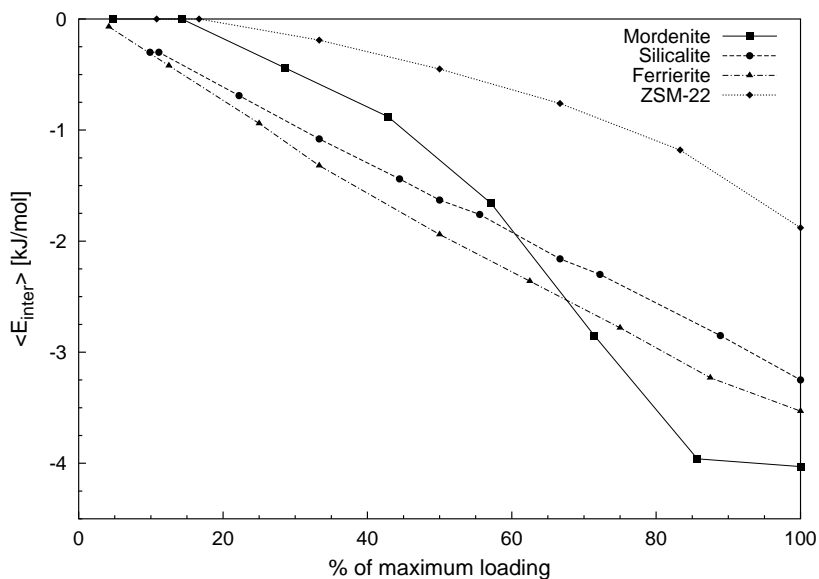


Figure 3.6: Ensemble-averaged alkane-alkane potential energy as a function of loading for n-butane in different zeolites.

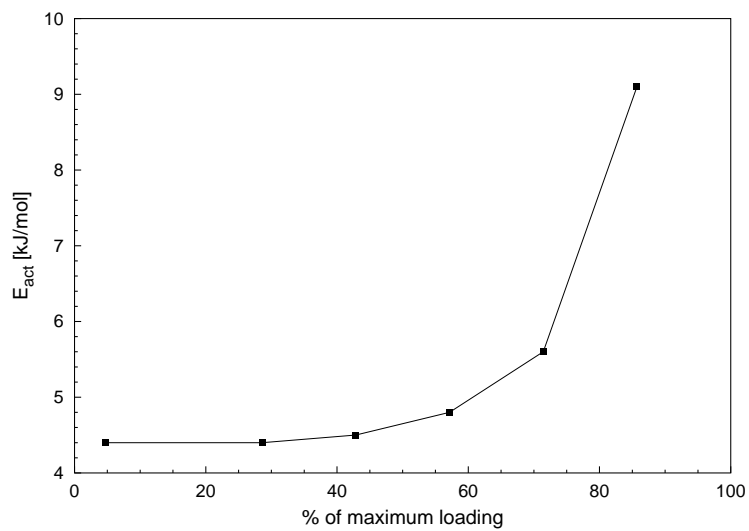


Figure 3.7: Activation energy of diffusion as a function of loading for n-butane in Mordenite. The activation energy strongly increases at higher loadings.

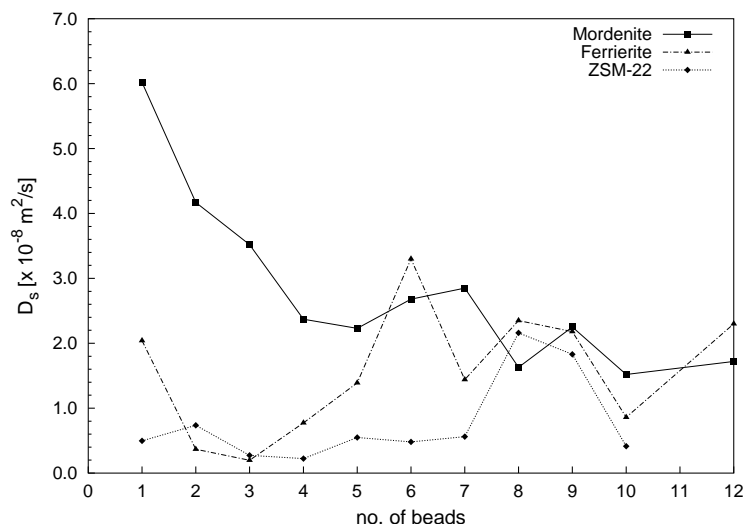


Figure 3.8: Self-diffusivities as a function of chainlength at 333K for zeolites Mordenite, Ferrierite and ZSM-22 at loadings of $\frac{1}{6}$, $\frac{1}{3}$ and $\frac{1}{4}$ molecules per unit cell, respectively. The lines merely serve as a “guide to the eye”.

3.6 Chainlength dependence

The number of carbon atoms in an alkane clearly influences the self-diffusivity of these molecules, as an increased number of atoms results in a larger interaction with the zeolite framework. That this does not necessarily result in a straightforward relationship between chainlength and diffusivity was already demonstrated by Runnebaum et al.¹⁵ for alkanes in Silicalite. The effects encountered in this study were ascribed to resonant diffusion effects, which occurs whenever the length of the diffusing molecule is an integral multiple of the periodicity of the host lattice.

Figure 3.8 shows the chainlength dependence of n -alkanes in zeolites Mordenite, Ferrierite and ZSM-22. The simulations were performed at a loading of $\frac{1}{6}$, $\frac{1}{3}$ and $\frac{1}{4}$ molecules per unit cell, respectively, at a temperature of 333K, with alkanes ranging from methane to n -dodecane. For the small alkanes up to propane, the diffusivity decreases with increasing chainlength in all zeolites. The magnitude of the diffusion constant furthermore reflects the pore sizes of the different zeolites: diffusion is fast for MOR, and much slower as the medium-pore zeolites FER and ZSM-22. For larger chainlengths, this relation however is not necessarily observed any more.

Most remarkable in figure 3.8 are the enhanced diffusivities of hexane in Ferrierite and octane/nonane in ZSM-22. The behaviour of Ferrierite can be partially explained by its topology consisting of 10-ring channels and cages with 8-ring windows. Van Well et al. showed that this topology resulted in a siting which depends

52 Molecular Dynamics of Alkanes in Zeolites

on the alkane chainlength.⁴⁴ The shorter alkanes up to *n*-pentane can easily adsorb into the complete pore system. The fraction of the molecules adsorbed in the cages however decreases with increasing chainlength. Due to the limited volume, *n*-hexane and longer alkanes no longer can reside in the cages, and for these molecules essentially a 1-dimensional network of 10-ring channels remains. Diffusion in these pores is relatively fast compared to the movement from one pore to the other via the cages, as the 8-ring windows result in a high activation energy for this process. These activation barriers are so high that on the timescale of the simulations these events do not occur, and the molecules inside the cages are essentially trapped. For methane up to *n*-pentane, the calculated diffusivity made up of two contributions: the relatively fast diffusion in the 10-ring pores and the slow inter-pore diffusion whereby the molecules pass the 8-ring windows and the cages. The diffusion coefficient merely reflects the fraction of the molecules adsorbed in the cages, resulting in an increased diffusivity for the bulkier alkanes. As *n*-hexane can no longer adsorb in the cages, the diffusivity is only determined by the fast motion in the 10-ring pores.

The enhanced diffusivity of *n*-octane and *n*-nonane in TON might possibly be caused by resonant diffusion. When the end-to-end chainlength of a molecule matches the lattice periodicity, an enhanced mobility might be observed because these molecules are smeared out of the low- and high-energy areas of the zeolite and thus experience a lower activation barrier. An examination of the end-to-end chainlengths reveals values of 8.9 and 10.3 Å, close to twice the lattice periodicity of 5 Å for the 10-ring channels. Resonant diffusion is also expected for *n*-pentane (end-to-end chainlength 5.1 Å), and indeed a small increase of mobility compared to *n*-butane is seen. This effect is however not that dramatic because the smaller molecules behave less “rigid” as the longer ones and are not that tightly aligned in the pores.

Resonant diffusion is also present in Mordenite. For this zeolite, *n*-heptane shows an increased diffusivity. Again, its end-to-end chainlength of 7.8 Å closely matches the channel periodicity of 7.5 Å, but the effects are less dramatic than in the case of the medium-pore zeolites. This might be caused by the fact that the conformations of the molecules are more constrained in the smaller pores than in the relatively large pores of MOR.¹⁶ These constraints force the molecules into straight conformations, making them better candidates for resonant diffusion. Furthermore the constraints in the medium-pore zeolites might explain why the calculated diffusivities for these systems lie close to or are sometimes even larger than in Mordenite.

More evidence for resonant diffusion is found when examining the activation energy of diffusion of the different alkanes. As was already observed by Runnebaum and Maginn,¹⁵ molecules that match the lattice periodicity of the alkane experience lower activation barriers. For *n*-octane in ZSM-22, an activation energy of -0.3 kJ/mol was found, almost equal to zero. This is much lower compared to the values of 4.7

Table 3.VI: Diffusivities (at 333 K) and activation energies of branched alkanes in various zeolites.

Alkane	Zeolite	D_s (333 K) [m ² /s]	E_{act} [kJ/mol]
<i>i</i> -butane	Mordenite	4.6×10^{-9}	4.7
2-methylpentane	Mordenite	3.7×10^{-9}	6.3
<i>i</i> -butane	ZSM-5	1.0×10^{-12}	34
<i>i</i> -butane	ZSM-22	1.6×10^{-12}	28

and 4.3 kJ/mol for *n*-butane and *n*-hexane, respectively. For longer chainlengths, the activation energy increases again (4.0 kJ/mol for *n*-decane). For Mordenite, a similar trend was observed. For *n*-hexane, an activation energy of 2.3 kJ/mol was found, again significantly smaller than the values for *n*-butane (4.4 kJ/mol) and *n*-octane (2.9 kJ/mol).

3.7 Diffusion of branched alkanes

Diffusion of branched alkanes in zeolites is much slower than their linear isomers, as these molecules are much bulkier and fit more tightly in the zeolite channels. As a result of that, activation energies for diffusion are expected to be much higher for these species. In order to still be able to observe sufficient movement of the particles, simulations of these species were conducted at elevated temperatures of 1000 K and higher for the medium-pore zeolites. Care was taken that on average the distance travelled by the molecules was equal to or greater than the length of the zeolite unit cell in the direction of diffusion. For Mordenite, the mobility was sufficient to conduct the simulations at the normal temperature range of 300 to 723 K. In table 3.VI the calculated diffusivities and activation energies are summarized. For comparison, diffusion constants were extrapolated to 333 K by using the determined values for the activation energy and pre-exponential factor. The calculated values for the branched alkanes should however be considered as upper bounds for the “true” values, as the use of a rigid instead of a flexible zeolite lattice significantly affects the diffusional behaviour of the bulky branched alkanes.⁴⁵

In the large-pore zeolite Mordenite, the diffusivity of *i*-butane is only a factor of two lower than for its linear counterpart. Differences in the activation energy are even smaller, 4.7 compared to 4.4 kJ/mol for *n*-butane. For the bulkier 2-methyl-pentane, the differences are larger, and the diffusivity is almost a factor of 10 lower while its activation energy is almost a factor of 3 higher. In the medium-pore zeolites, the differences in mobility of linear and branched alkanes is much larger. Both for ZSM-5

54 Molecular Dynamics of Alkanes in Zeolites

and ZSM-22, the diffusivities of *i*-butane are three orders of magnitude lower than for *n*-butane. The activation energies are in the order of 30 kJ/mol, compared to 4.2 and 4.7 kJ/mole for its linear counterpart in ZSM-5 and ZSM-22, respectively. Clearly, the bulky iso-alkanes fit tightly in the 10-ring channels. The slightly higher activation energy of ZSM-5 can be accounted for by the presence of the rather spacious channel intersections, where the molecules are preferentially sited.

3.8 Conclusions

Molecular dynamics simulations have been used to study the diffusion of a number of different linear and branched alkanes in zeolites Mordenite, Silicalite, Ferrierite and ZSM-22. This simulation technique can give useful insight in the effects of pore topology on the dynamical properties of the adsorbates and provides data which are difficult to obtain from experimental techniques. A comparison with PFG-NMR and QENS data shows that MD simulations provide good estimates for the diffusivity and the activation energy of diffusion. Unfortunately the amount of available data from these experimental techniques is rather limited making a comparison for systems other than Silicalite difficult.

A close examination of the mean-squared displacement revealed that no single-file diffusion behaviour was observed in the 1-dimensional zeolites Mordenite and ZSM-22. Changing the simulation box dimensions and, accordingly, the total number of molecules inside the box, did not influence the results, indicating that boundary effects are not the cause for the absence of single-file diffusion. For *n*-butane, no particle passages were observed during the simulation run, so this possible explanation could also be excluded. Possibly, the low activation barriers for diffusion in these zeolites might be the cause that this behaviour cannot be observed on the timescale of the simulations.

The diffusion constants strongly depend on the zeolite loading. These effects are most dramatic in the large-pore zeolite Mordenite. At high loadings, the diffusivity has the same order of magnitude for all systems, and the alkane-alkane interactions seem to have the largest influence on the alkane mobility. The activation energy was found to increase with zeolite loading. These results indicate that for comparison of experimental and/or theoretical data the adsorbate concentration has to be taken into close consideration.

The chainlength dependence of the diffusivity in different zeolites seems to indicate that a resonant diffusion mechanism occurs in all these systems. Due to its pore topology consisting of 10-ring channels and cages with 8-ring windows, Ferrierite shows a remarkable diffusive behaviour, because the smaller alkanes are trapped inside the cages. The effects of resonant diffusion are much more pronounced in the

medium-pore zeolites, because the molecules in these systems are more rigid and therefore better candidates for the occurrence of this phenomenon. A close examination of the activation energy of different alkanes gives further evidence for resonant diffusion, as these values are found to decrease when the end-to-end chainlength of the molecules matches the lattice periodicity. For all alkanes, the activation barriers are rather low.

By performing simulations at higher temperatures, it is possible to obtain diffusion constants and activation energies for branched alkanes. In Mordenite the differences in mobilities of *i*-butane and 2-methyl-pentane and their linear counterparts are rather small (about one order of magnitude), and activation barriers are still low. In the medium-pore zeolites the molecules fit tightly in the pores, and as a result the mobility is three orders of magnitude lower, and activation energies are in the order of 30 kJ/mole. The presence of channel intersections increases the activation barriers as the molecules are preferentially sited in these rather spacious regions.

3.9 References

- ¹ W. O. Haag, *Catalysis by zeolites - science and technology*, in: *Zeolites and Related Microporous Materials: State of the Art 1994*, J. Weitkamp, H. G. Karge, H. Pfeifer, and W. Hölderich, eds., vol. 84 of *Studies in Surface Science and Catalysis*, pp. 1375–1394, Elsevier, Amsterdam (1994).
- ² J. R. Hufton and D. M. Ruthven, *Ind. Eng. Chem. Res.* **32**, 2379–2386 (1993).
- ³ N. van den Begin, L. V. C. Rees, J. Caro, and M. Bülow, *Zeolites* **9**, 287–292 (1989).
- ⁴ B. G. Anderson, N. J. Noordhoek, F. J. M. M. de Gauw, L. J. van IJendoorn, M. J. A. de Voigt, and R. A. van Santen, *Ind. Eng. Chem. Res.* **37**(3), 815–824 (1998).
- ⁵ W. Heink, J. Kärger, H. Pfeifer, and F. J. Stallmach, *J. Am. Chem. Soc.* **112**, 2175–2178 (1990).
- ⁶ P. C. M. M. Magusin, D. Schuring, E. M. van Oers, J. W. de Haan, and R. A. van Santen, *Magn. Reson. Chem.* **37**, S108–S117 (1999).
- ⁷ H. Jobic, M. Beé, and G. J. Kearley, *J. Phys. Chem.* **98**, 4660–4665 (1994).
- ⁸ J. Kärger and D. M. Ruthven, *Diffusion in zeolites and other microporous solids*, John Wiley & Sons, Inc., New York (1992).
- ⁹ D. Frenkel and B. Smit, *Understanding molecular simulation: from algorithms to applications*, Academic Press, Inc., San Diego (1996).
- ¹⁰ B. Smit and J. I. Siepmann, *J. Phys. Chem.* **98**(34), 8442–8452 (1994).
- ¹¹ D. N. Theodorou and J. Wei, *J. Catal.* **83**, 205–224 (1983).
- ¹² X.-Y. Guo, Z.-W. Liu, and B. Zhong, *Microporous Mesoporous Mater.* **23**, 203–209 (1998).
- ¹³ C. Saravanan and S. M. Auerbach, *J. Chem. Phys.* **107**(19), 8132–8137 (1997).
- ¹⁴ R. L. June, A. T. Bell, and D. N. Theodorou, *J. Phys. Chem.* **96**(3), 1051–1060 (1992).
- ¹⁵ R. C. Runnebaum and E. J. Maginn, *J. Phys. Chem. B* **101**(33), 6394–6408 (1997).

56 Molecular Dynamics of Alkanes in Zeolites

- ¹⁶ S. P. Bates, W. J. M. van Well, R. A. van Santen, and B. Smit, *J. Am. Chem. Soc.* **118**(28), 6753–6759 (1996).
- ¹⁷ W. Heink, J. Kärger, H. Pfeifer, K. P. Datema, and A. K. Nowak, *J. Chem. Soc. Faraday Trans.* **88**(23), 3505–3509 (1992).
- ¹⁸ Molecular Simulations Inc., San Diego, CA, Cerius², version 3.8 (1998).
- ¹⁹ C. R. A. Catlow, C. M. Freeman, B. Vessal, S. M. Tomlinson, and M. Leslie, *J. Chem. Soc., Faraday Trans.* **87**(13), 1947–1950 (1991).
- ²⁰ J.-P. Ryckaert and A. Bellemans, *Faraday Discuss. Chem. Soc.* **66**, 95–106 (1978).
- ²¹ P. van der Ploeg and H. J. C. Berendsen, *J. Chem. Phys.* **76**(6), 3271–3276 (1982).
- ²² J. I. Siepmann, S. Karaborni, and B. Smit, *Nature* **365**, 330–332 (1993).
- ²³ B. Smit, L. D. J. C. Loyens, and G. L. M. M. Verbist, *Faraday Discuss.* **106**, 93–104 (1997).
- ²⁴ T. J. H. Vlugt, R. Krishna, and B. Smit, *J. Phys. Chem. B* **103**(7), 1103–1118 (1999).
- ²⁵ M. P. Allen and D. J. Tildesley, *Computer simulation of liquids*, Clarendon, Oxford (1987).
- ²⁶ A. V. Kiselev, A. A. Lopatkin, and A. A. Shulga, *Zeolites* **5**, 261–267 (1985).
- ²⁷ W. G. Hoover, *Phys. Rev. A* **31**(3), 1695–1697 (1985).
- ²⁸ S. J. Goodbody, K. Watanabe, D. MacGowan, J. P. R. B. Walton, and N. Quirke, *J. Chem. Soc., Faraday Trans.* **87**(13), 1951–1958 (1991).
- ²⁹ M. B. J. Caro, W. Schirmer, J. Kärger, W. Heink, H. Pfeifer, and S. P. Zdanov, *J. Chem. Soc., Faraday Trans. 1* **81**, 2541–2550 (1985).
- ³⁰ D. Dumont and D. Bougeard, *Zeolites* **15**, 650–655 (1995).
- ³¹ E. Hernández and C. R. A. Catlow, *Proc. R. Soc. Lond. A* **448**, 143–160 (1995).
- ³² E. J. Maginn, A. T. Bell, and D. N. Theodorou, *J. Phys. Chem.* **97**(16), 4173–4181 (1993).
- ³³ K. P. Datema, C. J. J. den Ouden, W. D. Ylstra, H. P. C. E. Kuipers, M. F. M. Post, and J. Kärger, *J. Chem. Soc. Faraday Trans.* **87**(12), 1935–1943 (1991).
- ³⁴ H. Jovic, M. Bee, and J. Caro, in: *Proc. 9th Int. Zeolite Conf.*, R. V. Balmoos, J. B. Higgins, and M. M. J. Treacy, eds., Butterworth-Heinemann, Boston (1993).
- ³⁵ K. Hahn and J. Kärger, *J. Phys. Chem. B* **102**(30), 5766–5771 (1998).
- ³⁶ K. Hahn and J. Kärger, *J. Phys. Chem.* **100**(1), 316–326 (1996).
- ³⁷ J. M. D. MacElroy and S.-H. Suh, *J. Chem. Phys.* **106**(20), 8595–8597 (1997).
- ³⁸ D. Keffer, A. V. McCormick, and H. T. Davis, *Mol. Phys.* **87**(2), 367–387 (1996).
- ³⁹ F. Jousse and S. M. Auerbach, *J. Chem. Phys.* **107**(22), 9629–9639 (1997).
- ⁴⁰ R. A. van Santen and J. W. Niemantsverdriet, *Chemical kinetics and catalysis*, Plenum Press, New York, New York (1995).
- ⁴¹ D. S. Sholl and K. A. Fichthorn, *Phys. Rev. Lett.* **79**(19), 3569–3572 (1997).
- ⁴² C. Saravanan and S. M. Auerbach, *J. Chem. Phys.* **110**(22), 11000–11011 (1999).
- ⁴³ W. J. M. van Well, *Adsorption of alkanes in zeolites*, Ph.D. thesis, Eindhoven University of Technology, Eindhoven (1998).
- ⁴⁴ W. J. M. van Well, X. Cottin, B. Smit, J. H. C. van Hooff, and R. A. van Santen, *J. Phys. Chem. B* **102**(20), 3952–3958 (1998).
- ⁴⁵ A. Bouermaouen and A. Bellemans, *J. Chem. Phys.* **108**(5), 2170–2172 (1998).

4

Diffusion in Single-File Systems

When a zeolite contains one-dimensional pores in which molecules are unable to pass each other a special type of diffusion, called single-file diffusion, occurs. One of the characteristic features which can result from this diffusion mode, is that the mean-square displacement of the molecules becomes proportional to the square root of time. Whether or not this characteristic behaviour can be observed, seems to be closely related on the pore geometry. In this chapter, this dependency will be investigated. A simple model of a narrow pore will be used in order to obtain a better understanding of the fundamentals of this single-file diffusion.

4.1 Introduction

When particles or molecules move inside a narrow one-dimensional channel in which they cannot pass each other, a special type of diffusion called single-file diffusion can be observed. Originally, interest in this subject was raised in the field of biophysics, where diffusion through very narrow pores in membranes was studied.¹ In the seventies and early eighties, interest in the subject was raised in the field of mathematical physics, resulting in a number of papers dealing with an analytical description of the behaviour of particles in these systems.²⁻⁴ The systems themselves are treated either as one-dimensional lines or arrays of lattice sites, in which the isolated particles move as random walkers. One of the important conclusions resulting from these papers was that, in the long time limit, the mean-square displacement of the particles in

[†]Reproduced in part from D. Schuring and R.A. van Santen, "Properties of Single-File Systems: What Determines the Typical Single-File Behaviour?", *J. Phys. Chem. B*, submitted for publication.

58 Diffusion in Single-File Systems

these systems would become proportional to the square root of time:

$$\langle z^2(t) \rangle = 2 \cdot F \cdot \sqrt{t} \quad (4.1)$$

in which F is the single-file mobility. This is in contrast with the behaviour of 3-dimensional systems, in which normal “Fickian” diffusion is observed, where this quantity is proportional to t .

More recently, the zeolite community has become interested in the field of single-file diffusion. A substantial number of zeolite structure types contain narrow, unconnected straight channels,⁵ making them excellent candidates for the occurrence of this phenomenon. As this type of diffusion is expected to strongly influence the transport behaviour, and consequently, the catalytic performance, a better understanding of this is not only important from a fundamental, but also from a practical point of view. Both the influence on reaction rates, as well as the long-time behaviour of particles in these systems were consequently studied by Kärger et al.^{6–8} With the advent of techniques such as PFG-NMR and QENS, it furthermore became possible to directly probe the single-file behaviour of molecules on a microscopic scale in these experiments.^{9–13} Discrepancies between different experimental studies¹⁴ recently shifted the interest to possible deviations from the single-file behaviour due to e.g. particle passages,^{15, 16} finite file lengths,^{17–19} or concerted cluster diffusion.^{20, 21}

Although the subject has been studied extensively, a lot of questions still remain about the fundamentals of this process. One of the most important ones to be answered is under what conditions the single-file diffusion behaviour will or will not occur. The criterium that particles cannot pass each other appears to be essential, but does not guarantee that the long-time behaviour of the mean-square displacement is actually observed. A hopping-like mechanism, where the individual particles move as random walkers as was often used as an assumption in early papers dealing with the theory of single-file diffusion, is also not strictly necessary. One thing that has become clear from previous studies, is that the observation of or deviations from the \sqrt{t} behaviour of the mean-square displacement strongly depend on the geometry (channel length, diameter, type of boundary) of the systems under study. In this chapter, this dependence will be the main focus.

To investigate the geometry dependence, it is not necessary to apply a detailed model of a zeolite pore. Instead, a much simpler model is used with a well-defined potential, thereby greatly reducing the computational costs of the simulations. Using these models, the dimensions of the pore and the shape of the pore wall and the particle-wall interaction potentials, the influence can be readily studied. As the interaction between the adsorbates can be easily switched off, the relation between the motion of non-interacting (isolated) particles and interacting particles in a single file system can be investigated as well. This is particularly interesting in view of the

common assumption that the single-file motion can be considered as the product of the motion of the individual particles, and a contribution due to the interaction between the different particles in the system.²² Finally, by varying the pore length for the different systems, the dependence of system size on the diffusive behaviour can be studied.

In this chapter, the different techniques to simulate the motion in narrow pores will be discussed. The special characteristics of these systems will be considered, and used to simplify the simulations and reduce computation time. Next, the results will be presented, starting with diffusion in a cylindrical pore and hard-sphere interactions, after which more complicated systems will be discussed. By comparing the behaviour in these systems, more information can be obtained on the exact mechanism of single-file diffusion. Possible implications for the theoretical understanding of this phenomenon, as well as for the occurrence of this behaviour in one-dimensional, narrow-pore zeolites, will be discussed.

4.2 Methodology

Although the main interest for single-file diffusion in this thesis is focussed on the transport of molecules through zeolites having a one-dimensional pore structure, a detailed description of these systems is not needed to gain insight in its fundamentals. A number of studies have indeed considered a detailed model of the zeolite pore structure (see e.g. Tepper et al.,¹⁵ and Keffer et al.²³), but due to the long-range correlations in these systems (requiring large system sizes), simulations using these models are very time-consuming. Therefore, a much simpler approach was chosen, whereby a system consisting of spherical particles, a cylindrically shaped pore and either hard-sphere or simple Lennard-Jones interactions is considered.

4.2.1 Hard-sphere dynamics

The easiest way to describe interactions in a single-file system is by using hard potentials (i.e. potentials which are discontinuous functions of the distance). Simulations of these type of systems stem from the early days of computational (statistical) physics, as these calculations are relatively easy to implement and at that time could be used to check approximative analytical theories of these systems.²⁴ Nowadays, the study of these type of systems still proves to be useful and are still applied in the field of fluids in confined geometries (see e.g. Suh and MacElroy,²⁵ Mon and Perkus,²⁶ and Henderson²⁷). As a result of the discontinuous character of the interactions, conventional molecular dynamics with continuous time integration cannot be used, as this would lead to infinite forces. Instead, the main task of the simulation algorithm

60 Diffusion in Single-File Systems

is to calculate, in chronological order, the collision times in the system.

A schematic representation of the system is shown in figure 4.1. It consists of a cylindrical tube of length L_{pore} , containing spherical particles with diameter σ_p and mass m . The z coordinate is defined along the pore axis, and in this direction periodic boundary conditions are applied. To simulate the presence of more and less favored regions in the pore, the diameter of the tube is periodically varied. This system will be referred to as a “structured” or “corrugated” tube. As shown in figure 4.1, the pore wall consists of narrow sections with radius R_{in} , and wide sections with radius R_{out} :

$$R_p(z) = \begin{cases} R_{in} & 0 \leq z < \frac{1}{2}\lambda \\ R_{out} & \frac{1}{2}\lambda \leq z < \lambda \end{cases} \quad (4.2)$$

and this “square-well” structure is periodically extended with the length of a single section equal to λ . The radii are measured from the center of the pore to the particle center, and the particles are thus unable to pass each other if the outer pore radius R_{out} is smaller than half the particle diameter. Hard sphere interactions are assumed and all collisions, both between different particles as well as between particles and the pore wall, are assumed to be elastic.

The main task of the simulation algorithm is to calculate the subsequent collisions taking place in the system, and updating the particle velocities accordingly. Particle-particle and particle-wall collisions are all assumed to be totally elastic. In case of a particle-wall collision, the velocity of the particle in a direction perpendicular to the wall is thus reversed. When two particles collide, their velocity components along the line of sphere centers ($\vec{r}_{12} = \vec{r}_2 - \vec{r}_1$) are exchanged. The simulation itself proceeds on a collision-by-collision basis, whereby the time is advanced to the time t_c at which the next collision takes place, after which the collision dynamics is calculated. The fundamental “time unit” in these simulations is thus the number of collisions, in contrast to conventional molecular dynamics in which the time is advanced in fixed steps. For hard-sphere dynamics, the total simulation time (in seconds) will thus depend on the properties of the system under study. Schematically, the simulation algorithm looks like this:

1. Calculate the next collision time t_c .

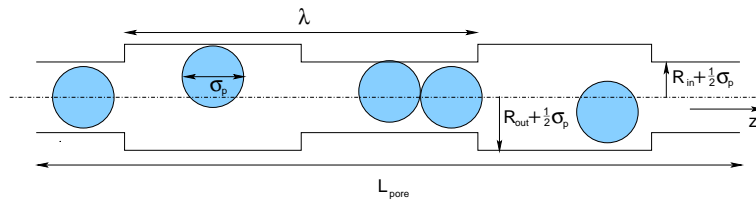


Figure 4.1: Schematic representation of the hard-sphere system used in the simulations.

2. Calculate the positions of the colliding particles at time t_c , and update these positions accordingly.
3. Implement the collision dynamics for these particles and update particle velocities.
4. Update the collision times of the collided particles and their direct neighbours.
5. When the important properties of the system need to be sampled, update all particle positions to the current time, and sample properties.

The scheme shown above is slightly different from a conventional hard-sphere dynamics system. Due to the special character of the system under study, a number of modifications were implemented to reduce computation time. As particles cannot pass each other only collisions with nearest neighbours occur, and consequently only collision times between adjacent particles, and of each particle with the wall have to be calculated. After a collision has occurred, only a limited number of collision times thus have to be updated instead of a complete recalculation of the collision times with all other particles in the system. A further reduction in computation time could be achieved by, after each collision, only updating the particle positions of the particles which have collided, and only updating the positions of all particles when sampling of properties is needed.

In addition to the structure shown in figure 4.1, simulations were also performed using a “sawtooth” structure to investigate the influence of the pore structure on the single-file behaviour. This structure was chosen because the time at which the particles collide with the wall can still be calculated analytically, as numerical evaluation of the collisiontime will be computationally expensive. In this case, for a single period the radius varies according to:

$$R_p(z) = \begin{cases} R_{in} + 2 \cdot \frac{R_{out} - R_{in}}{\lambda} \cdot z & 0 \leq z < \frac{1}{2}\lambda \\ R_{out} - 2 \cdot \frac{R_{out} - R_{in}}{\lambda} \cdot (z - \frac{1}{2}\lambda) & \frac{1}{2}\lambda \leq z < \lambda \end{cases} \quad (4.3)$$

As a result of this structure, a collision with the pore wall leads to a partial transfer of momentum both parallel and perpendicular to the channel axis.

4.2.2 Molecular dynamics with Lennard-Jones type interactions

By using Lennard-Jones type potentials, a system can be simulated that more closely resembles the situation inside the zeolite pore. Furthermore, these kind of simulations represent a much “softer” type of interactions, influencing the single-file behaviour. The small attractive contribution in the interparticle potentials might lead to an increased correlation between the motion of the individual particles. For the

62 Diffusion in Single-File Systems

particle-particle interactions, a shifted Lennard-Jones potential is used:²⁸

$$V_p(r) = \begin{cases} 4\varepsilon_p \left(\left(\frac{\sigma_p}{r} \right)^{12} - \left(\frac{\sigma_p}{r} \right)^6 \right) - c_1(r^2 - r_c^2) - c_2 & \text{for } r < r_c \\ 0 & \text{for } r > r_c \end{cases} \quad (4.4)$$

in which r is the radial distance of the particle center from the channel axis. σ_p can be regarded as the effective diameter of the particles. The constants c_1 and c_2 are chosen in such a way that both the potential and the forces are zero at the cutoff radius r_c . The cutoff radius is chosen to be 13.0 Å, a value commonly used in the simulation of small molecules in zeolites.

In zeolites, the potential energy felt by the particles moving inside the pores is determined by the interaction with many atoms of the surrounding zeolite lattice. Usually, this is described by two-particle Lennard-Jones type potentials. Assuming a pore with a cylindrical symmetry, the resulting potential energy consisting of the integral of all separate interactions is a function of the axial position and the distance from the center of the pore. As the calculation of the previously mentioned potentials is computationally rather expensive, and such a detailed description is not strictly necessary to study single-file behaviour, a much simpler approach is used. For the interactions with the pore wall, an inverse Lennard-Jones potential was used, as applied previously by Hahn et al.²⁸

$$V_t(r_t, z) = \begin{cases} 4\varepsilon_t \left(\left(\frac{r_t}{\sigma_t} \right)^{12} - \left(\frac{r_t}{\sigma_t} \right)^6 \right) + \varepsilon_t & \text{for } r_t > r_c \\ 0 & \text{for } r_t < r_c \end{cases} \quad (4.5)$$

In this equation, the variable r_t equals the distance from the center of the tube. σ_t is the parameter determining the radius of the tube, as at this radial distance the potential strongly increases. As the interactions are calculated between the center-of-mass of the spheres and the center of the tube, the effective diameter of the tube thus equals $2\sigma_t + \sigma_p$. The value of σ_t can be a function of axial coordinate z to mimic a structured pore. As zeolites are periodic structures, the tube radius is assumed to be a periodic function of z :

$$\sigma_t(z) = \sigma_{t,0} + \Delta\sigma_t \sin\left(\frac{2\pi z}{\lambda}\right) \quad (4.6)$$

The parameter λ determines the periodicity of the tube, $\sigma_{t,0}$ the average tube radius, and $\Delta\sigma_t$ the variation in the tube radius.

The simulation are carried out using a conventional leapfrog algorithm²⁹ in the microcanonical ensemble (i.e. at constant energy). For the integration, a step size of 2 ps proved to be sufficiently small in order to achieve a constant total energy of the

Table 4.1: Parameters used for the hard-sphere and Lennard-Jones systems.

Parameter	Value
R_{in}	1.0 Å
λ	14.92 Å
σ_p	3.73 Å
ε_p	148.0 k_B K
ε_t	150.0 k_B K
m	16.0 u

system over the integration time. The special character of the system can again be used to reduce computation time. As the particles cannot pass each other, the order of the particles is conserved, and once a particle falls outside the cutoff radius, all subsequent particles do not have to be considered any more. In this way, the number of particle-particle interactions to be calculated is greatly reduced.

4.2.3 Computational procedure

At the start of each simulation run, the particles are either placed randomly inside the pore, and given random velocities according to a Maxwell-Boltzmann distribution, or the final configuration from a previous simulation is used as input. The loading of the pore is defined as

$$\theta = \frac{N\sigma_p}{L_{pore}} \quad (4.7)$$

in which N is the number of particles in the system, σ_p the diameter of the particles, and L_{pore} the length of the pore. It should be remarked that in fact this occupancy in principle is only correct when dealing with a one-dimensional pore ($R_{in} = R_{out} = 0$), but the real occupancy would be a complex function of the pore shape, dimensions, interaction potentials, and this definition proved to be useful in previous studies.²⁸

The simulations are carried out either by using the hard sphere dynamics or the molecular dynamics algorithm, depending on the type of potentials used. The relevant parameters used in the simulations are summarized in table 4.I. Values for the particle dimensions, mass and interaction parameters were chosen as to reflect the diffusion of methane in a zeolite pore.³⁰ At the start of the simulation, the particles are either placed randomly inside the pore and assigned random velocities according to a Maxwell-Boltzmann distribution at the desired temperature, or the starting configuration is used from a previous simulation. Before recording data, the system is allowed to equilibrate for a certain amount of time. The total momentum of the particles is set to zero. In case of a molecular dynamics simulation, the velocities of the

64 Diffusion in Single-File Systems

particles are rescaled a number of times to reflect the desired temperature (because part of the kinetic energy is transferred to potential energy in the system), after which an additional equilibration run is performed. Because the kinetic energy in a hard-sphere simulation is conserved, in these simulations the temperature automatically remains constant. During the production phase, the positions and velocities of the particles are stored at fixed time intervals, so that multiple time origins can be used to calculate the displacement and velocity autocorrelation function, reducing the statistical errors in these quantities.³¹ Using these multiple time origins, the mean-square displacement at time τ is calculated via:

$$\langle \bar{r}^2(\tau) \rangle = \frac{1}{N \cdot n_0^\tau} \sum_{i=1}^N \sum_{j=1}^{n_0^\tau} \left(\bar{r}^i(t_j + \tau) - \bar{r}^i(t_j) \right) \quad (4.8)$$

in which n_0^τ is the total number of time origins that can be used to calculate the displacement over time interval τ , and \bar{r}^i is the position of particle i . Usually, only the axial (z) coordinate is recorded as this is the most interesting property. The velocity autocorrelation function can be calculated using:

$$\psi_z(\tau) = \frac{1}{N \cdot n_0^\tau} \sum_{i=1}^N \sum_{j=1}^{n_0^\tau} \left(v_z^i(t_j + \tau) \cdot v_z^i(t_j) \right) \quad (4.9)$$

in which v_z^i is the z -component of the velocity of particle i . For the calculation of the density distribution function in the axial direction, only a segment of the pore of length λ equal to the period of the structure is considered, and distribution function is thus the average distribution over all the identical segments in the tube.

4.3 Diffusion inside an unstructured tube

4.3.1 The mean-square displacement

The simplest possible system that can be regarded as a candidate for single-file diffusion is a cylindrical pore with an unstructured tube wall (i.e. $R_{out} = R_{in}$). In order to ensure that no particle passages take place, the pore radius is chosen to be smaller than half the particle diameter σ . Inside the tube, the particles interact with each other and the wall via hard-sphere interactions. To ensure that the periodic boundaries do not influence the results, a large system was used ($N = 10000$). The loading was set to $\theta = 0.1$. The resulting mean-square displacements in the axial direction from the simulations for different pore diameters are shown in figure 4.2. As is clear from this figure, after an initial regime in which the particles move ballistically because the particles do not interact with each other, the displacement is proportional to t , just as

can be observed in ordinary systems. Increasing the loading inside the pores (thereby increasing the number of collisions in the pore) leads to the same conclusions: the displacement remains proportional to t . Deviations from this behaviour only occur at large timescales, but this is due to the periodic boundaries, as will be discussed later.

Clearly, the condition that particles cannot pass each other in the channel is not sufficient to ensure that the \sqrt{t} behaviour in the long-time limit is visible. This can be understood by looking at the way the particles interact with the pore wall. When particles collide with an unstructured wall, the forces exerted on them is always perpendicular to the channel axis. In essence, the motion in the axial direction is thus only influenced by collisions between different particles, just as in the case of diffusion in unrestricted systems, and the usual Fickian type of diffusion behaviour is observed. This is in accordance with earlier studies of the diffusion of hard rods in a one-dimensional system.³² The inability of the particles to pass each other does however result in a decreased overall mobility, but as long as the pore diameter is small enough to not permit these passages, the motion is independent of this parameter. That this is indeed the case is illustrated in figure 4.2, showing identical displacements (within the accuracy of the calculations) in systems with different pore radii.

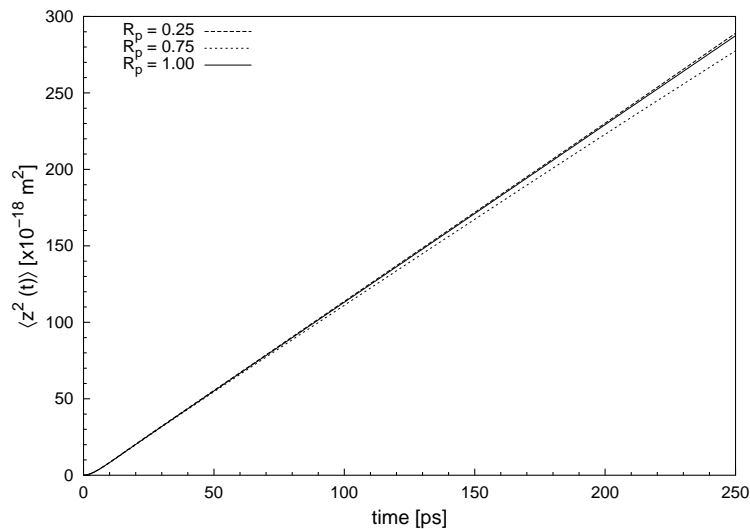


Figure 4.2: Mean-square displacement in the axial direction in an unstructured tube for different tube radii at a loading of $\theta = 0.1$.

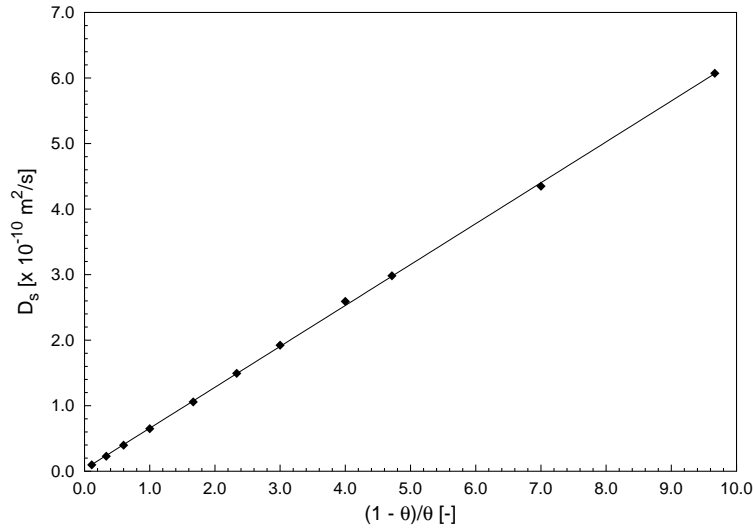


Figure 4.3: Loading dependence of the self-diffusion constant in an unstructured tube.

4.3.2 Concentration dependence

In a single-file system, the motion of the particles is strongly restricted by their neighbours, as there is no way to pass these particles. As a result, a decreased mobility and a stronger influence of the diffusivity on the pore loading should be expected than is the case in a system where the particle order can change. While the diffusion coefficient is proportional to $(1 - \theta)$ with a slightly stronger dependence for systems with lower connectivity,³³ previous studies have indicated that in the case of a single-file system the mobility (see eq. 4.1) is proportional to $(1 - \theta)/\theta$.^{3, 22} That this is indeed true for the simple system currently under investigation is shown in figure 4.3, in which the calculated self-diffusion coefficient is plotted against this quantity. Obviously, this concentration dependence is the most characteristic feature of a single-file system, while for the observation of the \sqrt{t} dependence additional conditions are required.

4.3.3 Influence of boundary conditions

As was already mentioned in paragraph 4.3.1, after a certain amount of time deviations occur from the linear dependency on time of the displacement. These deviations result from the finite size of the system, as is demonstrated in figure 4.4. In this figure, the calculated displacements are plotted using various numbers of particles, keeping the loading inside the pore (eq. 4.7) constant. After a regime in which the displacement is proportional to time and all systems behave identically, deviations

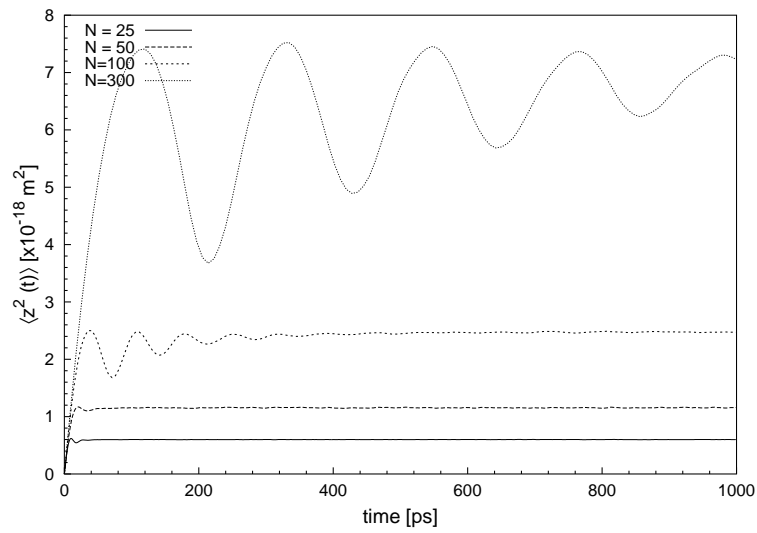


Figure 4.4: Mean-square displacement for different system sizes N at a constant loading of $\theta = 0.5$.

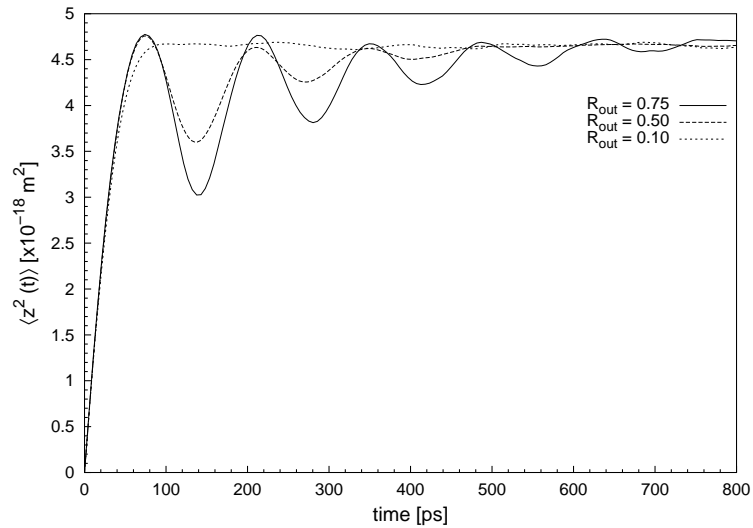


Figure 4.5: Mean-square displacement for a fixed number of particles ($N = 200$) and a fixed loading ($\theta = 0.5$) for different values of the pore radius.

from the normal diffusive behaviour start to occur until finally a limiting value for $\langle z^2 \rangle$ is reached. This can be understood by realizing that the amount of space the particles can travel is limited by the presence of its neighbours. In order to be able to travel in a certain direction, it is necessary that all the neighbouring particles shift as well. As the total momentum in the system is initially zero and is conserved, the center-of mass remains at the same position, and after a certain amount of time the optimum particle and velocity distribution is reached and a maximum is observed in the displacement. Due to the fact that the amount of available space at constant loading over which the particles can redistribute is proportional to the length of the pore, this maximum value also linearly depends on the system size N .²⁸

A remarkable feature in figure 4.4 is the oscillations visible in the displacement once deviations from the normal diffusive behaviour occur, especially visible for the larger systems. The period of these oscillations depends linearly on the system size N . When the pore radius is decreased, as shown in figure 4.5, the amplitude of the oscillations also decreases, until, in the case of a one-dimensional pore ($R = 0$), they completely disappear. This shows that the phenomenon is related to the occurrence of non-central collisions (i.e. collisions for which the collision vector $\vec{r}_{12} = \vec{r}_1 - \vec{r}_2$ is not parallel to the channel axis). When a non-central collision occurs, only part of the linear momentum in the axial direction is transferred from one particle to the other instead of the complete exchange of linear momentum in the extreme one-dimensional case. As a result, there is an increased chance that the particles are collectively moving in a certain direction. Only at longer timescales these correlations have decayed and the system essentially shows a behaviour as if it was one-dimensional. It is however surprising that the maximum displacement in the long-time limit is identical to this one-dimensional case, as a larger pore diameter leaves more space for the particles to rearrange.

4.4 Diffusion in a structured tube

As was obvious from the previous section, having a pore in which particles cannot pass each other is not sufficient to observe the \sqrt{t} behaviour as is often identified with single-file systems. In real-life systems the pore wall usually has some kind of structure and is divided in regions where adsorption is favorable and regions where the particles do not like to reside. When colliding with such a pore wall, part of the linear momentum of the particle is transferred to this (static) wall, resulting in the randomization of the velocity of the particles, essentially making them behave like random walkers. To further investigate the behaviour of these systems, simulations were performed using a structured pore as was described in section 4.2.1.

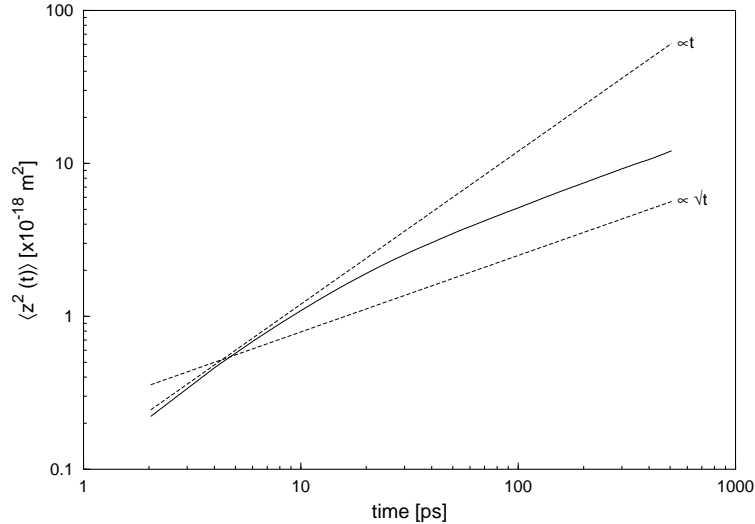


Figure 4.6: Log-log plot of the mean-square displacement of particles inside a structured tube with $R_{in} = 1.0 \text{ \AA}$, $R_{out} = 1.05 \text{ \AA}$, and $\lambda = 14.92 \text{ \AA}$. The dotted lines show a displacement proportional to t and \sqrt{t} , respectively.

4.4.1 The mean-square displacement in a structured tube

To compare the behaviour of a system with an unstructured and a structured tube, a system was simulated with identical parameters and conditions as the system in section 4.3.1, but now the outer pore diameter is not taken identical to R_{in} , but 5 % larger than the inner diameter. For λ , the periodicity of the pore structure, a value equal to four times the particle diameter is chosen. The calculated mean-square displacement is shown in figure 4.6. The behaviour in this system clearly is completely different from that of an unstructured tube. In this case, the typical \sqrt{t} dependence of the displacement is indeed observed. Obviously, the presence of this pore structure somehow ensures the occurrence of this behaviour.

When looking at the literature, the derivations of the long-time behaviour of the displacement in one-dimensional channels are based on the assumption that the isolated particles move like random walkers. At first sight, one would thus suspect that collisions with the wall in case of a structured tube lead to a randomization of the motion of the individual particles. That this is not exactly the case is illustrated in figure 4.7, showing the mean-square displacement of the non-interacting particles (i.e. the particle-particle interactions are shut off, they only collide with the wall) in the same system as was used in figure 4.6. When the particles would act like random walkers, this quantity should be proportional to t . Instead, the proportionality lies somewhere between that of ballistically moving particles and random walkers,

70 Diffusion in Single-File Systems

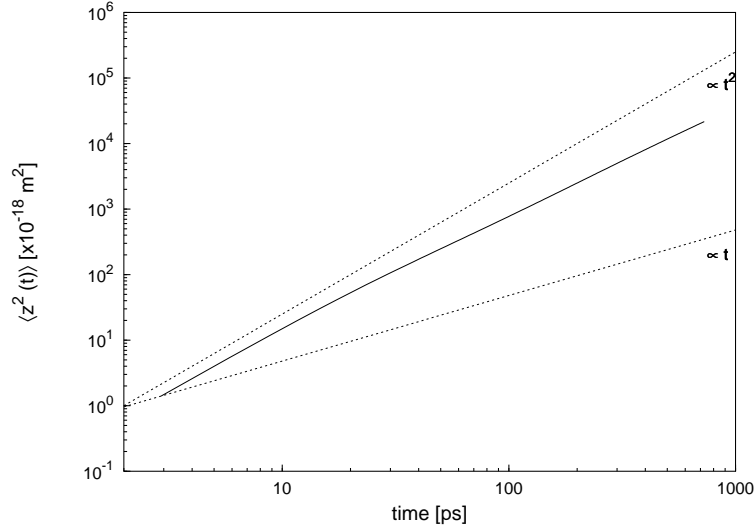


Figure 4.7: Mean-square displacement of particles inside a structured tube when particle-particle interactions are shut off. The same pore dimensions are used as in fig. 4.6.

with a displacement proportional to $t^{1.6}$ at the timescale in which for the interacting system the displacement is already proportional to \sqrt{t} . The isolated particles in the system thus do not necessarily have to move as random walkers in order to observe this behaviour, although a certain amount of randomization is present. What appears to be essential is the ability of particles to transfer (part of) their linear momentum in the direction of motion to the pore wall.

The current findings seem to be in contrast with the ones of Hahn and Kärger,²² who deduced a relation between the displacement of particles in a single-file system and the motion of the isolated particles (i.e. no particle-particle interactions take place) in the system. The derivation is based on the assumption that, when pointlike particles interact in the interior of a box, and one can only measure the velocities and times, one cannot distinguish systems with interacting and non-interacting particles. Consequently, the spatial distribution for these systems is identical. For finite particle sizes, only a small modification has to be made as the interaction takes place when the centers-of-mass are still separated by a distance $2 \cdot R_p$. Using this assumption, they deduced that the displacement can be calculated using the following relation:

$$\langle z^2(t) \rangle = \frac{1 - \theta}{\theta} \sigma \langle |s(t)| \rangle \quad (4.10)$$

in which $\langle |s(t)| \rangle$ is the average of the absolute value of the distance travelled by a non-interacting particle in the system. Clearly, this equation does not predict the \sqrt{t} behaviour in the present system. A similar observation was made in a subsequent

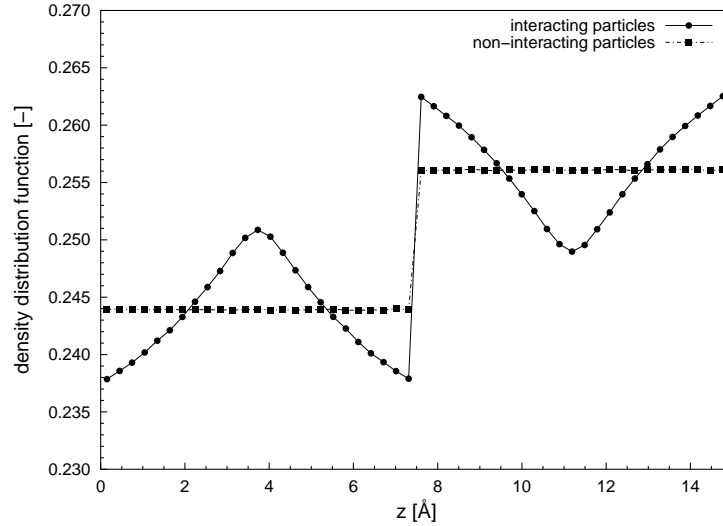


Figure 4.8: A comparison of the density distribution as a function of the axial coordinate z for a system with and without particle-particle interactions using $R_{in} = 1.0$, $R_{out} = 1.05$, and $\lambda = 14.92$ Å.

article published by Hahn and Kärger²⁸ for the diffusion of spheres in a single-file tube structured by a periodic potential. They attribute this to the coupling between the longitudinal and transverse degrees of freedom of the particles in the case of a structured tube, resulting in a particle velocity that only quasiperiodically varies with time. In the derivation of eq. 4.10, these effects are not accounted for as a truly one-dimensional system is used. That the single-file behaviour is still observed in these system can, according to these authors, be attributed to the random disturbance of the interactions with the tube by particle-particle interactions at random positions. In the present system, these particle-particle collisions and collisions with the tube wall are completely separated, and the latter interactions only result in the reversal of the velocity in either the longitudinal or transverse direction. In this case, the interactions with the wall thus do not lead to a coupling between the degrees of freedom in the transverse and longitudinal direction. Still, the occurrence of these collisions is sufficient to observe the single-file behaviour in a system with interacting particles.

The present simulations clearly show that it is only the combined effect of both particle-particle and particle-pore wall interactions that determines the dependence of the mean-square displacement on time. When interacting particles move in an unstructured tube, particle-particle collisions cause them to behave like random walkers with a mean-square displacement proportional to t . The additional ability of the particles to transfer linear momentum in the axial direction to (or from) the pore wall ensures that single-file behaviour occurs, although these collisions themselves do not

72 Diffusion in Single-File Systems

result in a complete randomization of the velocity of the individual particles.

The reason that eq. 4.10 breaks down in the present case is that, in the case of a three-dimensional system, one is able to distinguish between a system with and without interactions. This is illustrated in figure 4.8, which shows the density distribution function over a single segment of the tube (equal to 14.92 \AA) for a system similar as the one used in figure 4.6 with both interacting and non-interacting particles. In the case that the particles do not interact with each other, a higher probability is observed for the particles to be in the broad sections, due to the higher volume available in this region. Once the interaction between the particles is switched on, a completely different distribution occurs with an increased probability to find a particle near the edges in the broader sections while it is decreased near the edges of the smaller section. The increased chance of finding particles in the broad part of the pore in case of non-interacting particles results in a decreased available volume in the narrow section of the pore, and thus a lower number of particles near the edges. As the particles are unable to pass each other, the chance of finding the particles in the middle of the narrow sections is increased. In this case, particle-particle interactions thus indeed have an influence on the density distribution, and the assumptions used to derive eq. 4.10 no longer hold. For the unstructured tube, these effects are not visible on the density, and indeed for these systems the above equation holds perfectly.

4.4.2 Dependence on outer pore diameter

As was shown in the previous section a structured pore wall leads to the typical long-time behaviour of the mean-square displacement in a single-file system. The timescale at which this behaviour is observed is related to the randomization of the velocity of the particles, and will thus depend on the shape and height of the structure of the pore wall. To investigate this, simulations were performed with an identical system as in the previous section, but now with varying values for the outer pore radius (R_{out}). Figure 4.9 shows the resulting displacements in a log-log plot. For all values of R_{out} , a transition from the initial ballistic regime ($\langle z^2 \rangle \propto t^2$) to the \sqrt{t} behaviour is observed. With increasing width of the broad sections of the tube, the timescale at which the long-time single-file behaviour is observed decreases.

For large values of R_{out} , the number of collisions with the sections of the wall perpendicular to the channel axis (the side walls), leading to a transfer of linear momentum to the pore wall, is relatively high, and randomization of the particle velocities is fast. As a result, the transition time to single-file behaviour is short. The collisions with the side pockets furthermore decrease the mobility of the particles, as each collision reverses the direction in which the particles are moving, increasing the chance that particles are moving back and forth within a certain part of the tube.

While for large values of R_{out} there is a continuous transition from the ballistic to

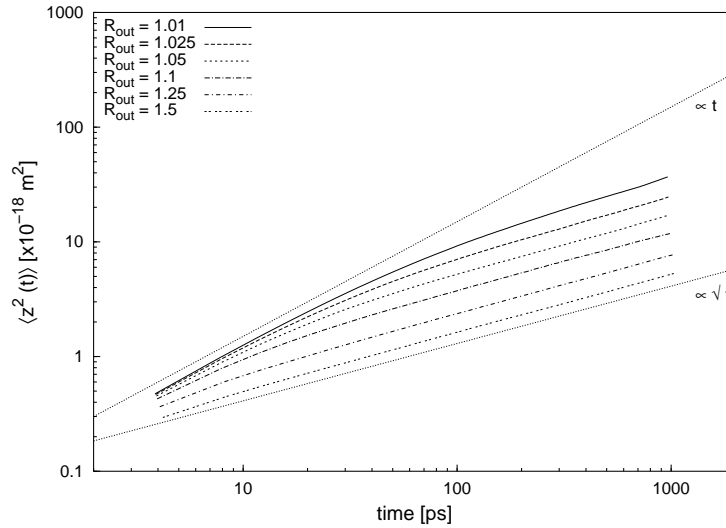


Figure 4.9: Log-log plot of the displacements for various values of the outer diameter, keeping the inner diameter of the tube fixed. The two lines show curves proportional to t and \sqrt{t} , respectively.

the single-file regime, for small values a distinct region is visible in which the displacement is proportional to t . In this case, the system obviously behaves identically as the unstructured tube. This is because the number of collisions with the side wall are so infrequent, that the diffusive behaviour in this region is entirely determined by particle-particle collisions and the randomization of the z -velocity takes place at a much larger timescale. For small differences in pore diameter between the narrow and broad sections (or in real-life systems for small activation barriers) the system on a certain timescale thus behaves as if ordinary diffusion takes place.

In figure 4.10, the transition time after which the single-file diffusion behaviour is observed, is plotted against the ratio between inner and outer pore radius for two different loadings. This transition time t_c is defined as the time at which the displacement reaches its \sqrt{t} behaviour. Initially, this transition time strongly decreases with increasing ratio R_{out}/R_{in} . At a ratio of 1, the transition time logically reaches an asymptotic value, as for an unstructured tube the single-file behaviour is not observed. For large ratios the transition time shows only a moderate dependency. In this case, the number of collisions with the side walls is already sufficiently large, and the degree of randomization of the velocity is mostly determined by particle-particle collisions.

That the interactions between the particles indeed play an important role in the crossover to single-file diffusion can be seen when comparing the curves at different

74 Diffusion in Single-File Systems

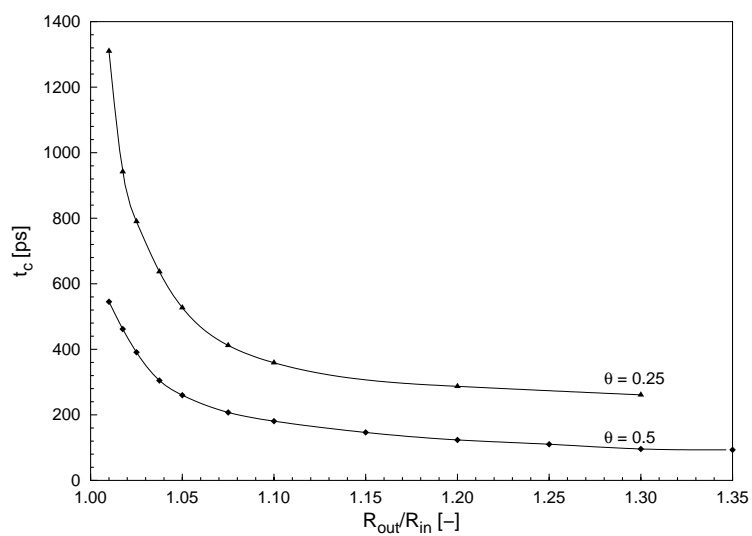


Figure 4.10: Time at which the long-time behaviour ($\propto \sqrt{t}$) of the displacement is reached plotted against the outer pore diameter with fixed $R_{in} = 1.0 \text{ \AA}$ for two different loadings.

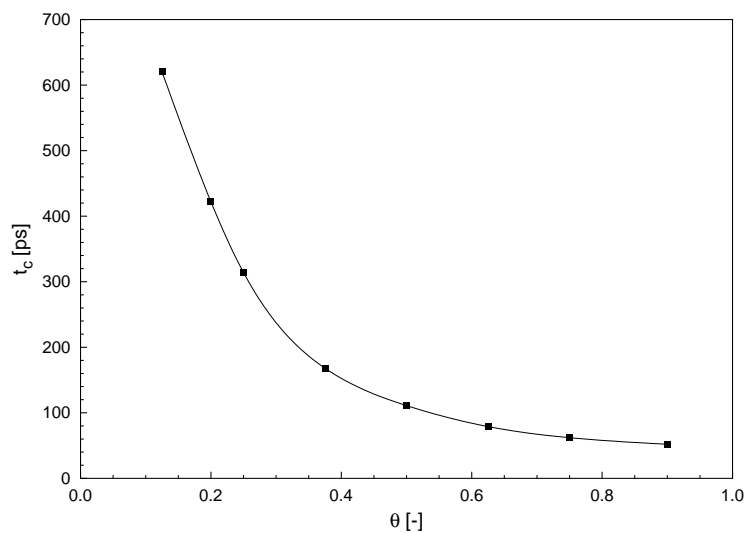


Figure 4.11: Transition time as a function of loading for a single-file pore for fixed $R_{out} = 1.25 \text{ \AA}$.

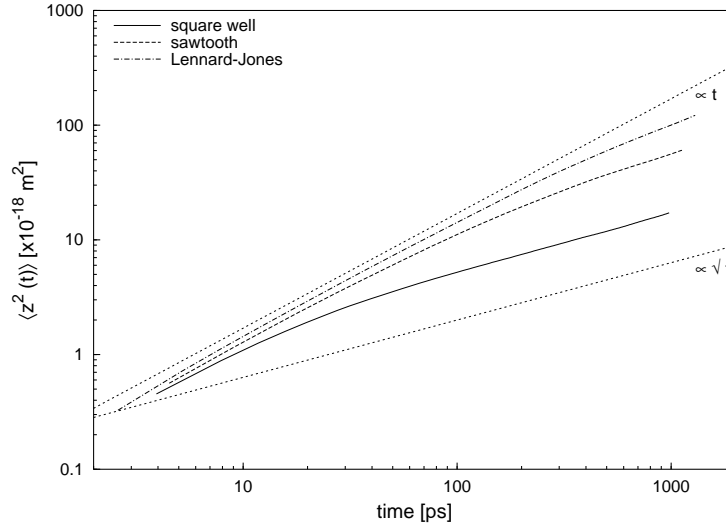


Figure 4.12: Comparison of the displacement in a square-well structure, a sawtooth structure, and a system with Lennard-Jones interactions. The pore and particle dimensions and loading were taken equal for all systems, for R_{out} a value of 1.05 \AA was used.

loadings in figure 4.10. This loading dependence is further investigated in figure 4.11, showing the transition time as a function of θ for fixed values of R_{in} and R_{out} . With increasing loading, the time at which the single-file behaviour occurs shifts downwards due to the increased number of collisions between the particles. The strong dependence on the loading indicate the vital importance of particle-particle collisions in this process.

4.4.3 Changing the pore geometry and interactions

The hard-sphere system with a “square-well” pore structure as studied previously represents an extreme case for studying single-file behaviour in a structured tube. In comparison, a zeolite pore has a much smoother structure as the pore used in the previous section. As the transition time from ballistic to single-file behaviour was shown to be a strong function of the size of the pore structure and the ability of the particles to transfer linear momentum (in the axial direction) to the pore wall, one could expect that the shape of the pore wall itself would also strongly influence this quantity. To investigate this, simulations were also performed with the “sawtooth” structure as described in section 4.2.1, and a system with Lennard-Jones interactions as described in section 4.2.2. In these systems, interactions with the pore wall lead to a transfer of linear momentum in both the transverse and longitudinal direction.

In order to be able to compare the different systems, for all systems the same

76 Diffusion in Single-File Systems

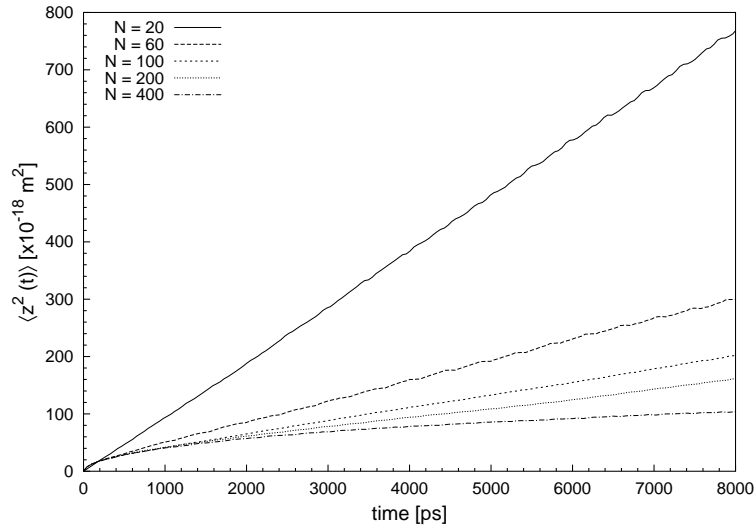


Figure 4.13: Mean-square displacement for particles inside a structured tube for different numbers of particles, keeping the loading constant at $\theta = 0.25$.

inner and outer pore radius, particle sizes, mass, and pore loading were chosen. The resulting mean-square displacements are shown in figure 4.12 for the square-well structure, as well as the sawtooth structure and the system with Lennard-Jones interactions. Compared to the square-well structure the mobility of the particles in both other systems is increased, because interactions with the wall now only lead to a partial deflection of the particle trajectory instead of a complete reversal of the velocity in the axial direction. The time it takes for the displacement to become proportional to \sqrt{t} is much longer in case of the “smoother” pore structures. Although for all structures the decay of the velocity autocorrelation function is fast, the complete reversal of the velocity in the z direction in the case of a collision with a side wall of the square-well structure contributes to a much faster onset of the single-file behaviour. For the other structures, there is even a distinct region in which the displacement is proportional to t , and where the diffusive behaviour is dominated by the particle-particle interactions only.

4.4.4 Finite size effects in a structured tube

As was mentioned previously, the presence of a structured pore wall enables the transfer of momentum in the axial direction to and from this wall. As a result, the total momentum of the particles need not be conserved, and a different kind of behaviour can be expected than was discussed in section 4.3. In figure 4.13, the mean-square displacement is plotted for different particle numbers at a fixed loading of $\theta = 0.25$.

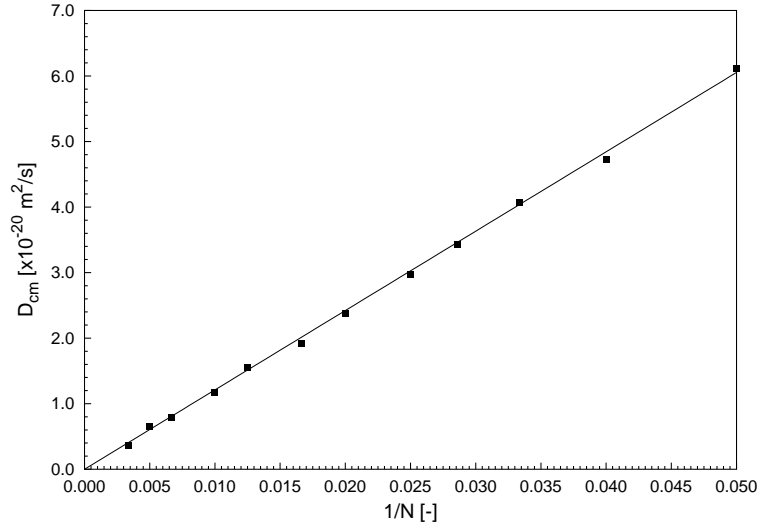


Figure 4.14: Self-diffusion constant in the long-time limit for finite-size systems plotted against the inverse of the file length L_{pore} . The loading inside the system was taken identical for all file lengths.

For large particle numbers, the normal time dependence of a single-file system is observed. However, with decreasing particle numbers, deviations from the \sqrt{t} behaviour occur after a certain amount of time. In the long time limit, the single-file systems again show the ordinary t -dependence of the displacement, and with increasing particle numbers, the mobility in this time regime decreases.

The behaviour shown in these simulations was already predicted by Van Beijeren *et al.*⁴ and Hahn and Kärger¹⁷ for the diffusion of random walkers on a one-dimensional lattice. According to their findings, in the long time limit the total center-of-mass diffusion (i.e. the collective motion of all particles) of the system takes over as the dominant diffusion mechanism inside the channel. In the systems considered by these authors, the individual particles are assumed to be moving as random walkers, meaning that the non-interacting particles would have a displacement proportional to t . The present results however show that even in a system where the individual particles do not show this behaviour, Fickian diffusion ($\langle z^2 \rangle \propto t$) is eventually observed. Again, it is the combined effect of both particle-particle and particle-wall interactions that are responsible for the onset of Fickian diffusion in the long-time limit.

As, in the long-time limit, ordinary diffusion can be observed, the slopes of the displacement curves can be related to a diffusion coefficient D_{cm} for this collective center-of-mass diffusion. According to the findings of Hahn and Kärger,¹⁷ this

center-of-mass diffusivity should be inversely proportional to the pore length L_{pore} (or, equally, the system size N). The calculated diffusivities for the hard-sphere system are plotted in figure 4.14 versus this system size N . As can be seen from this plot, the predicted dependency is clearly met. The decreased mobility with increasing system size is due to the fact that a shift of the center-of-mass requires the particles to move in a correlated fashion, which will be more difficult when the number of particles in the system increases. Although in this case periodic boundary conditions are used instead of open systems, similar behaviour can be expected as a system with periodic boundary conditions can be regarded as an open system which is in continuous equilibrium with the gas phase, and in which readsorption at the pore boundaries is infinitely fast. The present results provide a strong proof for the conclusions of Nelson and Auerbach¹⁸ that, in contrast to the suggestion made by MacElroy and Suh,³⁴ the diffusivity in the long-time limit for finite systems is proportional to $1/N$ instead of $1/\sqrt{N}$.

4.5 Implications and conclusions

Although the system of hard spheres in a narrow cylindrical pore itself is quite simple, the diffusion in these systems shows complex behaviour. The mean-square displacement, one of the important quantities to measure the mobility in a system, is strongly determined by the different parameters that make up the system. It is however difficult to find a description of the dynamic behaviour due to the three-dimensional nature of the problem, combined with the confinement of the particles in a restricted geometry. Therefore, the simulations presented here provide a useful way to investigate this.

If the pore wall is smooth, without any corrugations, Fickian diffusion is observed even when the particles are unable to pass each other. Systems that are commonly referred to as single-file systems (i.e. a system in which the particle order is conserved) thus do not necessarily have to show the typical \sqrt{t} behaviour of the displacement in the long-time limit. A characteristic feature of these systems is however the strong dependence on the concentration of particles in the pore due to the strong correlations between particles in the system. The characteristic loading dependence of the diffusivity associated with these systems, $D_s \propto (1 - \theta)/\theta$, is indeed observed in the unstructured tube and appears to be the most characteristic feature for systems in which particles cannot pass each other.

When the pore wall is corrugated, enabling the transfer of linear momentum in the axial direction to the pore wall, the single-file behaviour of $\langle z^2(t) \rangle$ is indeed observed after a certain amount of time. Although the predictions of single-file behaviour usually assume that the individual particles in absence of particle-particle interactions

move like random walkers, the present study shows that this is not necessary. Although a certain amount of decorrelation takes place due to collisions with the pore wall, the particle velocity is not completely randomized by these events. What appears to be essential for the observation of the characteristic \sqrt{t} dependence is that particles are able to transfer linear momentum in the axial direction to the pore wall. The combined effect of particle-particle and particle-wall interactions eventually is responsible for single-file behaviour, while it is difficult to separate these two contributions. This is furthermore illustrated when comparing the density distribution functions of a system with interacting and one with non-interacting particles, where the structure combined with particle-particle interactions leads to a preference of the particles to reside near the edges of the broad sections of the pore.

While in a tube without corrugations the dimensions of the pore are of little influence to the mobility of the particles, in a structured tube the exact dimensions of the pore structure strongly affect the diffusivity. Both the mobility of the particles, as well as the time it takes to observe the single-file behaviour are strongly related to the ratio between the radius of the narrow and broad sections of the pore structure. The ratio between these quantities determines the number of collisions with the sections perpendicular to the pore axis, during which a transfer of linear momentum in the z -direction can take place. As a result, a larger chance of these collisions results in a more efficient transfer of momentum and an earlier transition to the \sqrt{t} behaviour. When the number of collisions with these side walls is not too large (R_{out} is only slightly larger than R_{in}) Fickian-type diffusion behaviour is visible over a longer timespan before the single-file behaviour sets in. That also the particle-particle interactions play a very important role in the transition to the \sqrt{t} behaviour is shown by the strong dependency of the transition time on the loading of the pore.

The influence of a finite pore length on the diffusive behaviour is again dependent on the exact geometry of the system. In the case of a cylindrical pore, the fact that the total linear momentum in the axial direction has to remain zero combined with the limited amount of space available for the particles causes the displacement to become constant after a certain amount of time. This limiting value for the diffusivity is proportional to the number of particles in the system (or, as the loading remains constant, the length of the pore), in accordance with results found in previous studies. What is however interesting is the occurrence of oscillations in the displacement, which slowly decays until the limiting displacement is reached. As these oscillations disappear when the diameter of the pore decreases, these oscillations seem to be related to the occurrence of non-central collisions. Possibly these type of collisions result in stronger correlations of the motion of the individual particles that slowly decrease with time.

In a corrugated tube, the influence of periodic boundaries is completely different.

80 Diffusion in Single-File Systems

For finite system sizes, after a sufficient amount of time Fickian diffusion is again observed. Again, the correlated motion of particles is responsible for this behaviour. In this case a shift of the total center-of-mass of the system is possible, as the total linear momentum is no longer conserved due to collisions with the pore wall, and the center-of-mass diffusion becomes the dominant mechanism in the long-time limit. It is remarkable that although the isolated particles themselves do not show Fickian behaviour, the entire system still shows this diffusive behaviour. This again indicates the importance of the combined influence of particle-particle and particle-wall interactions. The center-of-mass diffusivity depends strongly on the system size, as this mode of diffusion requires the particles to move collectively. In accordance with the findings of Nelson and Auerbach,¹⁸ the diffusivity in this case is proportional to the inverse of the system time, in contrast with the conclusions from MacElroy and Suh.³⁴

Evidently, the present study shows that the observation of the long-time single-file behaviour of the displacement strongly depends on the timescale on which this quantity is observed. For very small timescales, when particles do not yet interact with each other, either ballistic motion or motion which is determined by the particle-wall interactions is observed. For systems in which the transfer of linear momentum to the pore wall is not too fast, a regime can then be observed in which the diffusion is essentially Fickian. After some time the long-time single-file behaviour, in which $\langle z^2(t) \rangle \propto \sqrt{t}$, finally sets in. The timescales at which this transitions take place all strongly depend on the pore shape. For very smooth pore structures, the transition to single-file behaviour takes much longer. In general, one can expect the pore structure of zeolites to be quite smooth, and especially for the zeolites with larger pore sizes, the activation energies to be quite small. It is however difficult to directly relate the present results with the real world, as one cannot easily define energy barriers in the systems used here. Furthermore, in real systems there is an additional contribution to the randomization of the particle velocities due to the thermal vibrations of the zeolite lattice.

In finite-size systems another transition takes place, after which Fickian diffusion is again observed. Again, the diffusivity in this regime is proportional to $(1 - \theta/\theta_c)$. The diffusivity in this regime furthermore strongly depends on the system size. This behaviour is characteristic for the diffusion in single-file systems, and provides another way of showing its occurrence. As all zeolites in the real world are of finite length, one should be able to study these effects using macroscopic experiments, for example by using the ZLC method or chromatographic experiments.³⁵ If one would thus be able to accurately control the size of the zeolite crystals (and the other experimental conditions), this would provide an indirect way of demonstrating that single-file diffusion occurs in a certain system. On the other hand, these results show

that one should be careful with direct measurements of the displacement using PFG-NMR or QENS. Whether or not the single-file time dependency is observed depends on the timescale at which these measurements probe the displacement. If measurements are being performed on very short timescales in systems with moderate energy barriers, Fickian diffusion could in principle be observed. The same holds for measurements that take place on a longer timescale. The exact time regime in which the \sqrt{t} dependency is indeed observed, strongly depends on the zeolite crystals used, and can be furthermore complicated by imperfections in the crystals or similar effects.

4.6 References

- ¹ E. J. Harris, *Transport and accumulation in biological systems*, Butterworths Scientific Publications, London (1960).
- ² D. G. Levitt, *Phys. Rev. A* **8**(6), 3050–3054 (1973).
- ³ P. A. Fedders, *Phys. Rev. B* **17**(1), 40–46 (1978).
- ⁴ H. van Beijeren, K. W. Kehr, and R. Kutner, *Phys. Rev. B* **28**(10), 5711–5723 (1983).
- ⁵ W. M. Meier and D. H. Olson, *Atlas of zeolite structure types*, Butterworths-Heinemann, London (1992).
- ⁶ J. Kärger, M. Petzold, H. Pfeifer, S. Ernst, and J. Weitkamp, *J. Catal.* **136**, 283–299 (1992).
- ⁷ J. Kärger, *Phys. Rev. A* **45**(6), 4173–4174 (1992).
- ⁸ J. Kärger, *Phys. Rev. E* **47**(2), 1427–1428 (1993).
- ⁹ V. Kukla, J. Kornatowski, D. Demuth, I. Girnus, H. Pfeifer, L. V. C. Rees, S. Schunk, K. K. Unger, and J. Kärger, *Science* **272**, 702–704 (1996).
- ¹⁰ V. Gupta, S. S. Nivarthi, A. V. McCormick, and H. T. Davis, *Chem. Phys. Lett.* **247**, 596–600 (1995).
- ¹¹ K. Hahn, J. Kärger, and V. Kukla, *Phys. Rev. Lett.* **76**(15), 2762–2765 (1996).
- ¹² H. Jobic, K. Hahn, J. Kärger, M. Bée, A. Tuel, M. Noack, I. Girnus, and G. J. Kearley, *J. Phys. Chem. B* **101**(30), 5834–5841 (1997).
- ¹³ H. J. K. Hahn and J. Kärger, *Phys. Rev. E* **59**(6), 6662–6671 (1999).
- ¹⁴ D. S. Sholl and K. A. Fichthorn, *J. Chem. Phys.* **107**(11), 4384–4389 (1997).
- ¹⁵ H. L. Tepper, J. P. Hoogenboom, N. F. A. van der Vegt, and W. J. Briels, *J. Chem. Phys.* **110**(23), 11511–11516 (1999).
- ¹⁶ D. S. Sholl, *Chem. Eng. J.* **74**(1), 25–32 (1999).
- ¹⁷ K. Hahn and J. Kärger, *J. Phys. Chem. B* **102**(30), 5766–5771 (1998).
- ¹⁸ P. H. Nelson and S. M. Auerbach, *J. Chem. Phys.* **110**(18), 9235–9243 (1999).
- ¹⁹ C. Rödenbeck and J. Kärger, *J. Chem. Phys.* **110**(7), 1–11 (1999).
- ²⁰ D. S. Sholl and K. A. Fichthorn, *Phys. Rev. Lett.* **79**(19), 3569–3572 (1997).
- ²¹ D. S. Sholl and C. K. Lee, *J. Chem. Phys.* **112**(2), 817–824 (2000).
- ²² K. Hahn and J. Kärger, *J. Phys. A: Math. Gen.* **28**, 3061–3070 (1995).
- ²³ D. Keffer, A. V. McCormick, and H. T. Davis, *Mol. Phys.* **87**(2), 367–387 (1996).
- ²⁴ J. M. Haile, *Molecular dynamics simulation: elementary methods*, John Wiley & Sons, New York (1992).

82 Diffusion in Single-File Systems

- ²⁵ S.-H. Suh and J. M. D. MacElroy, *Mol. Phys.* **58**(3), 445–473 (1986).
- ²⁶ K. K. Mon and J. K. Percus, *J. Chem. Phys.* **112**(7), 3457–3458 (2000).
- ²⁷ J. R. Henderson, *Mol. Phys.* **99**(10), 883–888 (2001).
- ²⁸ K. Hahn and J. Kärger, *J. Phys. Chem.* **100**(1), 316–326 (1996).
- ²⁹ M. P. Allen and D. J. Tildesley, *Computer simulation of liquids*, Clarendon, Oxford (1987).
- ³⁰ T. J. H. Vlugt, R. Krishna, and B. Smit, *J. Phys. Chem. B* **103**(7), 1103–1118 (1999).
- ³¹ D. Frenkel and B. Smit, *Understanding molecular simulation: from algorithms to applications*, Academic Press, Inc., San Diego, 1 ed. (1996).
- ³² J. L. Lebowitz and J. K. Percus, *Phys. Rev.* **155**(1), 122–138 (1967).
- ³³ M.-O. Coppens, A. T. Bell, and A. K. Chakraborty, *Chem. Engng. Sci.* **53**(11), 2053–2061 (1998).
- ³⁴ J. M. D. MacElroy and S.-H. Suh, *J. Chem. Phys.* **106**(20), 8595–8597 (1997).
- ³⁵ J. Kärger and D. M. Ruthven, *Diffusion in zeolites and other microporous solids*, John Wiley & Sons, Inc., New York (1992).

5

Measurement and Simulation of Binary Diffusion in Zeolites

*The positron emission profiling technique is extremely well suited to study the diffusion of mixtures in zeolites on a macroscopic scale. By labelling one of the components, the adsorptive and diffusive properties of that component can be determined. Although the diffusion in mixtures is an important topic, the amount of studies on this subject is rather limited. In this chapter, the PEP technique, together with a model to describe the transport behaviour inside a packed bed reactor, is being used to study the behaviour of a mixture of *n*-hexane and 2-methylpentane.*

5.1 Introduction

Diffusion and adsorption of hydrocarbons in zeolites has received a lot of attention in the last few decades.^{1,2} Not in the least place, this is due to the vast number of applications of these materials in the petrochemical industry, e.g. as catalysts in cracking and hydroisomerization processes, and as molecular sieves in separation processes. For all these applications, a thorough understanding of the diffusive and adsorptive properties of molecules inside these materials is of vital importance, as these greatly influence the performance of the catalytic or separation processes. When used as for example a catalyst or molecular sieve, at least two, or even more, species are present

[†]Reproduced in part from D. Schuring, A. O. Koriabkina, A. M. de Jong, B. Smit, and R. A. van Santen, "Adsorption and Diffusion of *n*-Hexane/2-Methylpentane Mixtures in Zeolite Silicalite: Experiments and Modeling", *J. Phys. Chem. B* **105**(32), 7690–7698 (2001). © 2001 American Chemical Society.

84 Measurement and Simulation of Binary Diffusion in Zeolites

inside the zeolite. Surprisingly, most studies are focused on the diffusion and adsorption of single components only. In the first place, this results from the fact that most conventional methods for studying mass transfer in zeolites, like the gravimetric and volumetric methods, are intrinsically unable to distinguish between different types of molecules. Furthermore, it is generally assumed that diffusion in multicomponent systems can be predicted from single-component data.

Only in recent years, the number of investigations on multi-component mixtures is increasing. However, most of these studies are concerned with small molecules only, like methane/xenon,^{3,4} ethane/ethene,⁵ and *n*-butane/methane,⁶ and the majority of these studies is focussed on the sorption thermodynamics, often making use of molecular simulations. Most experimental data are obtained with techniques like NMR and quasi-elastic neutron scattering, and at relatively low temperatures. Among the few papers dealing with longer hydrocarbons are the work of Choudhary et al. (aromatics in ZSM-5),⁷ Niessen and Karge (xylene-benzene mixtures),⁸ and work on cyclic, branched, and linear hydrocarbons in silicalite membranes by Funke and co-workers.⁹ Recently, Masuda and co-workers¹⁰ reported results on *n*-heptane/*n*-octane and *ortho*- and *meta*-xylene mixtures at elevated temperatures. They concluded that, while the diffusivity of the slow component with increasing amounts of the fast components remains constant, the diffusivity of the fast component decreases monotonically with the increasing fraction of slow components. This is in line with results obtained for the mixtures of smaller components.

A relatively new technique capable of studying adsorption and diffusion of multi-component mixtures is positron emission profiling (PEP), which makes use molecules labelled with a positron-emitting isotope. This technique is based on coincident detection of the γ photons resulting from the annihilation of a positron, emitted by the radioactive isotope, with an electron from the chemical environment. Because the annihilation produces a pair of γ photons travelling in (almost) opposite directions, the exact location of the decay event can be determined by coincident detection of these photons. Due to the high penetrating power of the γ -rays, a great advantage of this technique is the fact that in-situ measurements can be performed on ordinary laboratory-scale reactors at normal reaction conditions. Furthermore, as labelled molecules are used, one has the possibility of only labelling one component in a mixture, thus making it possible to study only this component. The positron emission profiling technique has been described in detail in Anderson et al.,^{11,12} and was already used successfully for studying single-component diffusion in biporous packed beds of zeolites.¹³ Recently, this technique has been extended to incorporate tracer exchange experiments.¹⁴ With these experiments, a continuous stream of labelled molecules is injected into a steady-state feed stream. The rate at which the exchange between labelled and non-labelled molecules takes place is determined by

the diffusion of the adsorbates inside the zeolite channels. By studying the exchange process, information can be obtained about diffusion and adsorption inside the zeolite crystals. The advantage of using tracer exchange experiments over transient experiments is that one is assured that the entire experiment is performed under steady-state conditions, so that the true self-diffusion constant is measured.

In this chapter, the tracer-exchange positron emission profiling (or TEX-PEP) technique is being used to study the adsorption and diffusion of *n*-hexane/2-methylpentane mixtures in zeolite silicalite. These systems were chosen because of their practical applications, the availability of other (theoretical) studies, and the peculiar adsorption behaviour observed for the single components.¹⁵ Using a constant total pressure, the adsorptive and diffusive behaviour of *n*-hexane and 2-methylpentane have been studied as a function of the *n*-hexane/2-methylpentane ratio in the gas phase. The remaining of this paper will deal with the experimental details, the model used for evaluating the experiments, and the results obtained.

5.2 Experimental setup

For the experiments conducted in this study, the same setup was used as was described earlier in the work of Schumacher et al.¹⁴ The positron-emitting ¹¹C isotope is produced by irradiation of a nitrogen target with 12 MeV protons from the 30 MeV AVF Cyclotron at the Eindhoven University of Technology. The resulting ¹¹C is then transferred as CO/CO₂ to the setup for the production of labelled hydrocarbons. Details of the homologation process used for the production of labelled *n*-hexane and 2-methylpentane can be found in Cunningham et al.¹⁶ After separation of the different products produced in this process, the desired labelled species is collected in a syringe.

Figure 5.1 shows a schematic diagram of the reactor system used in the TEX-PEP experiments. During the tracer exchange experiments, a constant flow of non-labelled hydrocarbons in a hydrogen carrier stream was fed into the reactor. The *n*-hexane/2-methylpentane/hydrogen mixture was produced using a CEM (Controlled Evaporator and Mixer)-mixing unit consisting of two branches, each of which equipped with a mass flow controller (MFC). Using these controllers for the *n*-hexane and 2-methylpentane branch, the composition of the mixture can be set. The total flowrate of hydrocarbons and carrier gas was set to a value of 80.2 ml/min.

For a tracer exchange experiment, a quantity of labeled molecules of either *n*-hexane or 2-methylpentane was produced and continuously injected into the feed stream using a syringe pump. The tracer exchange and tracer re-exchange process could then be monitored using the PEP detector by either turning the tracer flow on or off. The PEP detector measures the concentration by reconstructing the posi-

tion of the positron-emitting isotopes via coincident detection of the two γ -photons, emitted in opposite directions during an annihilation event. With the current setup, the concentration of the labelled alkanes is then measured at 17 different positions along the reactor axis with a spatial resolution of 3.05 mm and a minimum sampling time of 0.5 seconds. A detailed description of the detection system can be found in Mangnus et al.¹⁷ and Anderson et al.¹¹ Due to switching effects,¹⁴ the re-exchange process yields more reliable results, and only this stage of the experiments was used for determining the kinetic parameters.

For the experiments, a sample of silicalite-1 was obtained from the Shell Research and Technology Centre in Amsterdam. The zeolite crystals in this sample have a very regular shape with dimensions of $150 \times 50 \times 30 \mu\text{m}$. Due to the large size, it was not necessary to press these crystals into larger pellets. The large crystal size furthermore ensures that processes taking place inside the zeolite are really dominating the transport properties inside the bed. The bed porosity was determined from the pressure drop over the bed using the Ergun relation, yielding a value $\varepsilon = 0.44$. The length of the zeolite bed was equal to 3 cm. Prior to experiments, the zeolite sample was activated for at least one hour at 673K in a hydrogen stream. The *n*-hexane and 2-methylpentane gases used for the constant non-labelled flow had a purity of at least 99.9%.

5.3 Modeling the tracer exchange process

In order to be able to interpret the data from the TEX-PEP experiments, a mathematical model is needed for describing the re-exchange process in the zeolite reac-

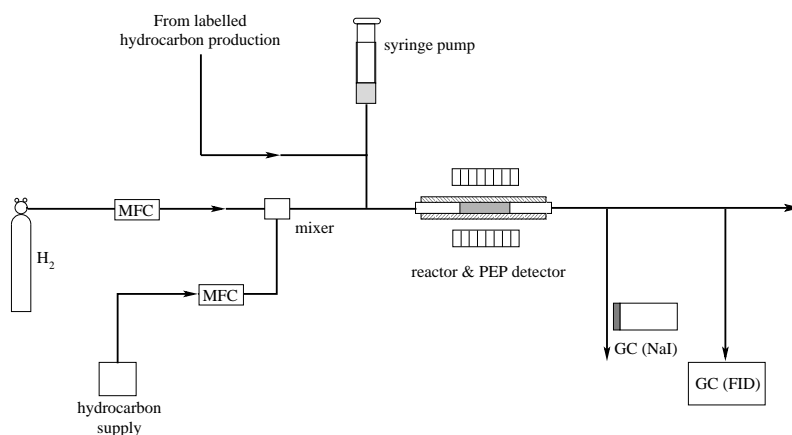


Figure 5.1: Schematic diagram of the reactor setup used for the tracer-exchange positron emission profiling measurements.

torbed. A common way to describe diffusion in packed beds is by using a system of diffusion equations, describing the mass transport in the zeolite bed and inside the crystals.^{1, 18, 19} The model used in this study basically is a modification of the equations used by Noordhoek et al.²⁰ It is assumed that the transport of molecules occurs via convection and axial diffusion in the space between the crystals, adsorption/desorption at the crystal surface, and diffusion inside the pores of the crystals. Furthermore, it is assumed that the crystals have a spherical shape. This approximation is commonly made in literature, and has been shown to be quite reasonable.¹ This is probably also due to the random orientation of the crystals inside the reactor, making it difficult to really explicitly account for the particle shape. As only one component is detected during the experiments, single-component equations can be used to model its behaviour. The parameters describing the different processes in the bed will then be effective values for the transport of this component in the mixture.

5.3.1 The model equations

Transport in the fluid phase inside the packed bed takes place through convection, axial diffusion, and flow to or from the zeolite crystals. A mass balance for a small volume element of the bed results in the following equation for the concentration C_z in the gas phase:

$$\frac{\partial C_z}{\partial t} = D_{ax} \frac{\partial^2 C_z}{\partial z^2} - v_{int} \frac{\partial C_z}{\partial z} + \frac{3(1-\varepsilon)}{\varepsilon R_c} N_c \quad (5.1)$$

In this equation, z is the coordinate along the reactor axis, D_{ax} is the axial diffusion coefficient, and v_{int} the interstitial velocity, which can be calculated from the gas flow speed v_{sup} using $v_{int} = v_{sup}/\varepsilon$. The axial diffusivity can be calculated from the molecular diffusion coefficient of the component. For R_c , the radius of the crystals, the equivalent spherical particle radius \bar{R}_c is taken, defined as the radius of the sphere having the same external surface area to volume ratio.¹ For the crystal size used in this study, this yields a value of 25 μm .

The boundary conditions used for the bed equation are identical as the ones in Noordhoek et al.²⁰ For the column entrance, a mass balance (and by neglecting the diffusional term just in front of the column) yields

$$\frac{\partial C_{z,0^+}}{\partial z} = \frac{v_{int}}{D_{ax}} (C_{z,0^+} - C_{z,0^-}) \quad (5.2)$$

in which $C_{z,0^-}$ and $C_{z,0^+}$ are the fluid phase concentrations just in front of and just after the column entrance, respectively. For TEX-PEP experiments, concentration just in front of the packed bed is given by the Heaviside step function:

$$\begin{aligned} C_{z,0^-}(t) &= C_0, & t \leq 0 \\ C_{z,0^-}(t) &= 0, & t > 0 \end{aligned} \quad (5.3)$$

At the column exit, the diffusional term is neglected, turning eq. 1 into a first-order equation which can be used as a boundary condition.

The term N_c equals the mass flux through the boundary of the zeolite, and is determined by the rate-limiting step for adsorption/desorption at the crystal boundary. It is assumed that external mass transfer resistance due to the diffusion through the laminar fluid film surrounding the particles can be neglected, as this process is much faster than diffusion inside the zeolite crystals. This has been confirmed by comparing simulations with and without this process included in the model, showing that neglecting the external film mass transfer resistance does not influence the results.

The model of Nijhuis et al.¹⁹ explicitly accounts for adsorption/desorption at the crystal boundary, assuming Langmuir adsorption kinetics. As the TEX-PEP experiments are conducted under steady-state conditions, this mechanism can be replaced by a simple first-order adsorption/desorption process:

$$N_c = k_d C_x(R_c, z, t) - k_a C_z(z, t) \quad (5.4)$$

in which k_a and k_d are the adsorption and desorption constants in [$\text{m}\cdot\text{s}^{-1}$]. This equation furthermore has the advantage that k_a and k_d have the same dimensions, and that there is no need to determine the number of adsorption sites.

Transport inside the zeolite crystals occurs through diffusion inside the zeolite pores. Although it is known that diffusion in zeolites is generally anisotropic,²¹ the random orientation of the crystals inside the reactor justifies the approximation that micropore diffusion can be described as an isotropic process. A mass balance for the zeolite crystals yields for the adsorbed phase concentration C_x in the crystals:

$$\frac{\partial C_x}{\partial t} = D_c \left(\frac{\partial^2 C_x}{\partial x^2} + \frac{2}{x} \frac{\partial C_x}{\partial x} \right) \quad (5.5)$$

in which D_c is the intracrystalline diffusivity, and x the radial coordinate of the crystal. In principle, the value of the diffusion constant depends on the concentration of both components. However, during the experiments, the total concentration does not change, and D_c can thus be regarded as constant during a single measurement. The boundary condition at the centre of the particle is obtained from symmetry reasons:

$$\left. \frac{\partial C_x}{\partial x} \right|_{x=0} = 0 \quad (5.6)$$

At the crystal boundary, the flow to the surface must be equal to the desorption rate at the crystal boundary at $x = R_c$:

$$D_c \left. \frac{\partial C_x}{\partial x} \right|_{x=R_c} = k_a C_z(z, t) - k_d C_x(R_c, z, t) \quad (5.7)$$

The initial conditions can be found by realizing that at the start of a tracer re-exchange process, the system is in equilibrium. Assuming that the injected tracer concentration initially is equal to C_0 , the initial conditions are given by:

$$\begin{aligned} C_z(z, t) &= C_0 \\ C_x(x, z, t) &= K_a \times C_0 \end{aligned} \quad (5.8)$$

in which K_a is the adsorption equilibrium constant, given by $K_a = k_a/k_d$.

5.3.2 Solving the model

The equations described above have been solved using the numerical method of lines.²² This procedure has been described in detail in Noordhoek et al.²⁰ In short, this is done by discretizing the spatial coordinates (and spatial derivatives), converting the system of partial differential equations into a set of ordinary differential equations (ODEs). These ODEs can then be solved using an ordinary numerical integration routine. Solving the model yields values for the concentration at the each bed and crystal gridpoint. As the PEP detector measures the total concentration of labelled molecules in a certain section of the catalyst bed, volume averaging has to be applied to simulate the response of the PEP detector. The average microparticle concentration at position z inside the reactor bed equals

$$\langle C_x(z, t) \rangle = \frac{3}{R_c^3} \int_0^{R_c} C_x(x, z, t) \cdot x^2 dx \quad (5.9)$$

As the crystal concentration C_x is only known at the gridpoints, this integral has to be evaluated numerically. The total concentration at position z can then be calculated by averaging over the bed and crystal concentration:

$$\langle C_{tot}(z, t) \rangle = \varepsilon \cdot C_z(z, t) + (1 - \varepsilon) \cdot \langle C_x(z, t) \rangle \quad (5.10)$$

Estimation of the different parameters, i.e. the adsorption/desorption and diffusion in the zeolite crystals, is done by fitting the modelled concentration profiles to the measured ones, using a least-squares Levenberg-Marquardt algorithm.²³ All the other parameters were determined experimentally.

5.3.3 Adsorption/desorption at the crystal boundary

If adsorption and desorption at the outer surface of the zeolite crystallites is fast compared to the diffusion inside the pores of the zeolite, adsorption equilibrium can be assumed at the crystal boundary. This seems a reasonable approach, as the diffusion

90 Measurement and Simulation of Binary Diffusion in Zeolites

inside the micropores is usually quite slow. An advantage of this approach is that the parameters describing adsorption/desorption at the boundary can be replaced by a single equilibrium adsorption constant K_a . This takes care of the problem that two parameters need to be fitted which are not completely independent, as was already reported by Nijhuis et al.¹⁹ In order to check if adsorption equilibrium can be safely assumed, results for the model described previously can be compared with that from a model assuming adsorption equilibrium.

On the assumption that adsorption/desorption is fast compared to diffusion in the zeolite micropores, the mass flux through the boundary of the zeolite is determined by diffusion to the boundary of the crystal. Eq. 4 then has to be replaced by

$$N_c = -D_c \left. \frac{\partial C_x}{\partial x} \right|_{x=R_c} \quad (5.11)$$

The boundary equation at the crystal surface, eq. 7, can be replaced by a simple equilibrium condition

$$C_x(x = R_c, z, t) = K_a \times C_z(z, t) \quad (5.12)$$

An estimate of the rate of adsorption can be obtained from kinetic gas theory.²⁴ The number of collisions between molecules and the surface can be calculated using the following relation:

$$\Phi_s = \frac{1}{4} C_{gas} \sqrt{\frac{R_g T}{2\pi M}} \quad (5.13)$$

which gives the collision rate per unit surface (in $\text{mol}\cdot\text{m}^{-2}$), with C_{gas} the concentration of the gas phase, R_g the gas constant, T the temperature, and M the molar mass of the molecules. The rate constant for adsorption can be calculated from this by dividing this expression by the gas phase concentration. It should however be realized that the value calculated from eq. 13 gives an upper bound for the true adsorption rate, as not all collisions with the zeolite crystal surface will result in the adsorption of a molecule inside the micropores (i.e. there exists a “surface barrier” for adsorption, and the sticking coefficient is smaller than 1). Estimation of the sticking coefficient is not straightforward, and it might have values ranging from approximately one to 10^{-3} .

In order to check in which regime the models give similar results, a number of simulations have been performed. For the bed porosity, crystal radius, flowrate, and temperature identical parameters were chosen as were used in the experiments. For the diffusion constant, D_c , a value of $5 \cdot 10^{-11} \text{ m}^2\cdot\text{s}^{-1}$ was chosen, which is the upper limit of this parameter found experimentally. The adsorption equilibrium constants found for these systems are typically in the order of 300 to 1000, so a value of 500 was chosen. This value was furthermore used to fix the ratio between the adsorption and

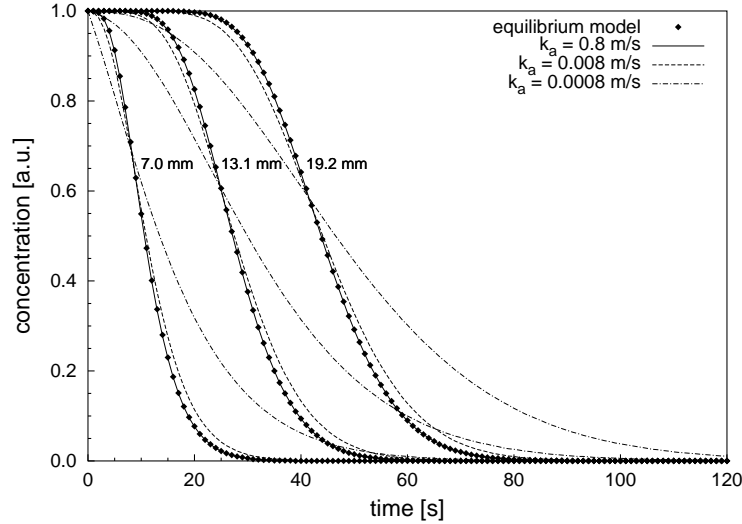


Figure 5.2: Simulated concentration profiles at $z = 7$ mm, 13.1 mm, and 19.2 mm along the reactor axis for the model assuming adsorption equilibrium (dots), and for different values for the adsorption rate using the model explicitly accounting for adsorption/desorption at the crystal boundaries (lines). deviations from the equilibrium model only start to be visible for adsorption rates smaller than $0.01 \text{ m}\cdot\text{s}^{-1}$.

desorption constant, as both models should yield equivalent loadings at equilibrium. The upper limit for the rate of adsorption was calculated using eq. 13, and was found to be in the order of $80 \text{ m}\cdot\text{s}^{-1}$. For $K_a = 500$, this corresponds to a desorption rate equal to $k_d = k_a/K_a = 0.16 \text{ m}\cdot\text{s}^{-1}$.

Figure 5.2 shows the simulated concentration profiles at different detector positions along the axis of the reactor (7 mm, 13.1 mm, and 19.2 mm) using the equilibrium model, and using the first-order adsorption/desorption model for different values of k_a . For a value of $k_a = 0.8 \text{ m}\cdot\text{s}^{-1}$, the equilibrium model is in perfect agreement with the full model. Only for values smaller than $8 \cdot 10^{-3} \text{ m}\cdot\text{s}^{-1}$, meaning that only one in 10^4 collisions will lead to adsorption, small deviations between the two models can be observed. For lower values of k_a , the re-exchange process is increasingly determined by the rate of desorption at the crystal boundary. Although exact values for the adsorption and desorption rate cannot be obtained, it seems unlikely that the sticking coefficient for the adsorption process on the zeolite crystal surface is smaller than 10^{-4} , and the use of the equilibrium model (thereby neglecting the existence of transport resistances due to a “surface barrier”) is justified under the conditions used in this study.

From these results, a criterium can be derived for the importance of adsorption/desorption at the crystal boundary by making use of a modified Biot number

92 Measurement and Simulation of Binary Diffusion in Zeolites

for mass transport, Bi_m . Usually, Bi_m is defined as the ratio of the time constants for external film to internal mass transfer resistance (see e.g. Emig and Dittmeyer²⁵), but in this case it can be defined as the ratio between desorption and micropore diffusion:

$$Bi_m = \frac{k_d R_c}{D_c} \quad (5.14)$$

Apparently, the intracrystalline diffusion is slow compared to desorption if the Biot number is greater than 10. For a Biot number smaller than 1, the mass transfer is strongly determined by the desorption process at the boundary.

5.3.4 Influence of the diffusion and adsorption constants

In order to be able to extract reliable data from the experiments, the different parameters of interest must have a significant influence on the shape of the exchange curves. Figure 5.2 shows that, under the conditions used in this study, this is indeed the case. For the values of the different model parameters, typical values were chosen as found during the experiments. In a previous study it was already shown that the influence of axial diffusion can be neglected in this system.¹⁴ Figure 5.3(a) shows the effect of varying the adsorption constant, having a fixed value for the micropore diffusion constant. Clearly, variation of this parameter has a large influence on the observed re-exchange curves at different positions along the reactor. The same holds for the diffusion coefficient when keeping the adsorption constant fixed, as shown in figure 5.3(b). Furthermore, it can be concluded that both parameters have a different influence on the measured exchange curves. The adsorption constant mainly determines the timescale at which the change in concentration travels through the bed without influencing the actual shape of the curves. The diffusion constant, however, mainly influences the shape of the curves, and causes an increasing amount of tailing with decreasing diffusivity. Clearly, analysis of the shape of the tracer re-exchange curves will yield both information on the diffusion constant, as well as the adsorption constant of the molecules under study.

5.4 Results and discussion

The model described above has been used for studying the adsorptive and diffusive behaviour of a mixture of *n*-hexane and 2-methylpentane as a function of the mixture composition. The total hydrocarbon pressure was fixed at 6.6 kPa, and the experiments were conducted at a temperature of 433 K. At different mixture ratios, the tracer re-exchange of both *n*-hexane and 2-methylpentane were recorded. Figure 5.4

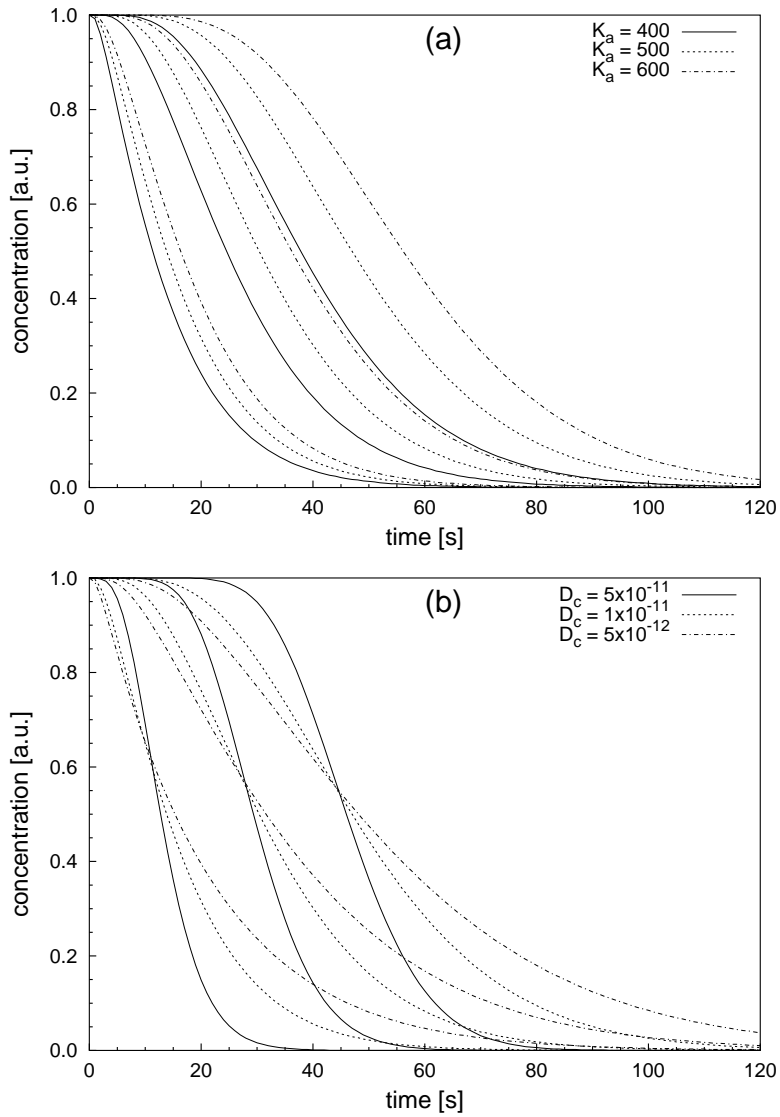


Figure 5.3: Modelled tracer re-exchange curves at three different positions along the reactor axis (7 mm, 13.1 mm, and 19.2 mm) for (a) different values of the adsorption constant K_a using a fixed value of $D_c = 1 \cdot 10^{-11} \text{ m}^2/\text{s}$ and (b) different values of D_c using a fixed value of $K_a = 500$.

Table 5.1: Single component loadings at a temperature of 433 K and a pressure of 6.6 kPa.

adsorbent	loading	loading
	[mmol/g]	[molecules/U.C.]
<i>n</i> -hexane	0.63	3.6
2-methylpentane	0.59	3.4

shows examples of the tracer re-exchange curves at different positions along the reactor for *n*-hexane and 2-methylpentane in a 1:1 mixture. As can be seen, the model accurately describes the measured concentration profiles. The somewhat larger amount of scattering in the experimental 2-methylpentane curves results from a slightly lower yield of this component during the production of labelled hydrocarbons. The plots furthermore show that the transport properties of *n*-hexane and 2-methylpentane in this mixture are different. The re-exchange of the branched molecule is slower than from the linear component, indicating that micropore diffusion is faster in the latter case. The larger separation in time of the exchange curves for the linear alkane indicates that this component has a larger adsorption constant.

5.4.1 Adsorption of single components: comparison with literature

Although the amount of data on the adsorption and diffusion of mixtures is really limited, there is a fair amount of data on single-component adsorption of *n*-hexane and also some data on 2-methylpentane. The adsorptive and diffusive properties of both components have been measured using the TEX-PEP technique. From the fitted adsorption equilibrium constants, the loading (in moles per gram of zeolite) can be calculated using the following relation:

$$\theta = \frac{K_a p_{hc}}{\rho_z R_g T} \quad (5.15)$$

in which p_{hc} is the hydrocarbon partial pressure, ρ_z the density of the zeolite, R_g the gas constant, and T the temperature. The calculated loadings for *n*-hexane and 2-methylpentane are shown in table 1. For *n*-hexane, this is in good agreement with the value obtained by Yang and Rees²⁶ (3.9 molecules per unit cell) and Van Well et al.²⁷ (3.7 molecules per unit cell). The slightly lower value obtained in this study might be attributed to the higher temperature used (433 instead of 423 K). For 2-methylpentane, extrapolating the data obtained by Cavalcante and Ruthven²⁸ to the conditions used in this study yields a value of 2.6 molecules per unit cell, somewhat lower than the value found here. The slightly reduced loading of the branched compared to the linear alkane under equal conditions is in accordance with other studies

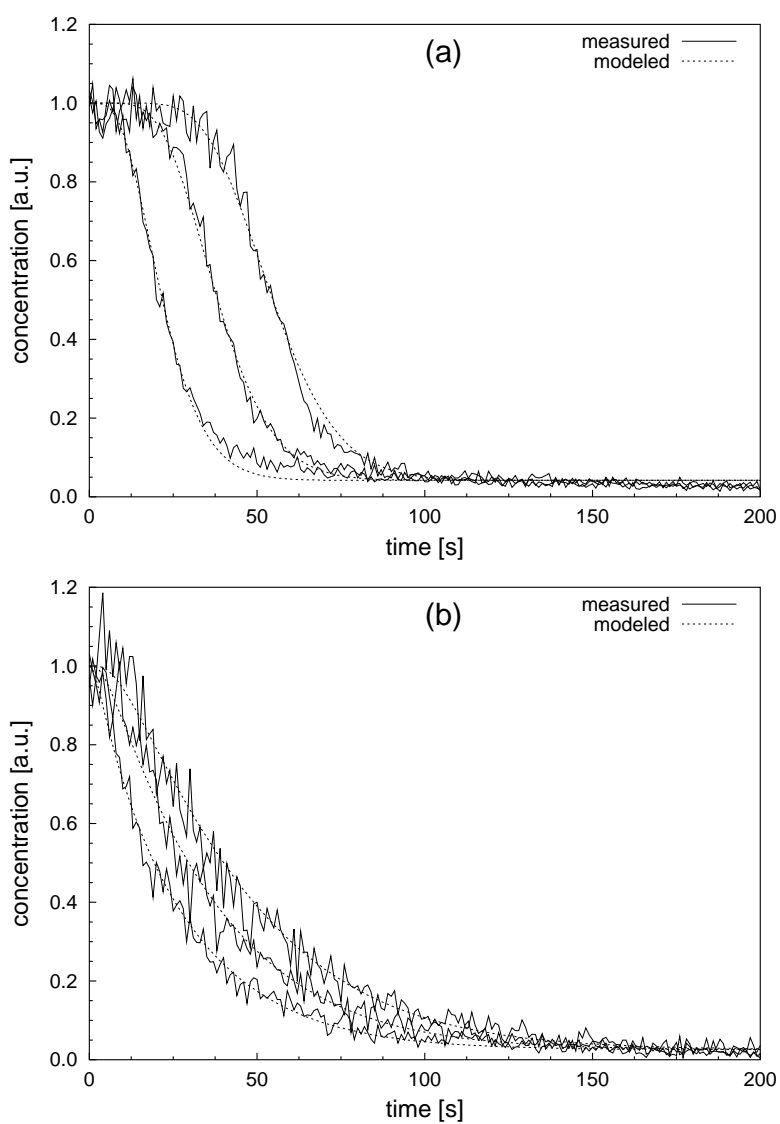


Figure 5.4: Experimental and simulated tracer exchange curves at different positions along the reactor axis for (a) n-hexane and (b) 2-methylpentane in a 1:1 n-hexane/2 methylpentane mixture at 433 K and 6.6 kPa total hydrocarbon pressure.

(see e.g. Vlucht et al.²⁹). This is an entropic effect, as the adsorption enthalpies of both components are approximately equal, but the conformations of the bulkier branched alkanes are much more restricted in the narrow pores of the zeolite. Adsorption of 2-methylpentane from the gas phase thus leads to a higher reduction in entropy compared to *n*-hexane, making it entropically less favourable to adsorb the branched isomer.²⁹

A comparison between single-component diffusivities obtained with this technique and values from literature has been discussed previously,¹⁴ showing that a reasonable agreement was obtained with previously reported values using other techniques.

5.4.2 Binary adsorption: Results and comparison with CBMC

Figure 5.5 shows the fitted adsorption constants (K_a) for both *n*-hexane and 2-methylpentane as a function of the mixture composition. The error margins in the calculated adsorption constants are around 10%. As can be seen from this plot, the equilibrium adsorption constant for both components increases with increasing 2-methylpentane fraction in the gas phase. This might be due to the slightly lower loading of the branched alkane in single-component systems, as can also be seen from the slightly lower adsorption constant for pure 2-methylpentane compared to *n*-hexane. The larger increase of the adsorption constant for *n*-hexane furthermore shows that competitive adsorption of both components is present. This can be seen more easily by plotting the loadings calculated from these adsorption constants.

The solid symbols in Figure 5.6 show the loadings of both *n*-hexane and 2-methylpentane, as well as the total loading, as a function of the gas phase mixture composition. Obviously, the *n*-hexane loading monotonically decreases, and the 2-methylpentane loading monotonically increases with an increasing partial pressure of the branched alkane. The total hydrocarbon loading varies only little (apart from experimental errors), and shows a slight decrease at high 2-methylpentane ratio, as was explained in the previous paragraph. The small deviations from a linear dependence on the mixture composition ratio indicate a small preferential adsorption for *n*-hexane compared to its mono-branched isomer. Although the preference for the adsorption of *n*-hexane is small, it does not entirely fall in the inaccuracy of the values determined, and was confirmed by repeated experiments.

In the literature, different types of adsorptive behaviour of binary mixtures have been reported. Cottier et al.³⁰ for example found that for the adsorption of a mixture of *para*- and *ortho*-xylene in various Y-type zeolites, both components essentially behaved similar to the single-component case, and adsorbed independently. A completely different behaviour was observed for ethane and ethylene in zeolite 13X by Buffham et al.,³¹ where the ethylene was preferentially observed at low ethane par-

tial pressures, and a non-linear dependence thus was observed. A similar behaviour was observed by Heuchel et al.³ for CF_4 and CH_4 in silicalite. The system under study appears to have an identical behaviour as the last two systems.

The adsorptive behaviour found in this study is in line with a recent configurational-bias Monte Carlo study on the adsorptive behaviour of linear and branched alkanes and their mixtures by Vlught et al.²⁹ Although their results cannot be directly related because they were performed with a fixed mixture ratio at a lower temperature (300 K), further insight can be gained from this study. From their simulations, they concluded that at a total loading of approximately 4 molecules per unit cell, the loading of the branched alkanes reaches a maximum value. At lower loadings, both components adsorb independently, while at higher loadings the branched alkanes will be squeezed out by the linear alkanes. The peculiar behaviour shown by this mixture could be explained when looking at the siting of both components. Vlught et al. found that, while the *n*-hexane could be adsorbed anywhere in the silicalite pores, 2-methylpentane was located at the intersections between the straight and zigzag channels. As a result of that, *n*-hexane has a higher packing efficiency, and it is thus easier (or entropically more favorable) to obtain higher loadings with the linear instead of the branched alkanes. For the CH_4/CF_4 system, different sitings for both components were also observed.³²

Apparently, under the conditions used in the present study, the system is in the regime at which the 2-methylpentane is starting to be pushed out. As a result of the

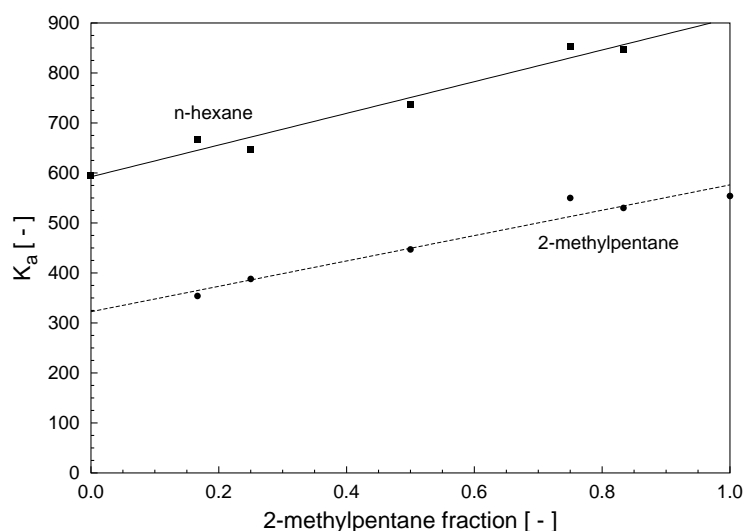


Figure 5.5: Fitted adsorption constants for *n*-hexane and 2-methylpentane as a function of the 2-methylpentane fraction in the gas phase of the binary mixture.

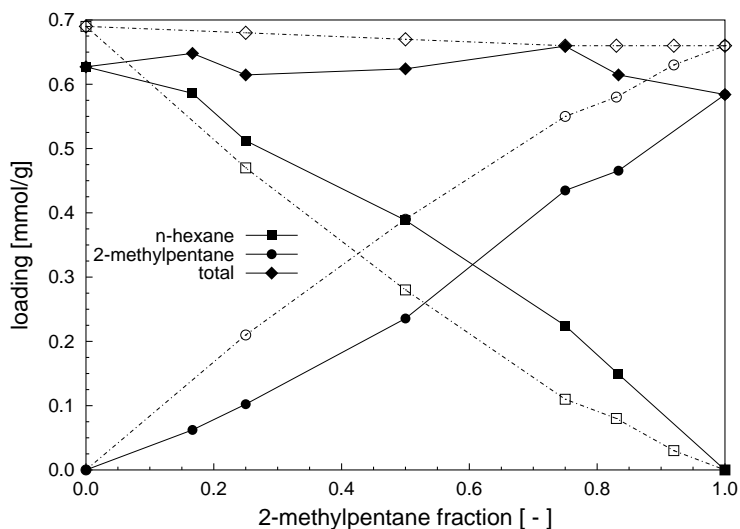


Figure 5.6: *n*-hexane and 2-methylpentane loading as a function of the 2-methylpentane fraction in the gas phase in a binary mixture. The solid symbols are measured loadings, the open symbols loadings as calculated from configurational-bias Monte Carlo simulations.

higher packing efficiency of *n*-hexane, as explained above, there is a preference of adsorbing this component. Only at higher 2-methylpentane fractions, the linear alkane is being replaced, and a non-linear dependence on the mixture ratio is observed.

To be able to better compare the results obtained from configurational-bias Monte Carlo simulations with the present study, a number of simulations have been performed under equal conditions as used in this work. The calculated loadings from these simulations are shown as open symbols in figure 6. Details about the CBMC simulation technique and the zeolite and alkane models used can be found in Smit and Siepmann³³ and Vlucht et al.²⁹ The calculated loadings of the single components are slightly higher than the values obtained from TEX-PEP measurements. This is probably due to the use of a perfect crystal structure in the simulations, and the presence of defects in the silicalite crystals used in this study. The slight decrease of the total loading is predicted correctly by the simulations. The slight preference for the adsorption of *n*-hexane however is not observed, but instead a (very) small preference for the branched alkane is seen. This can probably be attributed to imperfections in the model parameters used for the CBMC simulations.

5.4.3 Multicomponent diffusion

Figure 5.7 shows the diffusion coefficients as obtained from the TEX-PEP experiments for *n*-hexane and 2-methylpentane as a function of the gas phase composi-

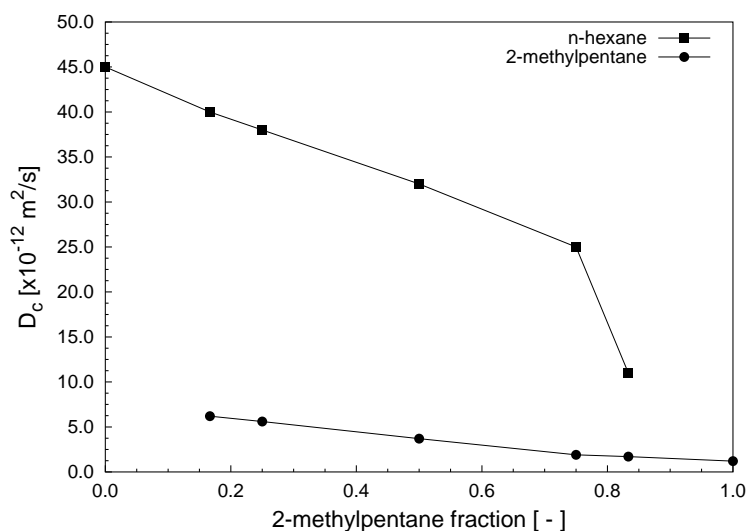


Figure 5.7: Self-diffusion constant as a function of 2-methylpentane fraction in the gas phase for *n*-hexane and 2-methylpentane at 433 K and a hydrocarbon pressure of 6.6 kPa.

tion. Obviously, the diffusivity of pure *n*-hexane is much higher as for the larger 2-methylpentane molecules (approximately a factor of 9). For both components, a decrease in mobility is observed with an increasing fraction of the branched alkane in the gas phase. The 2-methylpentane behaves essentially in a way one would expect for a single-component system (see e.g. Schumacher and Karge,³⁴ Schuring et al.³⁵), whereby the diffusivity monotonically decreases with increasing loading of this component. The diffusivity of the faster *n*-hexane depends more strongly on the composition of the gas mixture. As the loading of *n*-hexane decreases with increasing 2-methylpentane fraction, but the total loading remains approximately constant, this decrease in mobility must result from interactions with its branched isomer in the system. Most remarkable is the sudden drop in diffusivity above a 2-methylpentane fraction of 0.75.

The diffusivity of molecules inside the zeolite lattice depends strongly on the loading of the zeolite crystal.³⁵ The plot shown in figure 5.7 should therefore be treated with some caution, as the dependency of the diffusion constant on the gas phase composition is also influenced by the adsorptive behaviour of the alkanes. In this case, however, the influence of adsorption is limited because the total loading remains constant and there is only a small preferential adsorption for *n*-hexane. The results can therefore be directly related to MD studies from other authors, where one commonly uses a fixed total loading and diffusivities as a function of the adsorbed phase fraction.

100 Measurement and Simulation of Binary Diffusion in Zeolites

For 2-methylpentane fractions lower than 0.75, the behaviour found in this study is essentially identical as that obtained in other studies.^{4, 10, 36} In all these systems it was found that the diffusivity of the slow component is essentially unaffected by the presence of the fast component. The diffusive behaviour can be understood on the basis of a simple jump diffusion model, in which diffusion is thought of as a sequence of activated jumps from one site to another, as was already demonstrated by Masuda et al.¹⁰ Such a jump can only be successful if the site to which the molecule jumps is empty. Although the jump frequency itself does not depend on the composition of the mixture, the number of successful jumps will. When the amount of slowly moving molecules (2-methylpentane) increases, they will essentially block the channel segments, and the number of successful jumps of the fast component (*n*-hexane) will be determined by the rate at which an empty site is created by a jump of the slow component. At high 2-methylpentane loadings, the diffusivity of *n*-hexane will thus be strongly determined by the diffusion rate of its branched isomer. The dependency of the 2-methylpentane diffusivity itself on mixture composition observed in this study is mainly caused by the relatively high total loading at the conditions used. In this case, the interactions between the branched alkanes themselves play an important role and will seriously decrease the mobility of the slow-moving component at higher fractions in the gas phase. This was also observed in the work by Jost et al.,⁴ where the slow component (in this case xenon) showed an increasing dependency on the mixture composition with increasing total loading of the zeolite.

The sudden drop in the diffusivity of *n*-hexane at a ratio above 0.75 is due to the particular adsorptive properties of both components in silicalite. As was shown by Vlugt et al.,²⁹ 2-methylpentane preferentially adsorbs in the intersections between straight and zigzag channels. When a large part of the intersections is occupied by the slowly diffusing branched alkanes, the entire pore system will essentially be blocked, and diffusion of the fast component will be totally determined by the hopping rate of the slow component moving from one intersection to another. This is strongly supported by the fact that the sudden drop in diffusivity takes place at a 2-methylpentane loading of about three molecules per unit cell, meaning that 75% of the intersections is occupied as each unit cell of silicalite contains four channel intersections. A similar effect was observed in a system of methane and benzene in zeolite NaY³⁷ and silicalite.³⁸ In NaY, the benzene molecules effectively block the windows of the supercages for the faster methane. In zeolite silicalite, Förste et al.³⁸ showed that the decrease of methane diffusivity was also caused by blocking of the channel intersections by benzene.

The results obtained here emphasize the importance of the structure of the zeolite channels when looking at multi-component diffusion. The sudden drop in diffusivity of the fast component in this system is a direct result of the adsorptive be-

haviour of both components and the channel topology of the zeolite. This explains why a similar behaviour was not observed in previous studies. For example, for the methane/Xenon⁴ and methane/tetrafluoromethane³² mixtures in silicalite, both components are preferentially sited in the interiors of the (straight and zigzag) channels, causing the blocking by the slow components to be less dramatic. For the *n*-butane/methane system,³⁶ the fast component (methane) shows a slight preference for adsorption in the intersections, while the slow component resides in the channels. Although the results cannot be directly compared, an accelerated drop was indeed observed, but only at much higher loadings.

The dependency of multicomponent diffusion on adsorption properties and zeolite topology has some important consequences for the description of mass transfer in binary systems. Usually, the transport of these mixtures in a packed zeolite bed during transient experiments will be described by diffusion equations, using diffusion constants which are independent of the loading. The current results show that this is definitely not the case, as the diffusivity can be a strong function of the mixture composition. A more advanced approach for describing mass transfer is provided by the Maxwell-Stefan theory, which has been applied successfully to diffusion and adsorption in zeolites.^{39, 40} In a recent study, Krishna showed that this theory could indeed describe the behaviour as observed in MD simulations of methane/xenon, methane/CF₄, and methane/*n*-butane.⁴⁰ However, although the Maxwell-Stefan theory accounts for sorbate-sorbate interactions, it does not explicitly incorporate the pore structure and siting of the molecules, and will likely fail to describe the phenomena shown in this work. Whether or not the multi-component diffusivity can be predicted from single-component diffusivities will thus depend on the particular system under study, and a general application of the Maxwell-Stefan theory should be treated with caution. Instead, more detailed model descriptions are needed to gain insight in the diffusive behaviour. Among these descriptions are Monte Carlo lattice dynamics simulations^{41, 42} and percolation theory.⁴³

Also for systems in which reactions take place, the behaviour observed here might have some important implications. The *n*-hexane/2-methylpentane mixture could represent a reactant/product system. In that case, the mobility can become a strong function of the radial coordinate of the crystal. In extreme cases, reactants or products could be piled up inside the crystals, essentially blocked by the slow components present in the system, thus having a serious effect on the activity of the catalyst.

5.5 Conclusions

In this work, the tracer-exchange positron emission profiling (TEX-PEP) technique has been used for determining the adsorptive and diffusive properties of an *n*-hexane/2-

methylpentane mixture at elevated temperatures (433 K). With this technique, the re-exchange of radioactively labelled molecules can be studied as a function of time and position inside the reactor. By only labelling one of the components in the feed, the mass transport properties of each individual component can be determined. Determination of these properties is done by fitting a numerical model for mass transfer in a packed zeolite bed, accounting for convection, adsorption at the crystal boundary, and diffusion between and inside the crystals, to the measured concentration profiles. Under the conditions used in this study, the adsorption/desorption process at the crystal boundary does not have to be explicitly accounted for, as the diffusive process is the rate-determining process at the crystal surface.

The system shows a slight preference for the adsorption of *n*-hexane over 2-methylpentane. This is due to the fact that it is entropically more favorable to adsorb the linear alkane, as it can reside anywhere in the pore system, while the branched alkane is preferentially adsorbed in the intersection between straight and zigzag channels. This is in line with the conclusions obtained from CBMC simulations of Vlugt *et al.* at lower temperatures and a constant mixture ratio. CBMC simulations performed at similar conditions as in this work show a reasonable agreement, although a slightly different behaviour is predicted by these calculations.

As was also observed in earlier studies, the diffusion of the fast-moving *n*-hexane molecules is strongly influenced by the presence of the slowly diffusing 2-methylpentane. The measurements however show a large drop in diffusivity at a large 2-methylpentane fraction in the gas phase. Most likely, this is due to the blocking of the channel intersections by the slowly moving branched alkanes. This indicates that the adsorptive properties of the different components, together with the topology of the zeolite pores plays an important role in the behaviour of multi-component systems. Models based on mean field approximations of the diffusion, like Fick's law and Maxwell-Stefan diffusion, should therefore be treated with caution.

5.6 References

- ¹ J. Kärger and D. M. Ruthven, *Diffusion in zeolites and other microporous solids*, John Wiley & Sons, Inc., New York (1992).
- ² J. Kärger, *Determination of diffusion coefficients in porous media*, in: *Handbook of heterogeneous catalysis*, G. Ertl, H. Knözinger, and J. Weitkamp, eds., pp. 1253–1261, VCH, Weinheim (1997).
- ³ M. Heuchel, R. Q. Snurr, and E. Buss, *Langmuir* **13**, 6795–6804 (1997).
- ⁴ S. Jost, N.-K. Bär, S. Fritzsche, R. Haberlandt, and J. Kärger, *J. Phys. Chem. B* **102**(33), 6375–6381 (1998).
- ⁵ L. F. Gladden, J. A. Sousa-Gonçalves, and P. Alexander, *J. Phys. Chem. B* **101**(48), 10121–10127 (1997).

- ⁶ L. N. Gergidis, D. N. Theodorou, and H. Jobic, *J. Phys. Chem. B* **104**(23), 5541–5552 (2000).
- ⁷ N. V. Choudhary, R. V. Jasra, S. G. T. Bhat, and T. S. R. P. Rao, in: *Zeolites: Facts, figures, future, Proceedings of the 8th International Zeolite Conference, Amsterdam, The Netherlands, July 10–14, 1989*, P. A. Jacobs and R. A. van Santen, eds., vol. 49 of *Studies in Surface Science and Catalysis*, pp. 867–876, Elsevier, Amsterdam, The Netherlands (1994).
- ⁸ W. Niessen and H. G. Karge, *Microporous Mater.* **1**, 1–8 (1993).
- ⁹ H. H. Funke, A. M. Argo, J. L. Falconer, and R. D. Noble, *Ind. Eng. Chem. Res.* **36**(1), 137–143 (1997).
- ¹⁰ T. Masuda, Y. Fujikata, H. Ikeda, and K. Hashimoto, *Microporous Mesoporous Mater.* **38**, 323–332 (2000).
- ¹¹ B. G. Anderson, R. A. van Santen, and L. J. van IJzendoorn, *Appl. Catal. A* **160**, 125–138 (1997).
- ¹² B. G. Anderson, R. A. van Santen, and A. M. de Jong, *Top. Catal.* **8**, 125–131 (1999).
- ¹³ B. G. Anderson, N. J. Noordhoek, F. J. M. M. de Gauw, L. J. van IJzendoorn, M. J. A. de Voigt, and R. A. van Santen, *Ind. Eng. Chem. Res.* **37**(3), 815–824 (1998).
- ¹⁴ R. R. Schumacher, B. G. Anderson, N. J. Noordhoek, F. J. M. M. de Gauw, A. M. de Jong, M. J. A. de Voigt, and R. A. van Santen, *Microporous Mesoporous Mater.* **35–36**, 315–326 (2000).
- ¹⁵ B. Smit and T. L. M. Maesen, *Nature* **374**, 42–44 (1995).
- ¹⁶ R. H. Cunningham, A. V. G. Mangnus, J. van Grondelle, and R. A. van Santen, *J. Molec. Catal. A: Chem.* **107**, 153–158 (1996).
- ¹⁷ A. V. G. Mangnus, L. J. van IJzendoorn, J. J. M. de Goeij, R. H. Cunningham, R. A. van Santen, and M. J. A. de Voigt, *Nucl. Instr. and Meth. in Phys. Res. B* **99**, 649–652 (1995).
- ¹⁸ J. B. Rosen, *J. Chem. Phys.* **20**(3), 387–394 (1952).
- ¹⁹ T. A. Nijhuis, L. J. P. van den Broeke, M. J. G. Linders, J. M. van de Graaf, F. Kapteijn, M. Makkee, and J. A. Moulijn, *Chem. Eng. Sci.* **54**(4423–4436) (1999).
- ²⁰ N. J. Noordhoek, L. J. van IJzendoorn, B. G. Anderson, F. J. de Gauw, R. A. van Santen, and M. J. A. de Voigt, *Ind. Eng. Chem. Res.* **37**(3), 825–833 (1998).
- ²¹ U. Hong, J. Kärger, R. Kramer, H. Pfeifer, G. Seiffert, U. Müller, K. K. Unger, H.-B. Lück, and T. Ito, *Zeolites* **11**, 816–821 (1991).
- ²² W. E. Schiesser, *The Numerical Method of Lines: Integration of Partial Differential Equations*, Academic Press, San Diego (1991).
- ²³ D. Marquardt, *SIAM J. Appl. Math.* **11**, 431–440 (1963).
- ²⁴ P. W. Atkins, *Physical Chemistry*, Oxford University Press, Oxford, United Kingdom, 5 ed. (1994).
- ²⁵ G. Emig and R. Dittmeyer, *Handbook of heterogeneous catalysis*, chap. Simultaneous heat and mass transfer, 1209–1252, VCH, Weinheim (1997).
- ²⁶ Y. Yang and L. V. C. Rees, *Microp. Mater.* **12**, 117–122 (1997).
- ²⁷ W. J. M. van Well, J. P. Wolthuizen, B. Smit, J. H. C. van Hooff, and R. A. van Santen, *Angew. Chem. Int. Ed. Engl.* **34**, 2543–2548 (1995).
- ²⁸ C. L. C. Jr. and D. M. Ruthven, *Ind. Eng. Chem. Res.* **34**(1), 177–184 (1995).
- ²⁹ T. J. H. Vlucht, R. Krishna, and B. Smit, *J. Phys. Chem. B* **103**(7), 1103–1118 (1999).
- ³⁰ V. Cottier, J.-P. Bellat, and M.-H. Simonot-Grange, *J. Phys. Chem. B* **101**(24), 4798–4802

104 Measurement and Simulation of Binary Diffusion in Zeolites

- (1997).
- ³¹ B. A. Buffham, G. Mason, and M. J. Heslop, *Ind. Eng. Chem. Res.* **38**(3), 1114–1124 (1999).
- ³² R. Q. Snurr and J. Kärger, *J. Phys. Chem. B* **101**(33), 6469–6473 (1997).
- ³³ B. Smit and J. I. Siepmann, *J. Phys. Chem.* **98**(34), 8442–8452 (1994).
- ³⁴ R. Schumacher and H. G. Karge, *J. Phys. Chem. B* **103**(9), 1477–1483 (1999).
- ³⁵ D. Schuring, A. P. J. Jansen, and R. A. van Santen, *J. Phys. Chem. B* **104**(5), 941–948 (2000).
- ³⁶ L. N. Gergidis and D. N. Theodorou, *J. Phys. Chem. B* **103**(17), 3380–3390 (1999).
- ³⁷ S. S. Nivarthi, H. T. Davis, and A. V. McCormick, *Chem. Eng. Sci.* **50**(20), 3217–3229 (1995).
- ³⁸ C. Förste, A. Germanus, J. Kärger, H. Pfeifer, J. Caro, W. Pilz, and A. Zikánová, *J. Chem. Soc., Faraday Trans. 1* **83**(8), 2301–2309 (1987).
- ³⁹ F. Kapteijn, J. A. Moulijn, and R. Krishna, *Chem. Eng. Sci.* **55**, 2923–2930 (2000).
- ⁴⁰ R. Krishna, *Chem. Phys. Lett.* **326**, 477–484 (2000).
- ⁴¹ M.-O. Coppens, A. T. Bell, and A. K. Chakraborty, *Chem. Engng. Sci.* **53**(11), 2053–2061 (1998).
- ⁴² D. Paschek and R. Krishna, *Phys. Chem. Chem. Phys.* **2**, 2389–2394 (2000).
- ⁴³ D. Keffer, A. V. McCormick, and H. T. Davis, *J. Phys. Chem.* **100**(3), 967–973 (1996).

6

The Influence of Siting on Adsorption and Diffusion

A number of different factors determine the behaviour of diffusing molecules in zeolites. What is most important is the interaction between the different molecules. How strong they interact with each other is determined by the pore topology and the siting of the molecules. The influence of this siting is investigated using dynamic Monte Carlo simulations of a simple 2-dimensional model of the zeolite pore system. Both the adsorption and diffusion will be considered, and the influences of different model assumptions will be investigated.

6.1 Introduction

As in many applications of zeolites as catalysts diffusion and adsorption in these materials occurs under varying concentrations and composition of the adsorbents, a better understanding of these processes in these materials is of practical importance. A number of different techniques have been applied to describe the diffusion in zeolites, ranging from microscopic simulations such as molecular dynamics¹ and kinetic Monte Carlo simulations,² to phenomenological descriptions such as Fick's law of diffusion^{3,4} and Maxwell-Stefan theory.^{5,6} Although molecular dynamics studies have proven to be very useful in the study of diffusion on a microscopic level,⁷ these simulations are computationally rather demanding. As a result, their usefulness is mainly limited to species that move sufficiently fast through the zeolite, and most efforts on simulating single-component and binary diffusion have been focussed on smaller molecules.⁸⁻¹¹ The phenomenological descriptions on the other hand are di-

106 The Influence of Siting on Adsorption and Diffusion

rectly applicable to describe the flow in laboratory-scale systems and are thus of great practical importance, but lack any intrinsic information about the specific structure of the zeolite and its interactions with the adsorbates. As a result, these methods often have to rely on experimentally obtained information on the adsorptive and diffusive behaviour of the adsorbates of interest in the specific zeolite.

One of the questions that has been raised by previous investigations¹² is in what way the diffusive behaviour is influenced by the specific siting (the place where the molecules are preferentially located) of the molecules in the pore system. While the zeolite-alkane interactions determine the mobility of the individual species, the zeolite pore topology (i.e. the way in which the pores of the zeolite are connected) strongly determines how much hindrance these molecules experience from each other. This dependency is immediately clear when one considers zeolites with one-dimensional pore structures compared to the three-dimensional systems. In the one-dimensional case, once the particles are adsorbed they are unable to pass each other,¹³ while in the three-dimensional structure the particles are still able to overtake another by travelling via a different channel. A more subtle example of the structural dependency is the exact position inside the pore system at which the different components in the mixture reside. If a component strongly adsorbs in the intersections between different channels and essentially block the way for other molecules, a stronger influence on the mobility can be expected than when these particles adsorb in the channels.

As the main interest is the influence of the pore topology and the siting of the molecules in these channels, a detailed model of the interactions between adsorbates and the zeolite is not essential, and a less detailed type of simulation can be applied. Dynamic (sometimes also referred to as kinetic) Monte Carlo simulations have proven to provide useful insight in the influence of pore topology, strong adsorption sites and concentration on the diffusivity.¹⁴⁻¹⁶ In these simulations, the zeolite pores are treated as a sequence of adsorption sites, whereby diffusion takes place by jumping from one site to another. As a result, these simulations are computationally much less demanding than detailed molecular dynamics simulations. While in principle it is possible to construct a detailed model of the zeolite-sorbate system,¹⁷ the main interest in this chapter is to get some feeling of the influence of the siting on the adsorptive and diffusive behaviour. Therefore, a much simpler approach is chosen, in which a 2-dimensional lattice model is used in which only some of the essential features observed in real systems is built in.

This chapter will start with a short discussion of the dynamic Monte Carlo technique. Next, the lattice model used in this study will be discussed. For the construction of this simulation lattice, the behaviour of alkanes in silicalite will be considered, and some of the essential features of these systems will be incorporated. The models will first be used to study the adsorptive and diffusive behaviour of single compo-

nents in the system. The influence of preferential siting and interactions between the different molecules will be considered and compared with the behaviour of zeolite-adsorbate systems in literature. Next, the effect of site blocking on the self-diffusivity will be considered. Finally, binary mixtures will be considered, where the emphasis will be on the influence of siting on the diffusive behaviour of the mixture.

6.2 Modeling the diffusion in a 2-D pore network

6.2.1 Dynamic Monte Carlo simulations

The application of dynamic Monte Carlo simulations is based on the fact that the diffusion of molecules through a zeolite can be treated as a “random walk”, in which particles move by a sequence of random jumps occurring through time. In these simulations, the zeolite itself is modeled as a grid of coarse-grained adsorption sites which are connected by bonds.¹⁸ In order to jump from one site to another, the particles have to overcome a certain free energy barrier, and the hops between the different sites are thus activated. As the diameter of the pores inside the zeolites are typically of the same dimensions as the diffusing molecules, the adsorption sites can usually only hold a single particle. As a result, a jump from one site to another will only be successful when this site is empty. Furthermore, particles cannot pass each other when they are adsorbed in the same channel.

While it is customary to describe the mobility of species in terms of diffusion coefficients, in dynamic Monte Carlo simulations the mobility is determined by the elementary hopping rate or, analogously, the average residence time on the adsorption sites. At infinite dilution, these quantities can however be easily related to a diffusion coefficient:¹⁹

$$D_s = \frac{l^2}{2d\tau_h} = \frac{l^2 k_h}{2d} \quad (6.1)$$

in which D_s is the self-diffusion coefficient, l is the distance between two adsorption sites on the lattice, d the dimensionality of the lattice ($d = 2$ for a 2-dimensional system), τ_h is the average residence time on the site (or the average time interval between two attempted hops), and k_h the hopping frequency. At higher loadings it is much more difficult to relate these two quantities as in this case correlation effects play an important role. A mean-field approximation yields the result that the diffusivity at higher loadings should be proportional to $(1 - \theta)$, as this factor is equal to the average chance that the neighbouring site will be empty.²⁰ In reality, the decreased connectivity and correlation effects lead to much more complicated dependencies.²¹

The hopping rate k can be related to the energy barrier E_{act} between the different

108 The Influence of Siting on Adsorption and Diffusion

adsorption sites via an Arrhenius-type equation:

$$k = v_0 \exp \left[-\frac{E_{act}}{k_B T} \right] \quad (6.2)$$

in which v_0 is the pre-exponential factor, k_B is the Boltzmann constant, and T is the temperature. The activation energy will depend on the sorbate and the size and shape of the zeolite pores, and can furthermore be influenced by the presence of other particles. To account for these lateral interactions, a simple scheme analogous to that of Paschek and Krishna²² was used, although more complicated models for these interactions exist.²³ Using this procedure, two neighbouring particles at sites α and β each feel a repulsive interaction equal to $\delta E_{\alpha\beta}$. As these interactions are additive, the total repulsion felt by a particle at site α is equal to

$$\delta E_\alpha = \sum_{\beta} \delta E_{\alpha\beta} \quad (6.3)$$

in which β are the occupied nearest neighbour sites. The depth of the potential well of the adsorption site α is thus modified by δE_α , and assuming that the energy of the transition state is unchanged, the activation energy is thus also modified by an equal amount.

For the simulations, the first reaction method (or discrete event simulation algorithm) is used. In this method, a tentative time is calculated for all possible reactions. The time δt at which a reaction takes place, is randomly chosen from a Poisson distribution:

$$\delta t = -\frac{1}{k_h} \ln(u), \quad u \in [0, 1] \quad (6.4)$$

in which u is a uniform random deviate. This correctly accounts for the effect of the jump time distribution, something often neglected in the earlier simulations where jumps were assumed to take place with a fixed interval τ_h .²⁴ The tentative reaction times are stored in a list, after which the first occurring reaction is executed, the system time is updated to the time of this reaction, and the event list is updated. This procedure is repeated until the end of the simulation.

6.2.2 The lattice-gas model

For the simulations, a two-dimensional lattice was chosen to investigate the adsorptive and diffusive behaviour. Although most zeolites have a three-dimensional pore structure, simulations with two-dimensional lattices have already proven to be useful gaining more insight in the diffusive behaviour in these materials,^{19, 25, 26} and are

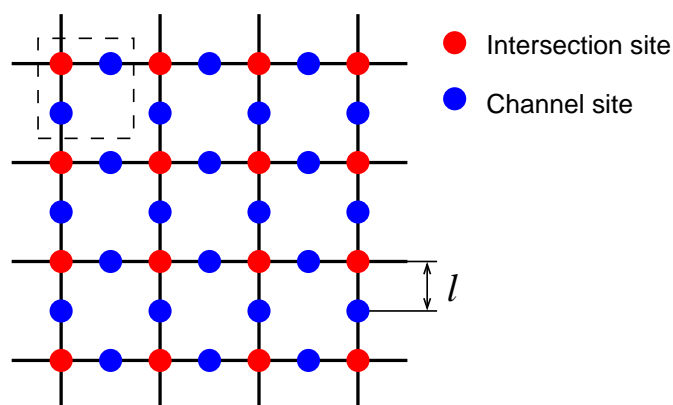


Figure 6.1: The two-dimensional grid used for the dynamic Monte Carlo simulations, containing intersection and channel sites. The unit cell is indicated by the square dotted box in the top left corner.

furthermore computationally less demanding. Most of the early studies have been focussed on simple square lattices in which all sites have an identical number of neighbours and adsorptive properties. It will therefore be worthwhile to study the behaviour of some more complex two-dimensional structures.

Although the aim is not to describe in detail the pore topology and behaviour of a specific system, it is worthwhile to review the behaviour of alkanes (specifically hexane and its isomers) in silicalite and try to incorporate some of the essential features in the present two-dimensional model. The sorption behaviour of alkanes in silicalite has already been studied extensively using equilibrium Monte Carlo simulations.^{27–30} For *n*-hexane, the observation of a transition in the adsorption isotherm due to commensurate freezing is now well-established.^{27, 28, 31} While at low pressures the *n*-hexane molecules are distributed evenly over the entire pore system, at higher pressures the molecules are localized in the zigzag channels, freeing the intersections and enabling the complete filling of the straight channels. As the branched alkanes are more bulky, these molecules are preferentially sited in the intersections of the zeolites.²⁸ Only at high pressures the molecules also adsorb between the intersections and reside in the zigzag channels only.

From the above description of the adsorptive behaviour, it is clear that one of the characteristic features of this zeolite is the presence of different adsorption sites at the intersections between the straight and zigzag channels, and in the channel segments themselves. In analogy, the two-dimensional model employed here is also built up of channel and intersection sites. A similar approach has already been used for more detailed three-dimensional models of the silicalite structure.^{15, 16, 32} The resulting lattice is shown in figure 6.1. The unit cell of this lattice contains only three sites:

110 The Influence of Siting on Adsorption and Diffusion

Table 6.I: Values used for the calculation of the hopping rates, and the calculated elementary hopping rates for the two species.

	<i>n</i>-hexane (fast species)	2-methylpentane (slow species)
D_c (433 K)	$1.0 \cdot 10^{-10} \text{ m}^2 \cdot \text{s}^{-1}$	$2.5 \cdot 10^{-12} \text{ m}^2 \cdot \text{s}^{-1}$
l	5 Å	5 Å
k_h	$4.0 \cdot 10^8 \text{ s}^{-1}$	$2.5 \cdot 10^6 \text{ s}^{-1}$
$k_a \cdot p$	$1.0 \cdot 10^7 \text{ s}^{-1}$	$1.0 \cdot 10^7 \text{ s}^{-1}$

one intersection and two channel sites. The intersection sites all have four nearest neighbours, while the channel sites have only two. Calculations of the free energy profiles along the different channels performed by some authors^{33, 34} furthermore indicate that more than one adsorption site can be present inside the channels, and some authors indeed include more than one site in their model.³² If one compares the lattice dimensions with the typical end-to-end chainlength of e.g. *n*-hexane, which is equal to 6.7 Å,³⁵ it is evident that for molecules of these dimensions not all sites can be occupied simultaneously, and these sites are usually energetically less favorable, these will not be considered. Comparisons between models with and without these additional sites furthermore showed that assuming additional adsorption sites did not lead to any significant differences in the diffusive behaviour.

For the diffusion simulations, two different species are considered. The choice of the hopping rates was made with the *n*-hexane/2-methylpentane system kept in mind. It should however be noted that the exact choice of these parameters can be rather arbitrary, as they merely determine the timescale of simulations and the absolute value of the calculated diffusion constants. For the qualitative behaviour these absolute values are of less interest, and what is most important is the ratios between the different hopping rates, and the diffusivities will usually be normalized on the diffusivity at zero coverage. The values of interest for the different species are summarized in table 6.I. From the diffusivities and the corresponding jump length, values for the rate constants were calculated using eq. 6.1.

The fast-moving species, representing the *n*-hexane molecules, have an equal probability to adsorb on the two types of sites. The slowly moving species, representing the branched alkane, has a preference for adsorbing in the intersections. This preference can be incorporated in the lattice model in two different ways. Paschek *et al.*^{22, 36} assumed that, for these species, diffusion only by direct hops from one intersection site to another. However, at higher pressures the branched alkanes can be forced into the channels although these positions are energetically not favorable^{33, 34} and the possibility to reside on the channel sites should thus be included in the model.

The other method that can be applied to account for this behaviour is to assume that the rate of jumping from an intersection site to a channel site ($k_{i \rightarrow c}$) is much slower than the backward step ($k_{c \rightarrow i}$). This model reflects that, in the narrow channels, the bulky branched isomer is destabilized due to steric constraints, leading to a much weaker adsorption and lower activation barriers for a jump to the intersections.³³ At lower loadings, an equilibrium will thus be reached, and the occupation of the intersection sites compared to that of the channel sites will be equal to the ratio between the forward and backward step.

Apart from diffusion, adsorption of molecules will also be considered. As the adsorption of molecules only takes place at the pore mouth, these processes are assumed to only occur at the edges of the lattice. The rate of adsorption can be estimated using gas kinetic theory:³⁷

$$k_a = \frac{1}{4\alpha} \frac{s_0 p}{\sqrt{2\pi m k_B T}} A \quad (6.5)$$

in which p is the gas-phase pressure, s_0 is the sticking coefficient at zero loading, A the surface area of the zeolite pore, and m the mass of the particle. The factor α accounts for the fact that not all collisions will lead to a successful adsorption, and that adsorption might also take place due to surface diffusion effects.³² From this equation, it can be seen that the rate of adsorption depends linearly on the gas-phase pressure. The value of α is difficult to determine, but in general this factor seems to be larger than one as the surface diffusion significantly enhances the adsorption rate. For the rate of desorption it is assumed that no surface barrier exists for this process, and the desorption rate is identical to the diffusion rate. Again, the exact values of these parameters are not important, as it is the ratio between the adsorption and desorption rate which in the first place determines the equilibrium loading in the simulation grid.

6.2.3 Computational details

The model described in the previous section provides a stochastic description for the diffusion of molecules through a two-dimensional lattice. The time evolution of such a system can be described by the chemical Master Equation (ME), which can be solved numerically using dynamic Monte Carlo simulations.^{38, 39} A number of different Monte Carlo methods can be used, all yielding similar result but varying in efficiency for different systems.⁴⁰ In this study, the general-purpose Monte Carlo code Carlos⁴¹ was used. This program implements the first reaction method and the variable step-size method, depending on the rate of the different reactions in the model. A detailed description of the program and algorithms can be found in Segers⁴⁰ and Lukkien *et al.*⁴¹

112 The Influence of Siting on Adsorption and Diffusion

At the start of the simulation, the lattice has to be defined. The number of sites was chosen to be sufficiently large in order to reduce finite size effects. Simulations conducted with different grid sizes showed that for lattices consisting of 100×100 sites and more yielded identical results, and all lattices were taken equal to or greater than this size. When the adsorption of a species is simulated, the lattice is initially empty. The boundary of the pore network is then subject to a gas phase, after which the simulation is run for a certain amount of time. During this run, the loading of the lattice is regularly monitored, and the run is continued until an equilibrium is reached after which the loading is determined. The loading or coverage θ is defined as:

$$\theta = \frac{N_{ads}}{N_{max}} \quad (6.6)$$

in which N_{ads} is the number of adsorbed particles, and N_{max} the maximum number of particles that can be adsorbed on a given lattice model. The coverage thus equals the ratio between occupied sites and the number of sites that can be occupied at infinite pressure (which is not necessarily the total number of adsorption sites). In case of simulations in which the dynamic properties are of interest, the particles are randomly placed on the lattice until the desired loading is reached. In this case, adsorption and desorption are not allowed, and periodic boundary conditions are applied. For the individual particles, the position is determined at different times so that the mean-square displacement can be calculated. From this displacement the self-diffusion coefficient (D_c) can then be calculated using the Einstein relation.

6.3 Adsorption of Single-component systems

Before binary diffusion and adsorption will be investigated, it is worthwhile to examine the single-component behaviour first. One of the interesting features present in the adsorption isotherms of single components is the inflection at certain loadings, as for example observed for linear and branched alkanes in silicalite.⁴²⁻⁴⁴ The existence of these inflections seem to be strongly related to the positions inside the zeolite pore network at which the molecules are preferentially located.^{27, 45} As some of these effects can be easily incorporated in the Monte Carlo model, the influence on the calculated adsorption isotherms can be studied.

6.3.1 Influence of preferential siting

Figure 6.2 shows the calculated adsorption isotherms for the lattice containing channel and intersection sites using the parameters as discussed in section 6.2.2, both with and without preferential adsorption in the intersections. For the system without preferential adsorption, a simple langmuir-type adsorption isotherm is observed. In this

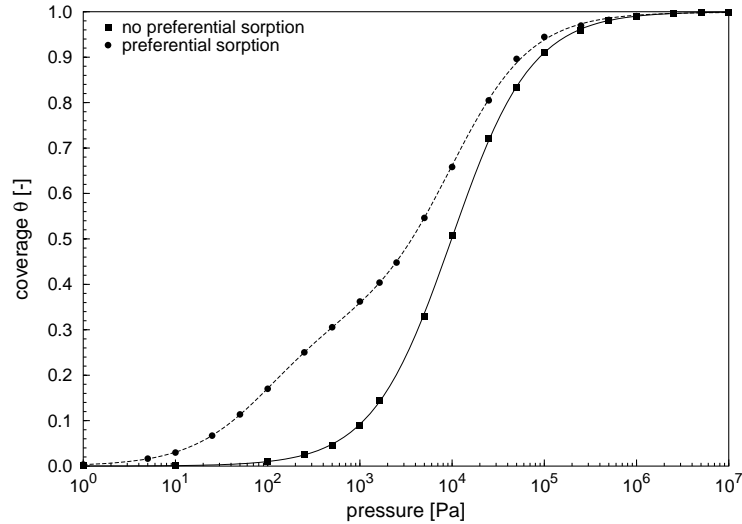


Figure 6.2: Adsorption isotherm for a single-component system without and with preferential adsorption in the intersections. The lines are fits of a Langmuir (—) and a dual Langmuir isotherm (- -), respectively.

case, in equilibrium the loading of all sites inside the lattice is identical and is thus determined by the coverage of the boundary sites. As the rate of adsorption at the edges is proportional to the pressure and the fraction of unoccupied sites and the desorption rate to the fraction of occupied sites, Langmuir adsorption occurs. The simulation results could be described excellently using a simple Langmuir isotherm:⁴⁶

$$\theta = \frac{K_{eq}P}{1 + K_{eq}P}; \quad K_{eq} = \frac{k_f}{k_b} \quad (6.7)$$

in which K_{eq} is the equilibrium constant, equal to the ratio between the adsorption rate k_f and desorption rate k_b . This again shows that, as stated before, it is not the absolute value of the adsorption and desorption rates that determines the adsorptive behaviour, but merely the ratio between them.

A completely different behaviour is observed for the system in which the particles are preferentially sited in the intersections of the pore system by assuming that the hopping rate to the intersections is much faster than in the reverse direction. In this case, adsorption already starts at much lower pressures. This is due to the fact that, in this model, the boundary is built up of channel sites only. Because of the strong preference of the particles to adsorb in the intersection sites, there is a high chance that a particle moves to such a neighbouring site before it can possibly desorb again. As a result, the coverage at the boundary sites remains low, decreasing the rate of desorption and increasing the rate of adsorption, leading to an increased loading at a

114 The Influence of Siting on Adsorption and Diffusion

given partial pressure. At a coverage of about 0.3, a “kink” is visible in the isotherm. At this point, almost all intersection sites are occupied, and the channel sites start to be filled. As the adsorption on these sites is unfavourable, adsorption only starts at higher pressures because the high loading on the intersections enhances the hopping rate to the channel sites and decreases the rate of jumps in the reverse direction.

Clearly, the assumption of a preference for a certain type of adsorption site in the zeolite network leads to the well-known inflection behaviour present in these systems. This furthermore supports the conclusions by various authors that the kink in the isotherms of branched alkanes^{28, 47–49} and benzene^{50, 51} in silicalite that this is due to the preferential siting of these components in the intersections of the zeolite. Already for small differences between the hopping rates to and from the intersection sites ($k_{c \rightarrow i}/k_{i \rightarrow c}$) the inflection could be observed in the simulations. In case of a system with two types of adsorption sites, a dual-site langmuir model can be used to describe the adsorption in these systems:^{48, 52}

$$\theta = \frac{\Theta_A K_A P}{1 + K_A P} + \frac{\Theta_B K_B P}{1 + K_B P} \quad (6.8)$$

in which Θ_A and Θ_B are the saturation coverages and K_A and K_B the adsorption constants for sites A and B, respectively. As can be seen in figure 6.2, the simulated isotherm can be described perfectly using this equation. The values found for the saturation coverages Θ_A and Θ_B indeed closely match the fraction of channel and intersection sites.

As there is a preference for adsorption in the intersections, the type of sites present at the boundary of the lattice is expected to have an influence on the calculated adsorption isotherm. That this is indeed the case is illustrated in figure 6.3, which shows the calculated isotherms using exactly the same parameters for the adsorption, desorption and diffusion processes, but with boundary sites consisting of channel sites only, and of both channel and intersection sites. When the lattice boundary also contains intersection sites, the higher loading on these sites causes a much higher rate of desorption and lower rate of adsorption at the edges, and higher pressures are needed to fill the lattice. Isotherm inflection is also observed in this case, and seems to be even slightly stronger while the inflection point is shifted to higher coverages. Although the type of simulations conducted here are an oversimplified representation of the adsorption processes taking place on real zeolites, these results do however raise some questions as to whether the exact composition of the surface might influence the adsorption properties of these materials. A similar question was raised in a recent molecular dynamics study conducted by Webb III and Grest,⁵³ in which the properties of liquid-zeolite interfaces was studied. The present results at least show that one should be careful with using these models to describe the adsorptive behaviour in zeolite networks, as the behaviour is significantly influenced by the

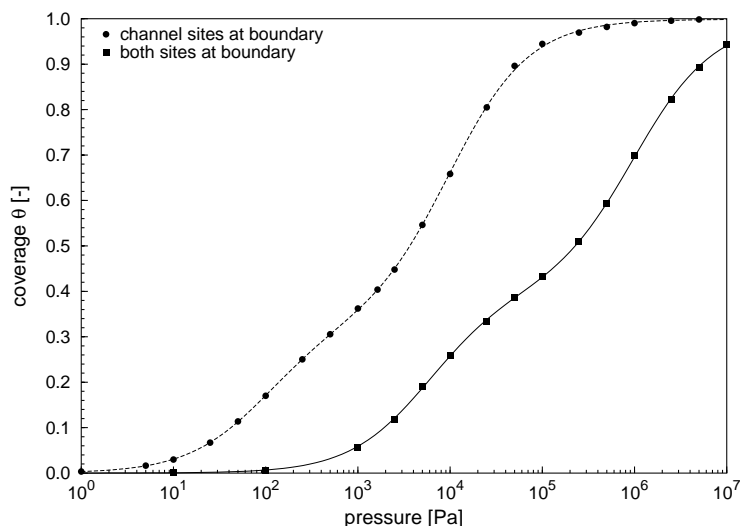


Figure 6.3: Adsorption isotherm for a single-component system on a lattice with only channel sites at the boundaries (—), and with both channel and intersection sites (- -).

model assumptions.

6.3.2 Influence of lateral interactions

For the inflection observed in the adsorption isotherms of certain linear alkanes (like ethane, hexane, heptane) in silicalite, an alternative explanation was originally forwarded by Smit and Maesen.²⁷ According to these authors, at low pressures these molecules do not show any preference to reside in a certain part of the zeolite pore network, while at higher loadings a certain ordering takes place where the molecules are preferentially located in the channels. The cause of this type of ordering must be due to interactions between the molecules themselves, as they are obviously caused by the increased loading inside the zeolite. These lateral interactions were incorporated in the model in two different ways. In the first model, it was assumed that nearest-neighbours feel a repulsive interaction which decreases the activation barrier of the particles to hop to another site, as was already explained in section 6.2.1. In this case, it is still possible that two neighbouring sites are occupied, although this is energetically not favourable. A second way to model this behaviour is by totally excluding the simultaneous occupation of two neighbouring sites.

The calculated isotherms using these models are shown in figure 6.4. For the first model, a distinct kink in the isotherm is also observed, but at higher coverages than the previous simulations. At low coverages the particles are adsorbed evenly across the entire lattice. With increasing loading the particles start to feel each others pres-

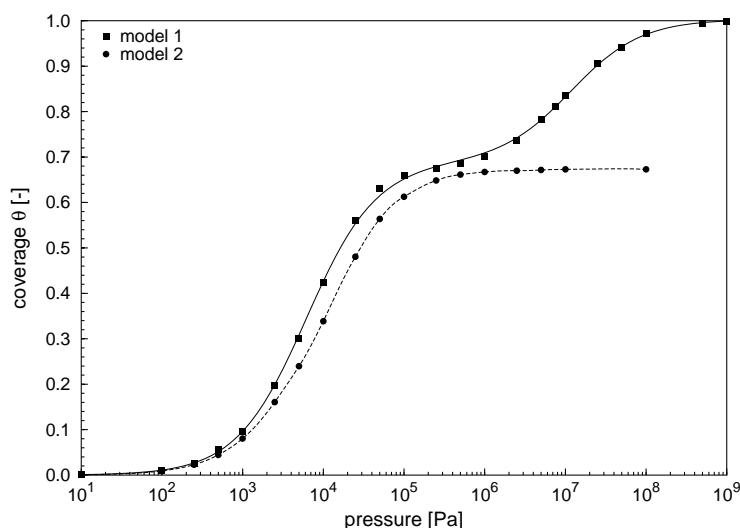


Figure 6.4: Adsorption isotherm for a single-component system when repulsive interactions are assumed between neighbouring particles. In model 1 (—) it is assumed that the presence of a neighbouring particle leads to a decreased adsorption energy, in model 2 (- -) the simultaneous occupation of two neighbouring sites is forbidden.

ence, and the lateral interactions start to become increasingly important. Due to the fact that these interactions are assumed to be additive, the channel sites are favoured by the particles as in this case they can only be surrounded by two instead of four other particles, minimizing the interactions. Once all the channel sites start to be occupied, an inflection of the isotherm is visible. As the simultaneous occupation of two neighbouring sites is energetically unfavourable but not prohibited, with increasing pressure the remaining sites also become occupied, until all intersection and channel sites are occupied.

The second model does not show any inflection behaviour. In this case not all sites of the lattice can be occupied, as the occupation of two neighbouring sites is forbidden. For this model the particles are also preferentially located at the channel sites at higher pressures, as this leads to the highest packing efficiency because in this case only two neighbouring sites cannot be occupied instead of four. The transition from no preference for the intersections at all to a preference for the channels in this case does also not lead to the observation of a kink in the isotherm.

Clearly, the present models used are not able to produce the isotherm inflections due to the commensurate freezing of particles as forwarded by Smit and Maesen.²⁷ This indicates that another mechanism, not incorporated in these coarse-grained simulations, results in this inflection behaviour. From the previous section, it was however concluded that only a small preference for one type of adsorption site is needed

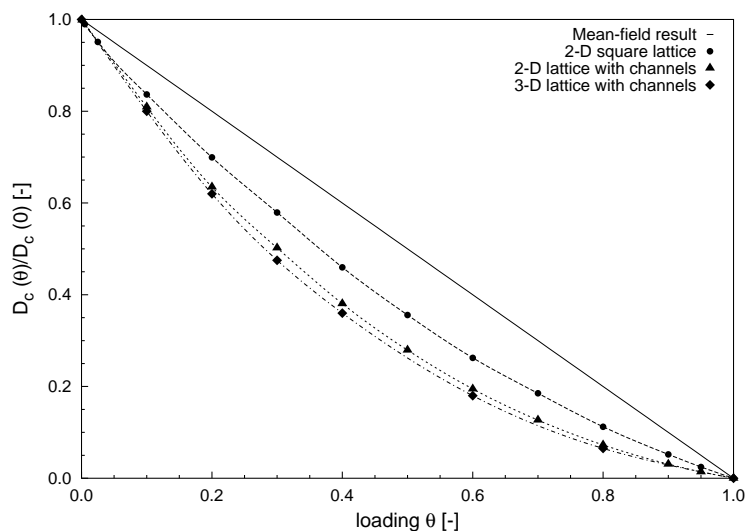


Figure 6.5: Normalized self-diffusivity as a function of occupancy for a simple square lattice, the 2-dimensional channel-intersection system, and a detailed 3-dimensional lattice model of silicalite. The latter data was taken from Coppens et al.¹⁶

to observe this behaviour. As some authors have indeed reported the presence of two distinct adsorption sites^{54, 55} or a preference of linear alkanes to reside in only part of the pore network,⁵⁶ this explanation cannot be ruled out.

6.4 Single-component diffusion

For the lattice models used in the previous section, the diffusive behaviour of single components was also studied. In this case adsorption and desorption no longer takes place, but the coverage of the lattice is kept constant and periodic boundary conditions are assumed. At different fixed loadings the particles were allowed to diffuse for a certain amount of time, after which the self-diffusion constant was calculated using the Einstein relation. Both the shape of the two-dimensional lattice, as well as the influence of preferential siting on one type of adsorption sites is considered.

6.4.1 Influence of the lattice topology

In figure 6.5 the influence of different lattice topologies on the concentration dependence of the self-diffusion constant is plotted. The self-diffusivity is normalized with respect to the diffusivity at zero coverage. To investigate the influence of a pore system containing both channels and intersections, simulations were performed with

118 The Influence of Siting on Adsorption and Diffusion

both a simple square lattice as well as a system containing channels and intersections, as shown in figure 6.1. The hopping rate was assumed to be equal on all sites, so there is no preference for either channel or intersection sites. For the 2-dimensional square lattice, deviations from the mean-field behaviour ($D_c \propto (1 - \theta)$) are already visible. The relation found in this study is in close agreement with previous studies.¹⁶ These deviations are due to correlation effects, as with increasing occupancy the chance that a particle returns to the position it previously came from increases.

For the system consisting of channels and intersections, even larger deviations from the mean-field results are visible. This is due to the lower connectivity of this lattice. While for the square lattice every site is surrounded by four neighbours, in this case two types of sites are present where the channel sites only have two nearest neighbours. Correlation effects can thus be expected to be stronger, as for these sites there is only one possibility for a subsequent jump to take place instead of three. For comparison, also the occupancy dependence for the three-dimensional lattice representing the silicalite structure, as calculated by Coppens *et al.*¹⁶ is shown in figure 6.5. Surprisingly, deviations of the results of the two- and three-dimensional systems are only small. Although for a three-dimensional lattice it is harder to block the entire pore system, for the diffusion the average connectivity of the individual sites seems to be the most important parameter. For the 2-dimensional channel-intersection system, the average connectivity \bar{Z} equals $(2 \times 2 + 1 \times 4)/3 \approx 2.67$, which is identical to the average connectivity of the 3-dimensional silicalite lattice model.

6.4.2 Influence of preferential siting

From the previous section it is clear that the coverage dependence of the diffusivity strongly depends on the connectivity of the pore system. One would thus also expect that the preferential siting on one type of site also influences the diffusive behaviour, as this also changes the “effective connectivity” the particles feel inside the lattice. The calculated diffusivities as a function of the coverage are shown in figure 6.6 for systems with both preference for adsorption in the intersections and in the channels. In this case, a monotonous decrease of the diffusivity is no longer visible, but instead a small increase is visible at a coverage where all preferred sites are occupied. For the system in which the particles adsorb in the intersections, initially a strong decrease of the diffusivity is visible. As the coverage increases the chance that a particle returns to its original position once it has hopped from an intersection to a channel becomes higher. As the hopping rate to the intersections is much faster than the rate in the reverse direction, the system can essentially be regarded as a system where particles only move from one intersection to the other. At these low coverages, the system thus essentially behaves identical to that of a simple square lattice with a maximum occupancy of 0.33 (all intersections occupied). As all intersections become occupied,

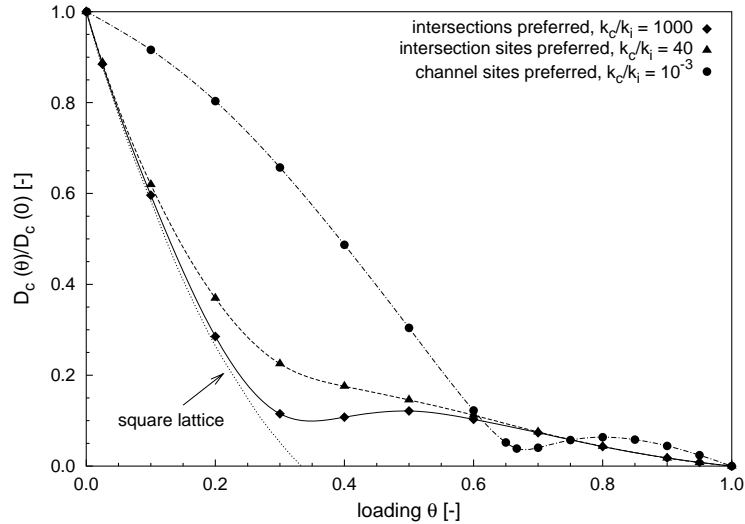


Figure 6.6: Normalized self-diffusivity as a function of occupancy for a system with preferential siting in the intersections with high (—) and lower (- -) k_c/k_i ratio, and for a system with preferential siting in the channels (- · -).

the channel sites start to be populated, increasing the number of channel-intersection hops and thus increasing the total rate of diffusion. The occupation of these channel sites furthermore has a less dramatic influence as the occupation of intersection sites, as now only the passage for two neighbouring sites is blocked. At even higher coverages the chance that such a hop will be successful drops rapidly, until finally the system is completely filled and the mobility drops to zero.

If the preference for adsorption in the intersections decreases (that is the ratio $k_{c \rightarrow i}/k_{i \rightarrow c}$ is smaller), the local minimum in the diffusivity eventually disappears. In this case the behaviour starts to deviate much sooner from that of a square lattice, as the channel sites become occupied at lower coverages. The occupation of the channel sites this time does not lead to such a dramatic enhancement of the diffusivity, as the hopping rate from this site is not that large any more, combined with the fact that a relatively smaller fraction of the particles is located at these sites. At high coverages, the two curves coincide indicating that it is the slow jump rate from an intersection to a channel site that is determining the overall mobility.

For the system with preferential siting in the channels, the initial decrease in mobility of the particles is much smaller. This is due to the fact that only the sites having two nearest neighbours are occupied, which makes it easier for the particles to still move around the lattice than when the intersections are blocked. With increasing coverages, more and more intersections also become occupied, and a greater decrease

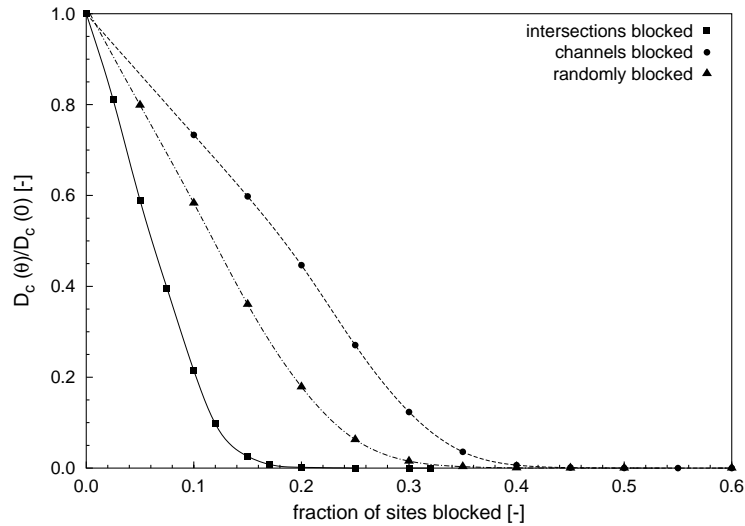


Figure 6.7: Diffusivity as a function of the fraction of blocked sites when only the intersections (—) and channels (- -) are blocked, and when both can be blocked (- · -), using a constant coverage of diffusing particles ($\theta = 0.05$).

of the mobility is observed. Again, a local minimum is observed at a coverage where all preferred sites are occupied ($\theta \approx 0.67$). As the lattice sites all become occupied it becomes harder and harder to move through the lattice, and eventually the mobility drops again.

6.5 Influence of site blocking

6.5.1 Diffusivity at varying coverages

Before the diffusion of binary mixtures will be considered, it is instructive to investigate the influence of a complete blockage of sites. This represents the extreme case of binary diffusion in which the mobility of one of the components is many orders of magnitude smaller than that of the other component, which for example occurs during deactivation of a catalyst. In figure 6.8, the diffusivity is plotted for a constant number of diffusing particles as a function of the fraction blocked sites. The particles have an equal hopping rate on the channel and intersection sites, so no preference for either of these sites is present. As the number of channel sites is twice as large as the number of intersection sites, all channel sites are blocked when the fraction of occupied sites equals 0.667, and all intersections are blocked when this fraction equals 0.333. Interestingly, the mobility of the particles is already reduced to very

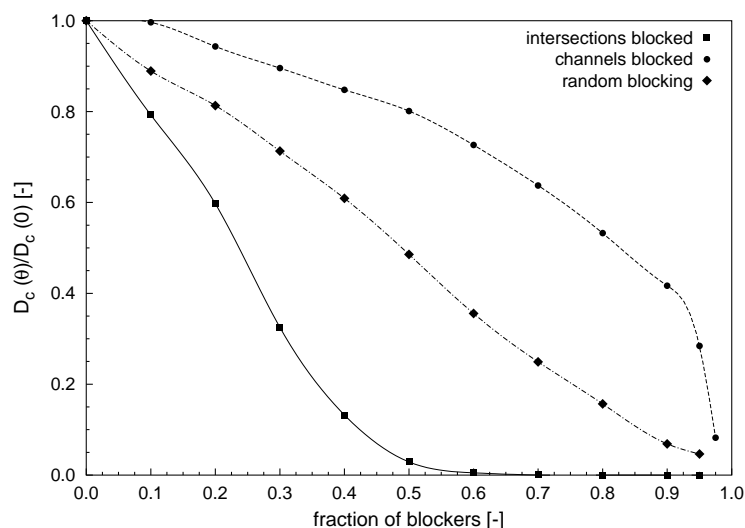


Figure 6.8: Normalized diffusivity at a constant total coverage of $\theta_t = 0.3$ as a function of the fraction of site blockers, located in the intersections (—), channels (- -), and randomly distributed (- · -).

low values when only 50% of the channel or intersection sites are blocked. Apparently, this is related to the percolation threshold p_c of the lattice as at fractions higher than $(1 - p_c)$ the diffusivity is expected to drop to zero.¹⁵ At this percolation threshold, a sufficient amount of sites is blocked to completely separate the lattice in two or more regions in which the particles are trapped. This is supported by the fact that close to fraction where the diffusivity drops to zero the mean-square displacement of the particles shows anomalous behaviour and is no longer proportional to time.⁵⁷

The blocking of intersection sites has a larger influence on the mobility than the channel sites, as these are the interconnect to four other sites. Resultingly, finding an alternative pathway will thus be much harder. When the sites are randomly blocked (i.e. both intersection and channel sites can be blocked), the behaviour lies somewhere inbetween the two extreme cases. The coverage at which the diffusivity reduces to zero is close to the value found by Trout *et al.*¹⁵ for their 3-dimensional MFI lattice. This further supports the previous findings that the differences between this more realistic model and the simplified 2-dimensional model used in this study are relatively small.

The models used in this section can be regarded as representative for the case where deactivation of a catalyst takes place. Similar models have already been used by a number of other authors to investigate the effect of coke formation on diffusion and reaction.^{19, 58–60} In these studies, however, coke formation is only permitted on

122 The Influence of Siting on Adsorption and Diffusion

one type of site. Present results show that the occurrence of coke formation on the intersection sites has a much larger influence on the mobility of the species inside the network, and will much sooner lead to a complete blocking of the pore network. Obviously, the formation of coke on the intersections will thus have a greater influence on the reactivity of a catalyst. As the coke formation primarily takes place on the reactive centers of the zeolite, it would seem advantageous to be able to control the exact location of these sites, so that the influence of coking can be decreased.

6.5.2 Blocking at constant coverage

To be able to compare the results with the ones in the case that both components are moving, all simulations are performed at a fixed total coverage $\theta_{total} = \theta_{particle} + \theta_{block} = 0.3$, while varying the fraction of immobile species. The total fraction of occupied sites thus remains constant. Figure 6.8 shows the calculated diffusivities as a function of this fraction for three different situations. For all models, a monotonous decrease of the diffusivity is visible. For the case where only the intersection sites are blocked, the diffusivity again drops much faster, and the mobility effectively drops to zero once the percolation threshold is reached. For the case that the channel sites are blocked, a sudden drop in the diffusivity is observed when the fraction of site blockers is greater than 90%. At this fraction, almost half of the channel sites are blocked, which is near the point that in figure 6.8 the diffusivity was reduced to very low values. It is however surprising that in this case a sudden drop is observed, while in the case of blocking of the intersections this is not the case. For the case that both types of sites are blocked, the behaviour lies somewhere inbetween the two extreme cases.

6.6 Binary diffusion

6.6.1 Diffusivity versus coverage

While the model in the previous section can be representative for the case where one species is essentially immobile, like for example in the case of catalyst deactivation, for most reaction mixtures the mobility of the different species lie closer to each other. In this case, the slow particles are, on a short timescale, essentially blocking the sites for the faster moving species. As the slowly moving species are still able to move from one site to another, total blocking should only occur when the lattice is completely filled. To investigate this, the diffusion of a 1:1 mixture of two components was investigated as a function of the total coverage. The slowly moving species in the mixture have a preference for adsorption on the intersection sites. The other species has an equal residence time on both types of sites.

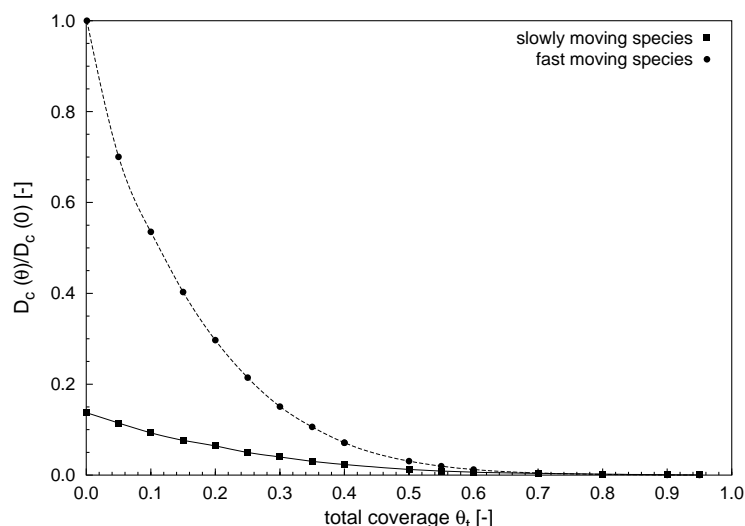


Figure 6.9: Normalized diffusivity as a function of the total coverage for a 1:1 mixture of slow and fast-moving particles. The slowly moving particles are preferentially sited in the intersections.

The results of these simulations are shown in figure 6.9. The values are normalized on the single-component diffusivity at infinite dilution of the fast moving species. When comparing this figure with figure 6.5, the diffusivity of the faster particles are significantly reduced due to the presence of the other component, and drops much faster as is the case in the single-component system. Interestingly, also for the other component the behaviour significantly differs from the single-component behaviour as shown in figure 6.6 as in this case the fast initial decrease of the mobility and the occurrence of a local minimum are not observed. Apparently, the presence of the mobile species reduces the chance that a particle moves back to its previous position, as there is a high likelihood that in the meantime it is occupied by these species.

At a total coverage of about 0.7 the diffusivity of both components becomes identical, as at this point all intersections are essentially occupied. At this point, the mobility is completely determined by the slowest component. This however occurs at much higher loadings than was the case when the particles are completely immobile, where the diffusivity was almost decreased to zero when only about 17% of the sites was blocked. It thus hard to directly relate the results obtained for slowly moving particles with the case that sites are completely blocked. The point at which the mobility of both species is completely determined by the slowest component (comparable to the percolation threshold in the case of site blocking) is significantly raised due to the fact that the particles are not completely trapped, and one thus has to be careful in

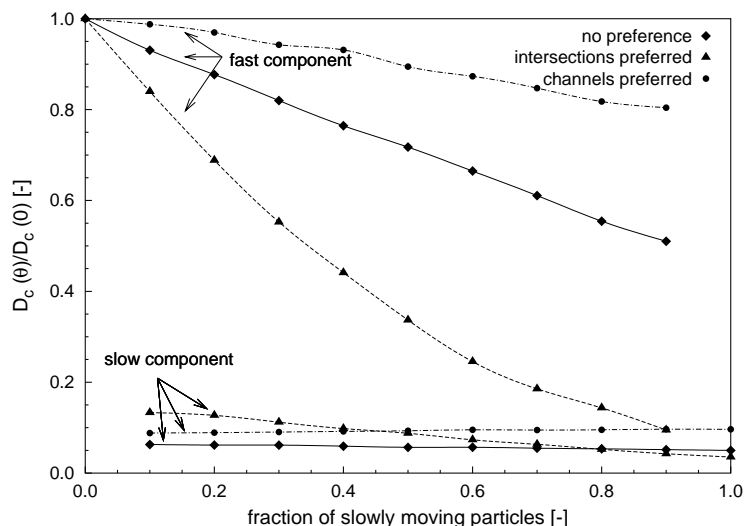


Figure 6.10: Diffusivity as a function of the fraction of slowly moving particles at a constant loading of $\theta = 0.3$ for models where the slow particles are preferentially sited in the intersections (---), channels (- · -), and without any preference (—).

predicting this point based on the simple picture of site blocking. The differences observed between completely immobile species and slowly moving species might also explain why Förster *et al.*⁶¹ had to assume a finite probability for methane to pass the immobile benzene molecules in their Monte Carlo model used for interpreting their NMR measurements of methane-benzene mixtures in silicalite. Assuming a certain chance that particles can pass the immobile benzene molecules will essentially have the same effect as having particles which can slowly move from one site to another, which effectively causes the pathway to be freed again for the fast moving methane species.

Again, a comparison with a system without preferential siting shows that the concentration dependence is enhanced by the adsorptive behaviour. Locating the slow particles in the intersections results in a more efficient blocking of the pathway for the faster moving particles. Without this preference, a higher total coverage is thus needed before both components reach identical values for their mobilities.

6.6.2 Influence of the mixture composition

To investigate the influence of the composition of the mixture on the diffusivity simulations have also been performed at a constant total coverage while varying the ratio between both components. Again, three different systems are considered: one without preferential siting, one in which the slow particles prefer the intersections, and

one in which the slow particles prefer the channels. The diffusivities of all simulations are normalized on the pure-component diffusivity of the fast component at the given coverage. The results of these simulations are shown in figure 6.10 for a total coverage of $\theta_t = 0.3$.

For all systems, a monotonous decrease of the diffusivity as a function of the mixture composition is observed. For the fast particles, the strongest decrease in mobility is again visible for the system in which the slow particles are preferentially sited in the intersections. In this case, an increase of the fraction of slow particles also increases the amount of occupied intersection sites which, due to the high connectivity of these sites, results in the most effective blocking of the pathway of the fast particles. As the fraction of slow particles is nearly one, these will occupy nearly all intersection sites, and the rate at which these particles move to the next intersection will become the rate-determining step. Resultingly, the mobility of both components will become equal to each other. The slow particles in this system are also significantly retarded as the fraction of slow particles increases. This is due to a strong increase of the coverage of the intersections with at higher fractions of these particles. As a result, the chance that a particle hops to a next intersection site once it has moved to a channel site is smaller. The decrease of the mobility of the slow particle is thus mainly due to interactions with species of its own kind.

If the slow particles are preferentially located at the channel sites, the hindrance of the other particles is the least efficient. In this case, the mobility of the fast component is only moderately dependent on the mixture composition, and the differences in mobility of both components is high. Interestingly, the diffusivity of the slow component is now increasing when the relative occupancy of these species becomes higher. Again, this can be related to the efficiency of blocking the pathway for other species when adsorbed on the different sites in the lattice. With increasing fraction, in this case the relative amount of intersections that are blocked decreases. Now, an increase of the relative amount of slow particles results in an increase of possibilities of particles to pass each other, and, resultingly, in an increase of the mobility of the slow component. This counteracts the effect that the slow particles have on the fast species, and thus only a moderate dependence on the composition is found for these.

When there is no preference for one of the types of sites, the behaviour of the system is somewhere in between the two extreme cases. In this case, a change of the mixture composition does not result in differences in the distribution of particles over the different sites, and a change in the blocking efficiency will thus not occur. Changes in the diffusivity are in this case only the result of interactions between the fast and slow species. As a result, the diffusivity of the slow component hardly changes with the mixture composition, as the timescale at which the other particles move is much smaller than for these particles. A stronger decrease of the diffusivity

of the fast component is indeed visible, but in this case these are not so efficiently hindered as in the case of preferential siting on the intersections, and at this total coverage there is still a significant difference in the mobility of both components.

Clearly, the present results show that the preferential siting of molecules in certain regions of the pore space has a distinct influence on the mobility of both species. As was expected, the fast component is influenced the most by changes in the mixture composition, and these species in all cases show a monotonous decrease of the diffusivity. The exact shape of this dependency seems to agree with simulations and experiments performed by other authors.^{6, 11, 62} The distinct drop of the diffusivity at higher ratios of the slow component (i.e. 2-methylpentane) as observed in the *n*-hexane/2-methylpentane system is not observed for these systems. Probably, the current models used are too simple to fully describe the behaviour of these systems. Recently, Krishna and Paschek⁶³ showed that, using Maxwell-Stefan theory, this drop in the diffusivity could indeed be described. Simply assuming that one species resides in the intersections and the other on all sites is not sufficient, as although the influence on the diffusivity is larger, the amount of intersections that are blocked by the slow particles is gradually increasing.

If one compares the behaviour of *n*-hexane/2-methylpentane mixtures in silicalite with the simple lattice model, the complete behaviour of these components cannot be totally simulated. In the real system, for both single components inflection behaviour is observed. This could be reproduced when assuming that particles prefer one type of sites above the other, but it is very hard to find a model describing the “commensurate freezing” behaviour of the linear compound. The interactions between the two species in the Monte Carlo simulations are also extremely simplified, as there is only a hard repulsion preventing two particles to reside on the same site on the lattice. In the real *n*-hexane/2-methylpentane system this behaviour is much more complicated, and one for example observes that at higher pressures the branched alkanes are being pushed out by their linear counterparts.²⁸ The observed drop in the diffusivity might thus be related to a certain re-ordering of the two components which takes place inside the pore network of silicalite due to intermolecular interactions. This could lead to a faster decrease of the diffusivity as the behaviour undergoes a change from a system that looks more like one where no preference is observed to one where the intersections are preferred.

6.7 Conclusions

Kinetic Monte Carlo simulations have been applied to investigate the influence of preferential siting on the diffusion of single components and mixtures in a two-dimensional pore system consisting of channel and intersection sites. Although these

simulations are a coarse-grained model of the diffusivity of molecules in the pores of a zeolite, they provide an excellent way of determining the influence of different parameters and assumptions on the behaviour of these systems. The complex interactions between the zeolite framework and the adsorbed molecules have to be reduced to a simple set of interactions and hopping rates between the particles.

Adsorption in zeolites takes place when, after a collision of a gas phase molecule with the surface of the particle occurs, the molecule is able to enter the pore. This can be simulated using dynamic Monte Carlo simulations by assuming a certain rate of adsorption on the outer lattice sites. When, for the two-dimensional lattice with channel and intersection sites, the residence time of the particles is identical on all lattice sites the system shows a simple langmuir-type behaviour. This is different for a system in which one of the type of sites is preferred. In this case, the preferred sites will be filled first, after which the less favoured sites become occupied. This leads to an inflection in the adsorption isotherm, in accordance with the behaviour that is observed for branched alkanes in silicalite. Although in all cases the inflection behaviour is observed, the exact definition of the boundary of the lattice has a large influence on the simulated adsorption isotherm. The presence of favoured sites at the edges leads to a much higher concentrations on these boundary sites and, resultingly, much lower adsorption rates, shifting the isotherm to higher pressures. The choice of the model for the zeolite lattice thus strongly influences the adsorptive behaviour one observes for these systems, and raises some questions in what sense the adsorptive behaviour in real zeolites is influenced by the exact structure of the crystal surface.

By assuming lateral interactions between nearest neighbours, the peculiar “commensurate freezing” behaviour of some linear alkanes in silicalite was tried to be simulated. Using these lateral interactions, this behaviour could indeed be observed as these indeed showed a shift from no preference to a preference for occupying the channel sites at high coverages. This re-ordering itself does however not lead to an inflection in the adsorption isotherm. In the case that the simultaneous occupation of two neighbouring sites is excluded, a langmuir-type isotherm is observed, while for a system where there is a smaller repulsive interaction between neighbouring particles an inflection is visible once nearest-neighbour sites have to be occupied. The behaviour as described by Smit and Maesen²⁷ thus cannot be reproduced using these simple models.

Due to the decreased connectivity of the channel-intersection-type lattice, in this type of lattice the self-diffusion constant depends much stronger on the diffusivity. Strong deviations from the mean-field concentration dependency can be observed, and deviations from a more detailed three-dimensional model of the silicalite pore system (also with channel and intersection sites) are small. Obviously, the average

128 The Influence of Siting on Adsorption and Diffusion

connectivity of the sites is the most important parameter determining this dependency. When the particles are preferentially located at the intersections the initial decrease in mobility is even higher. The system seems to behave essentially identical to one where only jumps from one intersection site to another can take place. Once the intersections are almost occupied, the decrease in diffusivity becomes more gradual and, when the preference is sufficiently large, a local minimum in the diffusivity is even observed. This is due to the more even distribution over both types of sites, leading to a larger contribution of the faster jumps from the channels to the intersections. When the channel sites are preferred, the mobility decreases much less than in the previous case, as the particles are less hindered by each other when they reside on these sites. Again, a local minimum in the diffusivity can be observed.

The influence of site blocking is also strongly dependent on the location at which the site blockers are located. Again, placing these blockers on the intersection leads to the fastest drop in the diffusivity, while placing them in the channels has the least influence. In order to completely block the channel systems, only about half of the respective sites have to be occupied. This is in good agreement with predictions from percolation theory. When the total coverage on the lattice was kept constant, a sudden drop in the diffusivity was visible at higher fractions of site blockers for the system in which the channel sites are blocked, while for the other systems the decrease is more gradual.

When a mixture of two moving compounds is used instead of having one immobile species, the largest influence on the mobility is visible for the faster-moving species. The changes in the diffusivity as a function of coverage at a fixed mixture composition is however much more gradual. The point at which both components start moving at the same speed cannot be easily related to the point at which in the case of immobile species the mobility is reduced to zero. When varying the mixture composition at a fixed total coverage, again the system in which the slow particles are preferentially located in the intersections shows the largest dependency on the diffusivity, especially for the fast moving particles. The slow moving particles even show a slight increase in diffusivity with an increasing fraction of these particles for the case that the channel sites are preferred. The sudden drop in the diffusivity of the fast moving species for the *n*-hexane/2-methylpentane mixture in silicalite could not be reproduced using the current models. Possibly, this is related to complex behaviour of the single components in this system, which could not be completely reproduced using the present models. A more detailed description of the intermolecular interactions in the dynamic Monte Carlo simulations thus appears to be important, as these seem to play an important role in the diffusive behaviour in zeolites.

The present simulations show that the diffusive behaviour of molecules inside a pore network is not only influenced by the way in which the separate adsorption

sites are connected, but also by the possible preferences particles have to adsorb on a certain type of site. When particles are preferentially located at the sites which have the highest number of nearest neighbours, they are much more effective in blocking the pathway for other particles. This leads to a much stronger dependence of the diffusivity on the concentration, and, in the case of mixtures, also on the mixture composition. In order to predict these dependencies, some knowledge of the adsorptive behaviour inside the pores of the zeolites is thus also required. In order to describe the diffusion on a reactor scale, some knowledge of the underlying microscopic mechanism of adsorption and diffusion inside the pores is thus required.

6.8 References

- ¹ P. Demontis and G. B. Suffritti, *Chem. Rev.* **97**(8), 2845–2878 (1997).
- ² D. Paschek and R. Krishna, *Langmuir* **17**(1), 247–254 (2001).
- ³ W. R. Qureshi and J. Wei, *J. Catal.* **126**, 126–146 (1990).
- ⁴ J. Kärger and D. M. Ruthven, *Diffusion in zeolites and other microporous solids*, John Wiley & Sons, Inc., New York (1992).
- ⁵ R. Krishna and J. A. Wesselingh, *Chem. Eng. Sci.* **52**(6), 861–911 (1997).
- ⁶ R. Krishna, *Chem. Phys. Lett.* **326**, 477–484 (2000).
- ⁷ F. J. Keil, R. Krishna, and M.-O. Coppens, *Rev. Chem. Eng.* **16**(2), 71–197 (2000).
- ⁸ R. Chitra and S. Yashonath, *Chem. Phys. Lett.* **234**, 16–20 (1995).
- ⁹ R. Q. Snurr and J. Kärger, *J. Phys. Chem. B* **101**(33), 6469–6473 (1997).
- ¹⁰ L. N. Gergidis and D. N. Theodorou, *J. Phys. Chem. B* **103**(17), 3380–3390 (1999).
- ¹¹ S. Jost, N.-K. Bär, S. Fritzsche, R. Haberlandt, and J. Kärger, *J. Phys. Chem. B* **102**(33), 6375–6381 (1998).
- ¹² D. Schuring, A. O. Koriabkina, A. M. de Jong, B. Smit, and R. A. van Santen, *J. Phys. Chem. B* **105**(32), 7690–7698 (2001).
- ¹³ J. Kärger, M. Petzold, H. Pfeifer, S. Ernst, and J. Weitkamp, *J. Catal.* **136**, 283–299 (1992).
- ¹⁴ P. R. van Tassel, S. A. Somers, H. T. Davis, and A. V. McCormick, *Chem. Eng. Sci.* **49**(17), 2979–2989 (1994).
- ¹⁵ B. L. Trout, A. K. Chakraborty, and A. T. Bell, *Chem. Engng. Sci.* **52**(14), 2265–2276 (1997).
- ¹⁶ M.-O. Coppens, A. T. Bell, and A. K. Chakraborty, *Chem. Engng. Sci.* **53**(11), 2053–2061 (1998).
- ¹⁷ S. M. Auerbach, N. J. Henson, A. K. Cheetham, and H. I. Metiu, *J. Phys. Chem.* **99**(26), 10600–10608 (1995).
- ¹⁸ B. Smit and R. Krishna, *Curr. Opin. Solid St. M.* **5**(5), 455–461 (2001).
- ¹⁹ D. N. Theodorou and J. Wei, *J. Catal.* **83**, 205–224 (1983).
- ²⁰ R. M. Barrer and W. Jost, *Trans. Faraday Soc.* **45**, 928–930 (1949).
- ²¹ Y. D. Chen and R. T. Yang, *AIChE J.* **37**(10), 1579–1582 (1991).
- ²² D. Paschek and R. Krishna, *Chem. Phys. Lett.* **342**, 148–154 (2001).
- ²³ C. Saravanan, F. Jousse, and S. M. Auerbach, *Phys. Rev. Lett.* **80**(26), 5754–5757 (1998).

130 The Influence of Siting on Adsorption and Diffusion

- ²⁴ K. A. Fichthorn and W. H. Weinberg, *J. Chem. Phys.* **95**(2), 1090–1096 (1991).
- ²⁵ L. J. P. van den Broeke, S. A. Nijhuis, and R. Krishna, *J. Catal.* **136**, 463–477 (1992).
- ²⁶ T. Masuda, Y. Fujikata, H. Ikeda, and K. Hashimoto, *Microporous Mesoporous Mater.* **38**, 323–332 (2000).
- ²⁷ B. Smit and T. L. M. Maesen, *Nature* **374**, 42–44 (1995).
- ²⁸ T. J. H. Vlugt, R. Krishna, and B. Smit, *J. Phys. Chem. B* **103**(7), 1103–1118 (1999).
- ²⁹ R. Krishna and D. Paschek, *Phys. Chem. Chem. Phys.* **3**, 453–462 (2001).
- ³⁰ R. Krishna, B. Smit, and S. Calero, *Chem. Soc. Rev.* **31**, 185–194 (2002).
- ³¹ H. Morell, K. Angermund, A. R. Lewis, D. H. Brouwer, C. A. Fyfe, and H. Gies, *Chem. Mater.* **14**(5), 2192–2198 (2002).
- ³² L. F. Gladden, M. Hargreaves, and P. Alexander, *Chem. Eng. J.* **74**(1), 57–66 (1999).
- ³³ B. Smit, L. D. J. C. Loyens, and G. L. M. M. Verbist, *Faraday Discuss.* **106**, 93–104 (1997).
- ³⁴ T. J. H. Vlugt, C. Dellago, and B. Smit, *J. Chem. Phys.* **113**(19), 8791–8799 (2000).
- ³⁵ R. C. Runnebaum and E. J. Maginn, *J. Phys. Chem. B* **101**(33), 6394–6408 (1997).
- ³⁶ D. Paschek and R. Krishna, *Phys. Chem. Chem. Phys.* **2**, 2389–2394 (2000).
- ³⁷ S. J. Lombardo and A. T. Bell, *Surf. Sci.* **245**, 213–224 (1991).
- ³⁸ N. G. van Kampen, *Stochastic processes in physics and chemistry*, North-Holland, Amsterdam (1981).
- ³⁹ A. P. J. Jansen and J. J. Lukkien, *Catal. Today* **53**, 259–271 (1999).
- ⁴⁰ J. Segers, *Algorithms for the simulation of surface processes*, Ph.D. thesis, Eindhoven University of Technology, Eindhoven (1999).
- ⁴¹ J. J. Lukkien, J. P. L. Segers, P. A. J. Hilbers, R. J. Gelten, and A. P. J. Jansen, *Phys. Rev. E* **58**(2), 2598–2610 (1998).
- ⁴² R. E. Richards and L. V. C. Rees, *Langmuir* **3**(3), 335–340 (1987).
- ⁴³ M. S. Sun, O. Talu, and D. B. Shah, *J. Phys. Chem.* **100**(43), 17276–17280 (1996).
- ⁴⁴ Y. Yang and L. V. C. Rees, *Microporous Mater.* **12**, 223–228 (1997).
- ⁴⁵ Z. Du, G. Manos, T. J. H. Vlugt, and B. Smit, *AIChE J.* **44**(8), 1756–1764 (1998).
- ⁴⁶ R. A. van Santen and J. W. Niemantsverdriet, *Chemical kinetics and catalysis*, Plenum Press, New York, New York (1995).
- ⁴⁷ T. J. H. Vlugt, W. Zhu, F. Kapteijn, J. A. Moulijn, B. Smit, and R. Krishna, *J. Am. Chem. Soc.* **120**(22), 5599–5600 (1998).
- ⁴⁸ W. Zhu, F. Kapteijn, and J. A. Moulijn, *Phys. Chem. Chem. Phys.* **2**(9), 1989–1995 (2000).
- ⁴⁹ W. Zhu, B. van der Linden, and J. A. Moulijn, *Phys. Chem. Chem. Phys.* **3**(9), 1755–1761 (2001).
- ⁵⁰ R. Q. Snurr, A. T. Bell, and D. N. Theodorou, *J. Phys. Chem.* **98**(19), 5111–5119 (1994).
- ⁵¹ Z. Du, L. J. Dunne, G. Manos, and M. F. Chaplin, *Chem. Phys. Lett.* **318**, 319–324 (2000).
- ⁵² A. Micke, M. Bülow, M. Kočičík, and P. Struve, *J. Phys. Chem.* **98**(47), 12337–12344 (1994).
- ⁵³ E. B. Webb III and G. S. Grest, *J. Chem. Phys.* **116**(14), 6311–6321 (2002).
- ⁵⁴ B. Millot, A. Methivier, and H. Jobic, *J. Phys. Chem. B* **102**(17), 3210–3215 (1998).
- ⁵⁵ W. J. M. van Well, *Adsorption of alkanes in zeolites*, Ph.D. thesis, Eindhoven University of Technology, Eindhoven (1998).
- ⁵⁶ R. L. June, A. T. Bell, and D. N. Theodorou, *J. Phys. Chem.* **94**(4), 1508–1516 (1990).
- ⁵⁷ M. Sahimi, G. R. Gavalas, and T. T. Tsotsis, *Chem. Eng. Sci.* **45**(6), 1443–1502 (1990).

- ⁵⁸ S. Sundaresan and C. K. Hall, *Chem. Eng. Sci.* **41**(6), 1631–1645 (1986).
- ⁵⁹ P. H. Nelson, D. M. Bibby, and A. B. Kaiser, *Zeolites* **11**, 337–344 (1991).
- ⁶⁰ X.-Y. Guo, Z.-W. Liu, and B. Zhong, *Microporous Mesoporous Mater.* **23**, 203–209 (1998).
- ⁶¹ C. Förste, A. Germanus, J. Kärger, H. Pfeifer, J. Caro, W. Pilz, and A. Zikánová, *J. Chem. Soc., Faraday Trans. 1* **83**(8), 2301–2309 (1987).
- ⁶² L. N. Gergidis, D. N. Theodorou, and H. Jobic, *J. Phys. Chem. B* **104**(23), 5541–5552 (2000).
- ⁶³ R. Krishna and D. Paschek, *Phys. Chem. Chem. Phys.* **4**, 1891–1898 (2002).

7

Concluding Remarks

A number of different techniques have been applied to study the diffusion in zeolites. A short overview will be given of the most important findings in this thesis. From the results obtained, some general conclusions can be drawn that are important for a better understanding of diffusion in zeolites.

In the previous chapters, a number of different techniques have been used to study the diffusion in porous systems, and specifically in zeolites. Diffusion in zeolites has already been studied for many decades now, but a lot of questions still remain regarding this subject. From the work in this thesis, it will have become clear that the diffusive behaviour of adsorbates in these systems is often complex and even counter-intuitive. Although a number of different problems have been studied, some general conclusions can be drawn from the obtained results. Before these will be considered, the results from the different chapters in this thesis will be reviewed.

7.1 Diffusion in zeolites: where do we stand now?

From the literature, a vast amount of experimental and also theoretical techniques are available to study the diffusion in zeolites. Not only do these methods differ in the methods employed, but also in the level of detail and the length- and timescale at which they study the diffusive properties in zeolites. From a fundamental point of view, methods that directly probe the microscopic mechanism of diffusion provide the most interesting information. From a practical point of view, however, these methods are of little use when the results obtained cannot be directly related to the properties of these systems on a laboratory or even an industrial scale. The coupling of the results obtained with these methods therefore is an important topic nowadays

addressed in zeolite research. The gap between these methods is still large, but due to the technical advances in the experimental and computational field, they are slowly closing in on each other.

7.2 The results: an overview

7.2.1 Molecular dynamics: modeling on microscopic scale

With molecular dynamics simulations, an atomistic model of the zeolite-adsorbate system is built. Using this method, the motion of the individual molecules can be followed, and a microscopic picture of the diffusive process can thus be obtained. This technique has the advantage that the conditions at which these simulations are conducted can be easily controlled, and all kinds of interactions can be readily calculated. In experimental techniques these conditions are much harder to control, and information about the interactions in the systems and the precise influence of changing these conditions is much harder to extract. MD simulations are thus an excellent tool to study the influence of the concentration, zeolite structure and alkane chainlength on the self-diffusivity.

As with almost every method, MD simulations only provide an approximative model of the real world. It thus remains important to compare the results with experimental data available in literature. Using the forcefields that have been optimized to describe the adsorptive behaviour of zeolites, a reasonable agreement is obtained with the available literature. The single-file behaviour, which was expected for some of the zeolite structures, was however not observed in this study. This might be due to the timescale at which these simulations are performed. For all systems considered in this study, the self-diffusivity decreases monotonically with increasing pore loading. It is however interesting that the diffusivity for all system tends to decrease to about identical values, irrespective of the shape of the diffusant or zeolite porestructure. At high coverages, it appears to be the intermolecular interactions which determine the diffusive behaviour instead of alkane-zeolite interactions. This change in mechanism is further supported by an increase of the activation energy of diffusion at higher coverages. For the mobility of the molecules as a function of chainlength, no general rule seems to apply, as the behaviour strongly depends on the zeolite. An important parameters in this respect seems to be the alkane chainlength compared to the length of the zeolite unit cell. When these two quantities closely match, resonant diffusion occurs and an enhancement of the diffusivity is observed.

The present study also shows that the molecular dynamics technique also has its limitations. Due to the computational demands of techniques, system sizes have to be kept small, and only relatively mobile species can be studied if computer resources are limited. The simulation of bulkier molecules, like branched alkanes, therefore is

not feasible. Simulations at elevated temperatures can in this case be helpful, but the interpolation of the results to relevant temperatures and the possibility of a different diffusion mechanism seriously reduced the reliability of the obtained results. Due to the small system size, some care also has to be taken when choosing the initial conditions of the simulations, as only a few pores, instead of many thousands, are probed. In the case of concentration dependence, a wrong definition of the starting configuration might seriously affect the results.

7.2.2 Single-file diffusion: simple systems with complex behaviour

From the MD simulations, it was already clear that single-file diffusion is not automatically observed when diffusion in a single-file pore is considered. To investigate the fundamentals of this phenomenon, a detailed model is not required, but simple models of a cylindrical pore in which the particles are unable to pass each other are sufficient. That even in these extremely simple systems the behaviour is quite complex is illustrated by the obtained results.

One of the characteristic features of single-file diffusion is the \sqrt{t} dependence of the mean-square displacement in the long-time limit. This behaviour however does not necessarily have to be observed in cylindrical pores in which the particles cannot pass each other. Only when the particles are capable of transferring linear momentum in the axial direction, the typical \sqrt{t} dependence is observed. The individual particles, however, do not have to behave like random walkers with a mean-square displacement proportional to time, as one is led to believe when reviewing the available literature on this subject. Instead, it appears to be the combined effect of particle-particle and particle-wall interactions which is most important. The time at which the \sqrt{t} -dependence starts to set in, depends strongly on the interactions with the zeolite wall. The smaller or smoother the interactions that enable the transfer of energy and momentum in the axial direction, the longer it takes before the single-file displacement is observed. For finite-size systems, a transition to ordinary diffusion ($\langle z^2 \rangle \propto t$) can again be observed. For these systems, the concentration dependence is still proportional to $(1 - \theta)/\theta$, which seems to be the most fundamental behaviour for systems in which particles are moving through a one-dimensional channel.

7.2.3 Diffusion in mixtures

An understanding of the behaviour of mixtures in zeolites is of practical importance as many applications of zeolites involve the diffusion of more than one component. The TEX-PEP technique is an excellent tool to study this phenomenon, as one of the components can be selectively labelled, and the (re-)exchange of the labelled components in a steady-state stream can be observed. Combined with a suitable

136 Concluding Remarks

model that describes the mass transfer in the zeolite bed, this method can then be used to determine the self-diffusion constants of the components in the mixture.

As a model system, the diffusion of a mixture of *n*-hexane and 2-methylpentane was chosen, also because of their peculiar adsorptive behaviour. The experiments are conducted at a constant total pressure while varying the composition of the mixture. The loading of the zeolite crystals slightly decreases with increasing fraction of the branched alkane in the gas phase. The diffusive behaviour as a function of the composition is characterized by a sudden drop of the diffusivity as the gas-phase composition consists of more than 75% of 2-methylpentane. Blocking of the intersections by the slowly moving branched alkanes, as these are preferentially located in the intersections, seems to be the most likely explanation for this. The results illustrate that the exact shape of the pore system, as well as the siting of the molecules inside the pores are important factors that determine the diffusive behaviour.

7.2.4 DMC: a coarse-grained model of diffusion

Using dynamic Monte Carlo simulations, it is possible to investigate the influence of pore topology and preferential siting of molecules in the pore system. As these simulations use a coarse-grained model of the zeolite, computational demands are limited, and larger systems can be considered. By using a simple, 2-dimensional model containing intersection and channel sites, the influence of siting was studied.

Assuming preferential siting on one type of site was shown to lead to the observation of an inflection in the adsorption isotherm of these models. This assumption also has a large impact on the single-component diffusivity, as this can lead to the occurrence of a local minimum in the mobility of the particles. Another important factor is the average connectivity of the sites, which seems to be more determining than whether the system forms a two- or three-dimensional network. When sites are essentially blocked, the largest impact can be observed when this is only done with the intersection sites, as this much more effectively limits the amount of escape routes for the particles. For binary mixtures, when the slowly moving particle takes over the role of the blockers, the same conclusion holds, but the effects are less dramatic. Care should thus be taken when treating the slow component of a binary mixtures as if it is essentially immobile.

7.3 The big picture

7.3.1 The importance of intermolecular interactions

One thing that is continuously returning throughout this thesis, is the importance of the intermolecular interactions for the diffusion in zeolites. As the molecules are

moving inside the narrow pores of the zeolite, the interactions appear to be completely dominated by the zeolite framework. While with increasing pore loading these interactions are quantitatively still dominating, the diffusive behaviour becomes more and more determined by adsorbate-adsorbate interactions. The confinement of the molecules inside the pores of the zeolite lattice causes an enhancement of these interactions compared to the gas phase. This complex interplay between particle-particle and particle-wall interactions also appears to be the fundamental cause for the peculiar \sqrt{t} -behaviour of the mean-square displacement in single-file systems. The same holds for the diffusion of a *n*-hexane/2-methylpentane mixture in zeolite silicalite, where the specific pore structure and the adsorptive behaviour of the components inside the pore systems cause the observed drop in diffusivity with increasing 2-methylpentane fraction.

7.3.2 The limitations of DMC

Related to the above mentioned point is the limitations of dynamic Monte Carlo simulations to simulate the diffusive behaviour in zeolites. Although this technique can provide useful qualitative insight, this method usually reduces the intermolecular interactions to extremely simple hard repulsive interactions, in which no two particles can occupy the same site. Therefore, the diffusivity in a completely filled system for example becomes zero at high coverages, while in reality there is still a finite mobility of the molecules. This might also be a possible explanation for the inability of the method to correctly describe the behaviour of the previously mentioned mixture of hexane isomers. A more suitable technique to study this system would be molecular dynamics, as the intermolecular interactions are more sophisticated, but due to the low mobility of the branched alkanes this is computationally still not very feasible.

7.3.3 Macroscopic versus microscopic viewpoints

Using different methods which both look at diffusion on a microscopic as well as a macroscopic scale of course raises questions about how these worlds link together. For the experimental method on a macroscopic level employed in this thesis, TEX-PEP, discrepancies still exist with the microscopic results from literature and the molecular dynamics simulations. What has however become clear from the research conducted in this thesis, is that an understanding of the processes taking place at a microscopic level can certainly help in explaining what happens on a macroscopic scale. The strong concentration dependence observed with MD simulations can, for example, partially explain discrepancies between different methods regarding the magnitude of the diffusivities found. These furthermore showed that, with increasing coverage, diffusivities of different species (linear and branched alkanes) come closer

138 Concluding Remarks

together. Often, microscopic mechanisms can have macroscopic consequences, as the strong concentration and pore length dependence of the diffusivity in single-file systems.

Linking macroscopic and microscopic results regarding the diffusion in zeolites has long been an important topic in this field of research. From the study on single-file diffusion, it can be concluded that the observed behaviour in this case is strongly dependent on the timescale at which it is observed. This conclusion might hold more generally, as different diffusion mechanisms might be dominating on different timescales as well in the case of diffusion in other systems. The introduction of new experimental techniques and improvement of theoretical methods will possibly provide a definitive answer for this.

7.3.4 Theory versus experiment

In science, a study can be conducted either by using experimental or theoretical techniques. Often, these two disciplines exist next to each other, without having any interactions, apart from reading each others articles. One of the biggest challenges, however, is trying to combine both methods and put the pieces of the puzzle together. As experimental and theoretical methods each have their own advantages and disadvantages, both are needed for a better understanding of physics and chemistry in general, and specifically of diffusion in zeolites. Experimental techniques are needed to provide us with an idea of how the real world is working, and enable us to check the theories we have developed. Experimental limitations however limit the regime in which measurements can be performed. Furthermore, the underlying microscopic mechanisms are not always revealed, as these are masked by other processes contributing to the overall behaviour of the system. In theoretical methods, the conditions (like e.g. the concentration inside a zeolite pore) can be easily controlled, and the level of detail can be chosen, so that the parameters of interest can be directly studied. Due to the complexity of the real system, these methods however have to rely on a greatly simplified models.

From this thesis, it will have become clear that theory and experiment cannot live without each other. Experimental data was used to check if the zeolite model used in the MD simulations provides us with reasonable values of the diffusivity. On the other hand, the PEP measurements require the use of a model which can accurately describe the flow in the zeolite system in order to extract the data. This model can furthermore be used to predict the experimental conditions at which the process of interest, micropore diffusion, is dominating over other contributions to the mass transfer resistance. In addition to the fact that they need each other, they also complement each other in the sense that insights from one of these approaches can help understand what is happening in the other, and provide ideas for new investigations

in the other field.

Even when choosing for either theory or experiment, further choices have to be made regarding the technique to use. Each has its own advantages and disadvantages, and it is thus important to know what the exact question is that has to be answered, in which technique is most suitable to do so. Unfortunately, one is often limited by the amount of resources available. Combining results from different methods furthermore often lead to additional complications, and it is thus tempting to stick to one or a small number of them. Notwithstanding these difficulties, however, a combination of different experimental and theoretical techniques seems to be the way to go in really tackling the different problems still present in zeolite science, and should be one of the primary focusses of future research.

Summary

Zeolites are extensively used in industry as catalyst and/or catalyst support in a large range of different processes. The diffusion in these microporous materials differs greatly from diffusion in liquids and gases. As it determines the ease and speed with which reactants can reach the catalytically active centers and products can leave the pores, a thorough understanding of this process is not only important from a fundamental, but also from a practical point of view. Although the industrial applications of these materials involve large time- and length scales, the mobility of the adsorbates in the first place is influenced by the interactions occurring on a molecular scale. Theoretical methods are extremely suited to investigate these influences, as one can easily build a model with the appropriate level of detail and the conditions can easily be varied. In this thesis, the diffusive process is studied in order to gain insight in its microscopic mechanisms and their consequences on a macroscopic scale. To accomplish this, different methods have been applied, ranging from an atomistic approach using molecular dynamics simulations, to the description of the flow in a laboratory-scale reactor by numerically solving the mass balances for the system.

Molecular dynamics simulations are capable of providing a detailed insight in the molecular mechanisms of diffusion. This method has been used to study the influence of the zeolite structure, sorbate concentration, and chainlength on the diffusivity of alkanes. Using forcefields which are optimized for the alkane-zeolite system, a fair agreement can be obtained with experimental data from PFG-NMR and QENS experiments. A strong dependence on the sorbate concentration is observed, and the present results indicate that the alkane-alkane interactions become dominant in determining the mobility at high coverages. As a result, the diffusivities in the different zeolite structures, and for different adsorbates, lie much closer to each other at higher coverage. The dependence on the chainlength is strongly non-linear, and is related to the structure of the pores (like e.g. the presence of side pockets) and also to the chainlength compared to the lattice periodicity, leading to the occurrence of “resonant diffusion”.

Another interesting phenomenon, occurring in zeolites with a one-dimensional pore structure, is single-file diffusion. Due to the fact that the particles are unable to pass each other, the mobility is greatly reduced, and a characteristic time-dependence of the mean-square displacement ($\langle z^2(t) \rangle \propto \sqrt{t}$ instead of $\propto t$) can be observed. Using

142 Summary

a simple model of a one-dimensional pore, it is shown that the occurrence of this behaviour is strongly influenced by the shape of the pore wall, and the length of the pore itself. It is the combined effect of both particle-particle and particle-wall interactions which is responsible for this time dependence. The type of behaviour is strongly dependent on the timescale at which the displacement is observed. For moderate activation barriers and “soft” potentials the displacement is first proportional to t , before the typical single-file dependence sets in. At large timescales, single-file systems of finite length will always show a displacement which is proportional to time again, as is the case in ordinary systems. What however remains characteristic for single-file systems, regardless of the behaviour of the displacement, is the strong concentration dependence of the mobility of the particles in these systems.

That insight in the behaviour on a microscopic scale can help in interpreting experimental results is shown in a study of the diffusion of a *n*-hexane/2-methylpentane mixture in silicalite using the positron emission profiling technique. With this technique, the concentration of radiochemically labelled species can be measured inside a zeolite packed-bed reactor. Using a numerical model of the mass transfer through the reactor, information can be obtained on the diffusivities of both components as a function of the mixture composition. With an increasing fraction of 2-methylpentane in the gas phase, a sudden drop in the diffusivity of the fast moving *n*-hexane species is observed. This is due to the fact that a significant fraction of the intersections between the different channels in the zeolite structure, where the branched alkanes are preferentially located, becomes occupied. The mobility of the slowly moving 2-methylpentane is hardly affected by the presence of the linear alkane.

The results from the PEP experiments indicate that the diffusive behaviour might also depend on the specific siting of the molecules in the zeolite pore network. This was investigated using dynamic Monte Carlo simulations, in which the zeolite is modelled as a simple network of channel and intersection sites, where the molecules move by jumping to an empty neighbouring site. Both in the single- and multi-component case, large differences can be observed in the diffusive behaviour when a preference for adsorption on one type of site exists. Generally, a preferential siting in the intersections leads to a much stronger concentration dependence. The results observed experimentally however could not be reproduced using these simple simulations. Apparently, the interactions described in these Monte Carlo simulations are too simple to account for the real behaviour, and lateral interactions play an important role in the diffusive behaviour.

Samenvatting

Zeolieten worden veelvuldig gebruikt in de industrie als katalysatoren en/of dragermaterialen voor een groot aantal verschillende processen. De diffusie in deze microporeuze materialen verschilt sterk ten opzichte van gasfase diffusie. Aangezien dit proces de snelheid en het gemak waarmee reactanten de katalytisch actieve centra kunnen bereiken en producten de poriën kunnen verlaten bepaalt, is het niet alleen vanuit wetenschappelijk, maar ook vanuit een praktisch oogpunt van belang om meer inzicht te krijgen in dit proces. Alhoewel in praktische toepassingen het transport plaatsvindt op grote tijd- en lengteschaal, wordt de mobiliteit van de molekulen in de eerste plaats beïnvloed door interacties op moleculaire schaal. Theoretische methoden zijn uitermate geschikt om deze invloeden te bestuderen, aangezien hiermee eenvoudig modellen gekozen kunnen worden met de juiste gedetailleerdheid, en de “experimentele” condities gemakkelijk kunnen worden gevarieerd. In dit proefschrift is het diffusie-proces bestudeerd om meer inzicht te krijgen in de microscopische mechanismen en de consequenties hiervan op macroscopische schaal. Hiervoor zijn diverse methoden gebruikt, variërend van een atomistische benadering via moleculaire dynamica simulaties, tot het beschrijven van de stroming door een katalytische reactor door het numeriek oplossen van de massabalansen voor het systeem.

Moleculaire dynamica simulaties geven gedetailleerde informatie over de moleculaire mechanismen van het diffusie-proces. Deze methode is gebruikt om de invloed van de zeoliet-structuur, concentratie van de adsorbaten, en ketenlengte te bepalen op de diffusie van alkanen. Door gebruik te maken van voor zeoliet-alkaan systemen geoptimaliseerde parameters voor de beschrijving van de krachten tussen de atomen, kan een redelijke overeenstemming worden bereikt met experimentele gegevens. De diffusiviteit blijkt sterk af te hangen van de concentratie van de adsorbaten, en bij hoge beladingen blijken vooral alkaan-alkaan interacties de mobiliteit van de moleculen te bepalen. Ten gevolge hiervan zijn de verschillen in de gevonden diffusie-constanten voor verschillende zeolieten en adsorbaten veel kleiner bij hoge concentraties, en is er een sterke toename te zien van de activeringsenergie voor diffusie. The afhankelijkheid van de ketenlengte is sterk non-lineair, en is gerelateerd aan de poriestructuur (zoals bijv. de aanwezigheid van kooien) en de verhouding tussen de ketenlengte en de periodiciteit van het zeoliet-rooster, wat kan leiden tot het optreden van “resonante diffusie”.

144 Samenvatting

Een ander interessant fenomeen, wat waarneembaar is zeolieten met een 1-dimensionale poriestructuur, is het optreden van single-file diffusie. Doordat de moleculen elkaar in de smalle poriën niet kunnen passeren, wordt hun mobiliteit sterk gereduceerd, en kan een karakteristieke tijdsafhankelijkheid worden waargenomen van de “mean-square displacement”, waarbij deze evenredig wordt met \sqrt{t} in plaats van t . Een eenvoudig model voor een 1-dimensionale porie is gebruikt om dit gedrag te onderzoeken. Het al of niet optreden van de \sqrt{t} -afhankelijkheid blijkt sterk af te hangen van de vorm en de lengte van de porie. Verantwoordelijk voor dit gedrag is een complex samenspel van interacties tussen deeltjes onderling en met de wand. Belangrijk is de tijdschaal waarop de verplaatsing gemeten wordt. Wanneer de interacties tussen zeoliet en adsorbaten niet al te groot zijn (de activeringsbarrières zijn laag), zal deze aanvankelijk evenredig zijn met de tijd, waarna pas na zekere tijd de \sqrt{t} -afhankelijkheid kan worden waargenomen. Op grote tijdschaal zal voor systemen met eindige afmetingen altijd een evenredigheid met t worden waargenomen.

Dat inzicht in het microscopische gedrag helpt bij de interpretatie van experimenten, is gebleken uit het bestuderen van de diffusie van een n -hexaan/2-methylpentaan mengsel in silicaliet met behulp van de positron emissie profilering techniek. Met deze techniek is het mogelijk om de concentratie van radio-actief gelabelde moleculen in een zeoliet reactor te meten. Met behulp van een numeriek model voor de stroming door de reactor kan informatie worden verkregen over de diffusieconstanten van de componenten als een functie van de samenstelling van het mengsel. Hierbij bleek dat met een toenemende fractie van 2-methylpentaan in het mengsel, er een sterke afname te zien is in de mobiliteit van het snel bewegende n -hexaan. Dit is het gevolg van het adsorptiegedrag van beide componenten, aangezien de vertakte alkanen bij voorkeur in de kruispunten tussen de verschillende kanalen gaat zitten. Het langzaam bewegende 2-methylpentaan ondervindt daarentegen nauwelijks hinder van de lineaire alkaan.

Aangezien de hiervoor genoemde resultaten erop wijzen dat het diffusie-gedrag ook sterk bepaald wordt door de plaatsen waar de moleculen zich in de poriën het liefste ophouden, is de invloed hiervan onderzocht met behulp van dynamische Monte Carlo simulaties. Bij deze simulaties wordt een zeoliet beschouwd als een eenvoudig netwerk van kruispunt- en intersectie-sites, waarbij de moleculen voortbewegen door naar een naburige lege site te springen. De voorkeur voor adsorptie op één type site blijkt inderdaad een grote invloed te hebben op het diffusiegedrag, zowel voor enkele componenten als wel voor mengsels. Over het algemeen leidt een voorkeur voor adsorptie op de kruispunten tot een veel sterkere concentratie-afhankelijkheid. Dat dynamische Monte Carlo simulaties niet tot in detail in staat zijn om het gedrag in zeolieten te beschrijven, blijkt wel uit het feit dat het gevonden gedrag bij de PEP experimenten met de huidige modellen niet kon worden gereproduceerd.

Dankwoord

Hij is af! Na vier jaar en-een-beetje ligt het resultaat van mijn promotie-onderzoek voor je neus. En zoals het geval is met alle proefschriften, is het niet alleen de persoon genoemd op de kaft van 't boekje die dit alles tot stand heeft gebracht. Vandaar ook dat ik graag van de mogelijkheid gebruik wil maken om een aantal mensen te bedanken.

In de eerste plaats wil ik natuurlijk Rutger van Santen bedanken voor het bieden van de mogelijkheid om binnen SKA een promotie-onderzoek te doen. Je enthousiasme, suggesties en niet aflatende ideeënstroom heb ik altijd als zeer stimulerend ervaren. Vooral de vrijheid en het vertrouwen om een eigen richting te geven aan mijn promotie hebben dit tot een erg leerzame ervaring gemaakt.

Dank ook aan Peter Hilbers, Berend Smit en Freek Kapteijn voor jullie bereidheid om plaats te nemen in de kerncommissie. Peter, het feit dat je de problemen vaak net vanuit een iets andere invalshoek wist te bekijken heb ik als zeer nuttig ervaren. Berend, bedankt voor het gebruik van de software en de continue interactie tussen de simulaties in jouw groep en onze experimenten, wat ons ook bij het onderzoek beschreven in hoofdstuk 5 erg geholpen heeft. Freek, bedankt voor de nuttige suggesties ter verfijning van dit proefschrift.

Gedurende mijn promotie heb ik het genoeg gehad om met een aantal mensen regelmatig te kunnen samenwerken en/of van gedachten te wisselen. Alina, bedankt voor de experimentele gegevens waarop ik mijn simulaties kon loslaten en de mogelijkheid om me toch nog met experimenten te kunnen bemoeien. Darek en Jeroen wil ik graag bedanken voor de gelegenheid om me eens met een ander probleem bezig te houden. Ook de mogelijkheid om eens wat meer te weten te komen over NMR-metingen, en de diverse discussies die ik heb gehad met Pieter Magusin heb ik als erg interessant en nuttig ervaren. Emiel van Kimmenade wil ik ook graag bedanken voor verrichtte werkzaamheden als afstudeerder onder mijn hoede. En natuurlijk dank aan Frank de Gauw, Niels Noordhoek, Arthur de Jong, Tonek Jansen en Bruce Anderson voor discussies en advies op wetenschappelijk gebied.

Werken als AiO in de vakgroep is uiteraard ook meer dan werken alleen. Dank dan ook aan iedereen die mijn vier-en-een-half-jarig verblijf tussen de chemici tot een aangenaam geheel hebben gemaakt. In het bijzonder denk ik hierbij aan oud-collega's Robin en Eric en de heren van de koffie-, lunch-, en virtuele forumtafel. De vele,

146 Dankwoord

wetenschappelijk uiterst verantwoorde, discussies en andere bezigheden waren voor mij altijd een waar genoegen! Chrétien en Xavier, bedankt voor de immer aanwezige koffie zo vroeg in de ochtend! En natuurlijk dank aan de SKA borrelcommissie, die de vrijdagmiddag toch altijd weer een speciaal tintje wisten te geven. En natuurlijk ook dank aan alle andere groepsleden die voor de nodige gezelligheid hebben gezorgd tijdens het werk, de diverse conferentie- en cursusbezoeken, en tijdens het organiseren van de TMR Summerschool in Dronten.

Rest mij nog om alle vrienden te bedanken die ook buiten het AiO-schap om hun bijdrage hebben geleverd door via stapavondjes, feestjes, Ardennenweekenden, MTB- en fietstochten en andere bezigheden voor de nodige afleiding te zorgen. Dank ook aan de leden van Squadra, die ervoor gezorgd hebben dat ik in topconditie mijn laatste promotie-jaar heb kunnen doorkomen, en op een uitermate gezellige manier kennis heb kunnen maken met de triathlon. Ruben, bedankt voor het feit dat je me altijd weer een trainingsdoel geeft (mijn tijd komt nog wel ...), en alle anderen die als prestatie-verhogende factor en trainingspartner hebben gefungeerd.

Als laatste (maar zeker niet als minste) wil ik graag Mirjam bedanken, niet alleen omdat je op het laatste moment nog optrad als spellingscorrector, maar ook voor het doorstaan van vooral de laatste fase van mijn promotie. Het zit erop!

Publications

- *Imaging of hydrocarbon reactions in zeolite packed-bed reactors using positron emission profiling.*
B.G. Anderson, N.J. Noordhoek, D. Schuring, F.J.M.M. de Gauw, A.M. de Jong, M.J.A. de Voigt, and R.A. van Santen; *Catal. Lett.* **56**, 137–144 (1998).
- *n-Pentane hopping in zeolite ZK-5 studied with ^{13}C NMR.*
P.C.M.M. Magusin, D. Schuring, E.M. van Oers, J.W. de Haan, and R.A. van Santen; *Magn. Reson. Chem.* **37**, S108–S117 (1999).
- *Concentration and chainlength dependence of the diffusivity of alkanes in zeolites studied with MD simulations.*
D. Schuring, A.P.J. Jansen, and R.A. van Santen; *J. Phys. Chem. B* **104**(5), 941–948 (2000).
- *Adsorption and diffusion of n-hexane/2-methylpentane mixtures in zeolite Silicalite: experiments and modeling.*
D. Schuring, A.O. Koriabkina, A.M. de Jong, B. Smit, and R.A. van Santen; *J. Phys. Chem. B* **105**(32), 7690–7698 (2001).
- *Adsorption and diffusion of alkanes and their mixtures in silicalite studied with positron emission profiling.*
A.O. Koriabkina, D. Schuring, A.M. de Jong, J. van Grondelle, and R.A. van Santen; In: *Studies in Surface Science and Catalysis, Vol. 135*, A. Galarneau, F. Di Renzo, F. Fajula, and J. Vedrine (eds.), Elsevier, Amsterdam, 2001.
- *In situ study of alkane conversion on Pt-loaded acidic zeolites.*
N.J. Noordhoek, D. Schuring, F.J.M.M. de Gauw, B.G. Anderson, A.M. de Jong, M.J.A. de Voigt, and R.A. van Santen; *Ind. Eng. Chem. Res.* **41**(8), 1973–1985 (2002).
- *Influence of the acid sites on the intracrystalline diffusion of hexanes and their mixtures within MFI-zeolites.*
A. O. Koriabkina, A.M. de Jong, D. Schuring, J. van Grondelle, and R.A. van Santen, *J. Phys. Chem. B* **106**(37), 9559–9566 (2002).

148 Publications

- *Diffusion of 3-methylpentane in silicalite: concentration dependence.*
A.O. Koriabkina, D. Schuring, A.M. de Jong, and R.A. van Santen, submitted to *J. Phys. Chem. B*.
- *Properties of single-file systems: what determines the typical single-file behaviour?*
D. Schuring and R.A. van Santen, submitted to *J. Phys. Chem. B*.
- *Adsorption assisted desorption of NH₃ on γ -alumina studied with the positron emission profiling technique.*
D. Sobczyk, J.J.G. Heszen, J. van Grondelle, D. Schuring, A.M. de Jong, and R.A. van Santen, to be submitted to *J. Catal.*
- *Diffusion of n-hexane in MFI zeolites: anisotropy effects and the concentration dependence.*
A.O. Koriabkina, A.M. de Jong, D. Schuring, E.J.M. Hensen, and R.A. van Santen, to be published.

Curriculum Vitae

Danny Schuring werd geboren op 11 mei 1974 te Amersfoort. In 1992 behaalde hij het Atheneum diploma aan het Vallei College te Amersfoort, waarna hij aan de Technische Universiteit Eindhoven begon aan een studie Technische Natuurkunde. Tijdens zijn studie liep hij enkele maanden stage bij Philips Lighting in Eindhoven, waar hij werkte aan een niet-destructieve methode voor de bepaling van de hoeveelheid kwik in fluorescentielampen. Zijn afstudeeronderzoek werd uitgevoerd bij de vakgroep Kernfysische Technieken onder leiding van prof.dr. M.J.A. de Voigt en dr. L.J. van IJendoorn. Tijdens dit onderzoek werkte hij aan het *in-situ* meten van transporteigenschappen en reactiekinetiek van alkanen in zeolieten met behulp van Positron Emissie Profileren, en de interpretatie van deze metingen met behulp van numerieke simulaties van de stroming en reacties in deze systemen. In maart 1998 trad hij in dienst als AiO bij de vakgroep Anorganische Chemie en Katalyse onder leiding van prof.dr. R.A. van Santen. Tijdens zijn promotie-onderzoek hield hij zich bezig met de bestudering van diffusie in zeolieten met behulp van diverse (voornamelijk theoretische) methoden, zowel op microscopische (moleculaire) als macroscopische (reactor) schaal. De resultaten van dit onderzoek zijn beschreven in dit proefschrift.